THREE-DIMENSIONAL ANATOMICAL ATLAS OF THE HUMAN BODY

by

António Manuel Teixeira Barbeito

A thesis submitted in partial fulfillment of the requirements for the degree of Doctor in Information Management, Geographic Information Systems.

Supervisors: Marco Painho, Ph.D.

Pedro Cabral, Ph.D.

October 2015

Committee:

Prof. Doutor Pedro Miguel Pereira Simões Coelho, President

Prof. Doutor Marco Octávio Trindade Painho, Supervisor

Prof. Doutor João Erse de Goyri O'Neill

Prof. Doutora Maribel Yasmina Campos Alves Santos

Prof. Doutor José Tadeu Marques Aranha

Prof. Doutor José Paulo Elvas Duarte de Almeida

Prof. Doutor Roberto André Pereira Henriques

DEDICATION

To Ana, Rita and Magui.

ACKNOWLEDGMENTS

I would like to thank all those who contributed in a constructive way to the development and completion of this thesis.

My supervisors, Professor Marco Painho and Professor Pedro Cabral, for their guidance, support and patience throughout this process.

The directors of ESTGA, Professor Estima de Oliveira and Professor Gonçalo Paiva Dias, by providing me with favorable conditions for carrying out this research.

The colleagues who kindly had a word of encouragement.

My parents and sisters for their endless love and concern.

Most of all, my girls, Ana, Rita and Magui, for the indefinable feeling that unites us and that gives meaning to everything else.

I would also like to thank the contribution of the U.S. National Library of Medicine for making available the datasets used in this work.

RESUMO

Os atlas anatómicos permitem mapear as estruturas anatómicas do corpo humano. As primeiras versões consistiam em documentos analógicos com representações pictóricas do corpo humano associadas a texto descritivo. Com o aparecimento dos sistemas computorizados, surgiram versões digitais e os modelos tridimensionais foram introduzidos. Desta forma, estes sistemas tornaram-se mais eficientes, permitindo visualizações mais realistas e um grau de interatividade superior. O desenvolvimento de atlas anatómicos em ambientes de sistemas de informação geográfica (GIS) permite criar plataformas com um elevado grau de interatividade e com ferramentas que facilitam a exploração e análise do corpo humano.

Nesta tese, desenvolve-se um protótipo para representar o corpo humano. O sistema inclui um modelo topológico 3D GIS, uma interface gráfica e funções para explorar e analisar o interior e a superfície das estruturas anatómicas do corpo humano. A aproximação GIS baseia-se essencialmente nas caraterísticas topológicas do modelo e no tipo de funções criadas que incluem diversos tipos de medição, identificação, seleção e análise.

Com estas funções, o protótipo tem a capacidade de replicar a informação disponibilizada pelos atlas anatómicos tradicionais e acrescenta um nível superior de funcionalidade. Efetivamente, algumas das limitações encontradas nos atlas anatómicos correspondem precisamente a caraterísticas presentes nos GIS, nomeadamente, as capacidades interativas, a gestão de um sistema em que a informação está organizada em camadas, as ferramentas de medição, o modo de edição para expansão da informação contida no sistema e as operações de análise espacial.

PALAVRAS-CHAVE

Segmentação; Reconstrução 3D; 3D GIS; Topologia; Análise espacial; Atlas anatómicos

ABSTRACT

Anatomical atlases allow mapping the anatomical structures of the human body. Early versions of these systems consisted of analogic representations with informative text and labelled images of the human body. With the advent of computer systems, digital versions emerged and the third dimension was introduced. Consequently, these systems increased their efficiency, allowing more realistic visualizations with improved interactivity. The development of anatomical atlases in geographic information systems (GIS) environments allows the development of platforms with a high degree of interactivity and with tools to explore and analyze the human body.

In this thesis, a prototype for the human body representation is developed. The system includes a 3D GIS topological model, a graphical user interface and functions to explore and analyze the interior and the surface of the anatomical structures of the human body. The GIS approach relies essentially on the topological characteristics of the model and on the kind of available functions, which include measurement, identification, selection and analysis.

With the incorporation of these functions, the final system has the ability to replicate the kind of information provided by the conventional anatomical atlases and also provides a higher level of functionality, since some of the atlases limitations are precisely features offered by GIS, namely, interactive capabilities, multilayer management, measurement tools, edition mode, allowing the expansion of the information contained in the system, and spatial analyzes.

KEYWORDS

Segmentation; 3D reconstruction; 3D GIS; Topology; Spatial analysis; Anatomical atlases

INDEX

LIST OF FIGURES

LIST OF TABLES

LIST OF ABBREVIATIONS AND ACRONYMS

2D	Two-dimensional
3D	Three-dimensional
4IM	4 intersection model
9IM	9 intersection model
BMI	Body mass index
BVH	Biovision hierarchical data file
CAD	Computer aided design
CGIS	Canada Geographic Information System
CT	Computed tomography
FDS	Formal Structure Data Model
GI	Geographic information
GIS	Geographic information system
GISc	Geographic information science
GPS	Global positioning system
GTP	Generalized tri-prism model
GUI	Graphical user interface
ID	Identifier
LM	Layer matrix
LOD	Level of Detail
MRI	Magnetic resonance imaging
NLM	National Library of Medicine
OGC	Open Geospatial Consortium
RGB	Red, Green, Blue colors
RMSE	Root mean squared error
ROI	Region of interest
RS	Remote sensing

SI	Spatial information
SPECT	Single-photon emission computed tomography
SQL	Structured Query Language
TEN	Tetrahedral network model
TIN	Triangulated irregular network
TOC	Table of contents
VCH	Visible Chinese Human
VHP	Visible Human Project
VKH	Visible Korean Human
WHO	World Health Organization

1. INTRODUCTION

This thesis focuses on the study, conceptualization and implementation of a geographic information system (GIS) prototype, named with the acronym 3DBodyGIS, with the aim of developing a 3D anatomical atlas of the human body. The motivation to develop an atlas in this type of platform was based on two fundamental aspects: (i) both GIS and 3D anatomical atlases deal with alphanumeric information aggregated to spatial information (SI); and (ii) the tools provided by GIS, in particular the ones regarding spatial analysis, could add value to the degree of functionality of the atlases.

Given the aim of the thesis, the work to be performed involves the study of 3D GIS models and current anatomical 3D atlases. After consultation of the scientific literature in each of these areas, there was an attempt to understand to what extent there would be studies proposing methodologies involving the approach of GIS to anatomical atlas or, at least, to some form of representation of the human body. The existence of this type of work would create a direct link to the object of this study. However, in contrast to the volume of existing research exclusively on 3D GIS or 3D anatomical atlas, the use of a GIS approach in the development of representations of the human body does not go much beyond its recognition of interest.

The first section of this chapter presents the GIS context and the actual representations of the human body, in particular, the anatomical atlases. After this overview, the section proceeds bringing these two areas together. Data used in this study are obtained from medical imaging. Its use in the reconstruction of 3D models requires image segmentation, which is, then, an essential topic included in this thesis. The literature review presented in this chapter covers the following topics: 3D GIS models, representations of the human body, anatomical atlases, GIS approach to anatomical atlases, segmentation of anatomical structures and 3D reconstruction methods. Throughout the text, the literature review provides clues to the conceptualization of the system to be developed.

The second section presents the objectives and working assumptions. The chapter ends with the description of the thesis structure.

1.1. CONTEXTUALIZATION AND LITERATURE REVIEW

1.1.1. Geographic Information Systems

Geographic information science (GISc) is related to various technologies and data with which these operate, i.e., geographic information (GI). GISc was initially defined by Goodchild (2005) as the "research on the generic issues that surround the use of GIS technology, impede its successful

implementation, or emerge from an understanding of its potential capabilities". More recently, Painho & Curvelo (2012) defined GISc as an experimental research field that has geographic space as its object of study, geographic information as its means of representing knowledge and geographic information systems as its disciplinary tool. According to these authors, this definition points to the manner in which GISc relies on the way it reconciles the technological, cognitive and conceptual aspects of geographic information, generates new contexts for the (re)formulation of geographical problems and (re)creates environments that stimulate and challenge spatial reasoning and spatial knowledge. These contexts and environments depend on the way in which theory, concepts, data, technology, methods, individuals and society interact and go through the continuum GISc – GISystems. Although this is a recent area of knowledge, the same cannot be said about the manipulation of GI by humans.

Geographic Information and Spatial Information

Statements such as "80% of all information contains some geospatial reference" come up regularly in the context of GI in order to highlight the importance of this kind of information. In ESRI (2012) a similar statement is dedicated to the information integrated in the corporate databases: "Approximately 80% of an organization's data has a location component". Hahmann & Burghardt (2013) start from the statement that "80% of all information is geospatially referenced" and develop a methodology to certify its veracity. At the conclusion of this work the authors state that "57% of the information within the German Wikipedia is geospatially referenced", considering that the value, despite being below the estimate of geo-community, remains as a strong evidence of the importance of GI.

References to GI and SI are often made with the same sense. Heywood et al. (2011), for example, states that GIS uses geographic data, and concludes that these systems can add value to spatial data. Jones (2014) states that the GI refers to phenomena with a spatial reference. However, when exemplifying this type of information, this author mentions exclusively entities on the Earth's surface, such as cities, streets, and administrative areas. The concept of GI associated to a coordinate or a set of spatial coordinates is common in the literature. Subsequently, the space referred by these coordinates can be identified as a neighborhood near the Earth's surface, including this one (Longley et al. 2005).

The adjective contained in the GI name comes from the coordinates usually used in cartography, latitude and longitude, known as geographical (Bonham-Carter 2014). The GI definition associated to the Earth's surface can be distinguished from the definition of SI. Longley et al. (2005) address this question in an elucidative way stating that SI refers to any space, while the GI refers to places related

to the Earth's surface. GI appears, then, as a kind of SI circumscribed to the space in which runs the current human activity.

GI has been expressed by human beings through cartography. According to Harley & Woodward (2001) "it is in Upper Paleolithic societies that one might expect to find the earliest evidence of maps". Casaca et al. (2005) refer that the need and the corresponding capability to create maps are phenomena of ancient and universal character. The tradition of mapping the Earth's surface and entities related to it has remained until today, having evolved with the techniques and technologies that have emerged. Casaca et al. (2005) identified two stages in the cartographic representation process: (i) the stage of geodesy, in which the Earth's surface points are projected on a reference surface of double curvature, generally ellipsoidal; (ii) the phase of mathematical cartography, which makes the projection of the reference surface on surfaces of simple curvature, such as the cone, cylinder or plane. Regarding the map concept, Thurston et al. (2003), state that "the map is a representation of reality, in color or black and white, and 2D, 3D, or 4D. The map might represent the backyard, neighborhood, city, country, or the world, or might constitute the pattern of microbes or blood vessels within the human body", which indicates that mapping is not limited to GI, and may use SI in general.

From 2D GIS to 3D GIS

The emergence and evolution of GIS can be defined through several stages. According to Coppock & Rhind (1991), “These overlap in time and occur at different moments in different parts of the world. The first, or pioneering age, extended from the early 1960s to about 1975; in this, individual personalities were of critical importance in determining what was achieved. The second phase, approximately from 1973 until the early 1980s, saw a regularization of experiment and practice within and fostered by national agencies; local experiment and action continued untrammeled and duplication of effort was common. The third phase, running from about 1982 until the late 1980s, was that of commercial dominance. The fourth (and current) phase is one of user dominance, facilitated by competition among vendors, embryonic standardization on open systems and increasing agreement on the user’s perception of what a GIS should do and look like.”

It is in the tradition of the planar cartography that GIS appears and this was the first reason for these systems being initially developed as 2D frameworks. The Canada Geographic Information System (CGIS) (Tomlinson et al. 1976) is recognized as the first GIS, having been developed with the support of the existing computerized systems by request of the Canadian government in order to identify natural resources of the territory and its potential uses.

The literature is profuse in defining GIS as evidenced by the list of definitions in Maguire et al. (1991). GIS definitions range from those that specify in detail the components or the functionality of systems (Burrough 1986; Burrough et al. 2015), considering GIS as a set of powerful tools to collect, store, retrieve, process and display SI of the real world with a view to a particular set of purposes, and those who hold few key elements (Bonham-Carter 2014), featuring GIS as computerized systems designed to manipulate GI.

The World Health Organization (WHO) after defining GIS as "computer systems for capturing, storing, checking, integrating, manipulating, analyzing and displaying data related to positions on the Earth's surface" concludes on the definition, mentioning a fundamental aspect of these systems, the link between databases and GI (by referencing maps): "It is thus the way of linking databases with maps, to display information, perform spatial analyzes or develop and apply spatial models" (World Health Organization 2015).

A key aspect in GIS is how to model the represented reality. GIS models can be classified as either vector or matrix. According to de By (2004) among the matrix models, the ones which are composed by square cells - in 2D version - are by far the most used, being called raster or raster maps. The vector and raster models have clearly distinct characteristics making them complementary regarding the application scope (Figure 1.1).

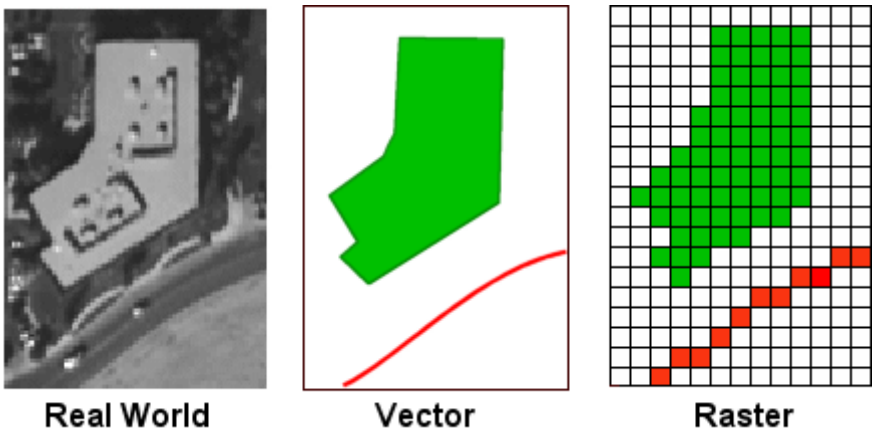

Figure 1.1 – Modeling the real world with vector and raster models.

Source: http://www.geography.hunter.cuny.edu/~jochen/GTECH361/lectures/lecture05/concepts/03%20-%20Geographic%20data%20models.html [Accessed June 9, 2015]

de By (2004), refers to the concepts of field, a geographic phenomenon for which, for every point in the study area, a value can be determined, and object, a phenomenon that occurs discreetly and with well-defined borders. Using these concepts, we can say, generally, that the raster models are suitable for the representation of the field concept, and vector models are suitable to the representation of the object concept. However in many situations both models can represent both concepts.

Davis (2001), when characterizing the two models, presents a set of advantages associated with each of them: the raster systems have a simple structure, are easy to use and allow to perform, in a simple way, some analysis operations. The vector models provide a more familiar form of map representation, allow describing the information with high precision in which the display does not degrade with zooming, generate lower amounts of data than raster models since the information is encoded in nodes or vertices that have representation and can be topological. Regarding the analytical capabilities of the two models, Heywood et al. (2011) point out that "Traditionally, vector spatial data models have been considered more appropriate for answering topological questions about containment, adjacency and connectivity. However, with the advent of more intelligent raster data structures such as the quadtree that contains information about the relationships between cells, this distinction is closing" (Figure 1.2).

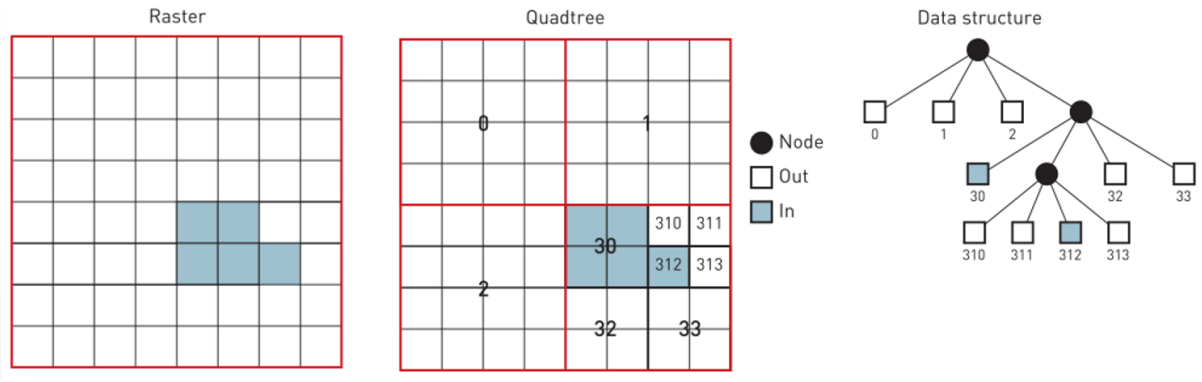

Figure 1.2 – Quadtree data structure.

Source: Heywood et al. (2011).

The strong development of GI technologies, that include global positioning systems (GPS), remote sensing (RS) and GIS (Heywood et al. 2011), allowed to generate and deliver large volumes of 2D and 3D GI. In parallel, the development of techniques, algorithms and the GISc, have contributed together

to create systems that enable an increasingly efficient and more accurate representation of reality providing, simultaneously, analysis tools.

According to the literature, 2D GIS have been described as widely tested and efficient systems (LI 1994). In 2D GIS data models is common to define three different classes to accommodate the various geometric entities: points, lines and areas. Stored by themselves, these entities originate a data model called spaghetti (Peuquet 1984). The establishment of spatial relationships between the several represented geometric entities leads to a topological data model. In these models, the points are the most elementary entities, being materialized through nodes. de By (2004) defines the following representations for GI:

- Points are given by a coordinate pair (x, y) in 2D, or by a 3-tuple (x, y, z) in 3D;
- The lines consist of a list of nodes: the two extreme nodes and none or a finite number of internal nodes (also called vertices);
- The areas use a frontier model, i.e., each area is represented by an arc/node structure that materializes a polygon as boundary.

The need to update the 2D systems with the introduction of the third dimension and the 3D GI demand have been growing (Gröger & Plümer 2012). This phenomenon stems from the inability of 2D systems to solve key issues involving the nature of 3D entities. The difficulties of 2D systems to model 3D objects occur not only at the representation level but, especially, in terms of performing analysis operations (Abdul-Rahman & Pilouk 2008). To reinforce the importance of the 3D systems, these authors present an extensive list of areas in which 3D spatial models have been studied and used: geology, hydrology, civil engineering, and environmental engineering. However, the transition from 2D to 3D entails a substantial increase in the volume of data involved, the complexity of reality to represent and, hence, the structures of the models, the algorithms that implement the GIS methods and the topological relationships among 3D objects. This is why 3D GIS have become a topic of research with the development of several studies about the conceptualization and implementation of models within specific applications (Abdul-Rahman & Pilouk 2008).

Between 2D and 3D systems emerged the 2.5D concept. From a geometrical point of view, these systems have intrinsically 2D data models and record altitude values in an attribute table. This means that the 2.5D systems are not able to represent objects having different Z values for a given (X, Y) pair, since each pair of planimetric coordinates corresponds to only a record which will be connected to the

respective altitude in the table of attributes. Thus, although 2.5D systems perform efficiently certain 3D viewing of objects in 3D environments (Zlatanova et al. 2002), their capacity is limited when it is necessary to represent more complex objects (Figure 1.3). Therefore, the dissatisfaction with the 2D models extends to 2.5D models when it comes to model 3D objects (Wu 2004).

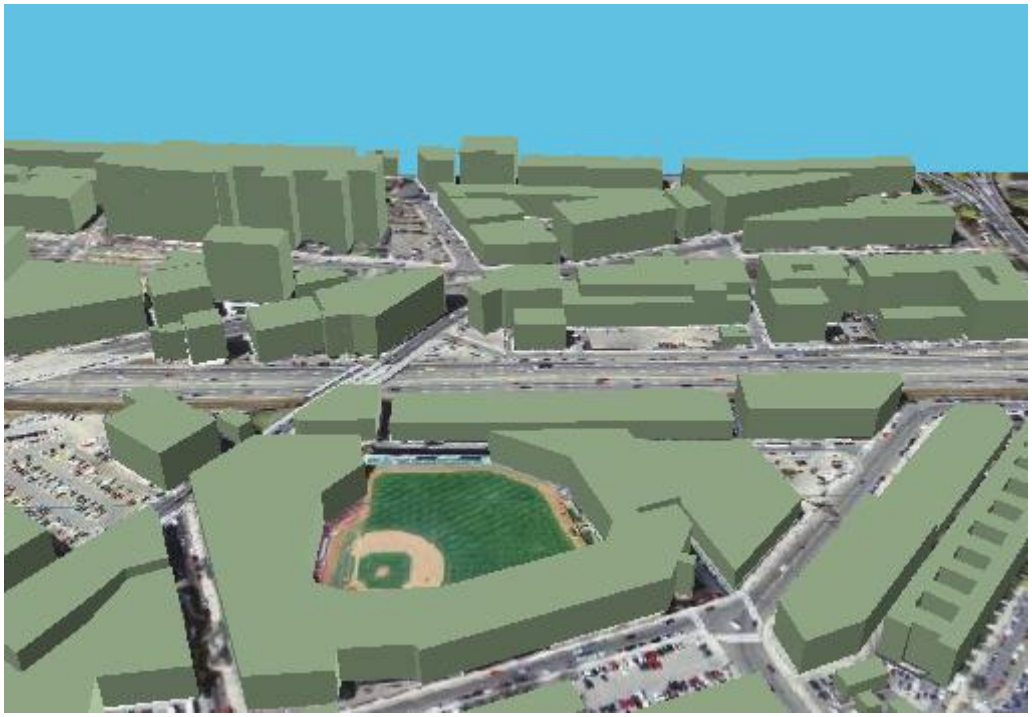

Figure 1.3 – The use of 2.5D data to model the 3D reality.

Source: http://www.gsd.harvard.edu/gis/manual/landmarks/ [Accessed June 9, 2015]

The 3D representations have distinguishing characteristics from 2D representations with regard to the data types and represented entities: a first aspect to consider is the need to store 3D coordinates, that is, the nodes become associated with coordinates (x, y, z). One second important aspect relates to the introduction of a new class of objects: the body class (Frank et al. 1986). A similar class to the area of the 2D models is the surface class: while the areas in 2D models are two-dimensional elements in the plan, in the 3D model the surfaces exist in the three dimensional space, being made up of faces bounded by edges and may have more complex shapes. Also the linear entities of 3D models may have more complex shapes than those occurring on the plane in the 2D models.

In current systems, Milner et al. (2014) state that, despite visualization being a common aspect of 3D GIS, the editing and analysis have not advanced much. The difficulties with the 3D spatial analysis result

from the greater complexity associated with the use of the third dimension and the fact that the existing algorithms in the traditional GIS have been developed for 2D systems. Thus, research continues in this area, with some of these papers referenced herein (Figure 1.4).

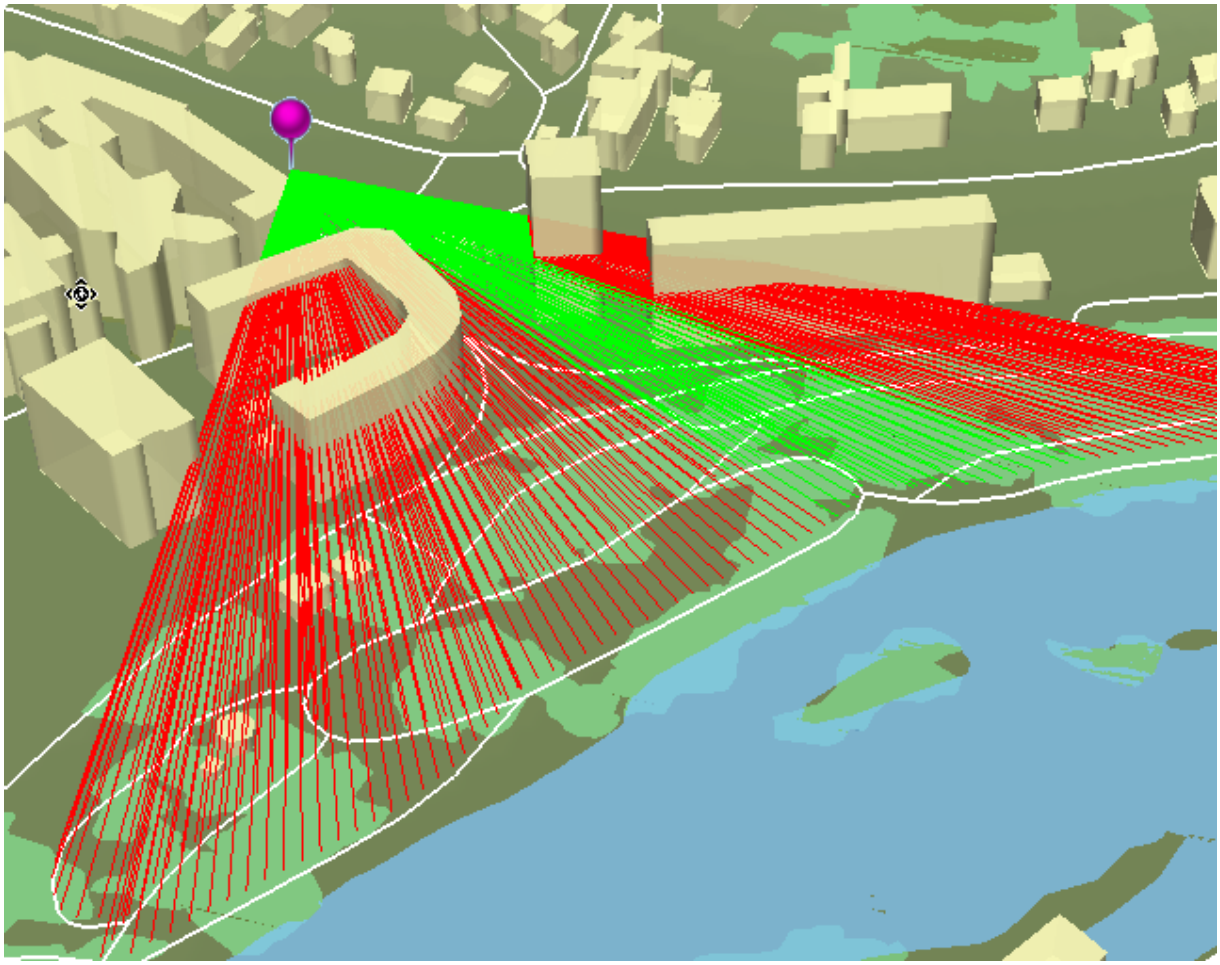

Figure 1.4 – Spatial analysis in 3D.

Source: http://www.arcorama.fr/2010/06/les-grands-themes-darcgis-10-28.html [Accessed June 9, 2015]

Like the 2D GIS, 3D GIS have been used to represent the Earth's surface and related entities. The 3D visualization of digital terrain models that represent the Earth's surface and the analysis which allows, for example, to determine if a point is above or below a surface, are issues easily solved by 2.5D models. However, the representation of a closed surface upon itself and the inclusion analysis of a given point relative to that surface become difficult to solve in these systems.

In the current language of the GISc, the "geographic" adjective is replaced by "spatial" when the analyzes are related with positions are mentioned. Indeed it is unusual to speak about geographical analysis, being the term “spatial analysis” unanimously used. This issue is not just casual because, in reality, it has a very concrete meaning: although GIS operate almost exclusively in a given space, their analysis tools are comprehensive and can be used in other spaces. The measurement of a length along a spatial object, for example, may be carried out both on a street or on a blood vessel: although the two situations are totally different, the same measurement function can be used in both cases.

GIS Functionalities

The knowledge of the typical functionality of the GIS is important in order to take advantage in the exploration of spatial models. de By (2004) distinguishes the following groups of analytical functions in a GIS: (i) Measurement, spatial query and classification; (ii) Overlay; (iii) Neighborhood; (iv) Network and (v) 3D analysis.

In the 3D space, the measurements may include distances between two entities or along an entity, areas and volumes. The approaches to take measurements differ in the case of vector and raster data. The measurements of raster areas and volumes, for example, involve cell counting, which are then scaled by the value of each cell. The vector measurements use mathematical formulae and results may be stored in attribute tables, which prevents recalculation whenever requested.

Spatial queries consist in identifying objects through logical conditions. These selections can be interactive on the geometric component or on a table of attributes, based on the "select by attributes" operations, usually defined through Structured Query Language (SQL), or based on "select by location", using topological properties. The location-based selections involve the initial determination of the source object(s) and the choice of the function that will make the selection. Once the source object is defined, it is possible to determine, with respect to this source, the objects with the following spatial relations: interior / exterior, intersection, adjacency, location within a predetermined distance.

The classification consists in rearranging the data by using certain attributes. The attributes with quantitative domain enable classifications based on methods that include Equal Interval, Quantile (equal frequencies), Jenks Natural Breaks, Geometric and Standard Deviation, which are used depending on the characteristics of the data. The proper selection of a classification method for a set of geographic data is an important requirement regarding the cartographic communication.

Overlay operations consist in combining layers of information through map algebra operations, carried out on overlapping areas. The overlay functions can be implemented with vector or raster data, although the latter is preferred due to their particular suitability for overlaying operations.

The neighborhood functions enable to assess the characteristics of an area around a given entity. They involve proximity calculations (buffer zones and Thiessen polygons), spread computation or least-cost paths analysis (de By 2004).

The network functions are based on the analysis performed on networks (arcs connected together). This type of analysis is more common on vector data. Network analysis involves determining optimal paths, finding closest facilities and determination of service areas.

The 3D functions are an extension of the 2D GIS functions with application on 3D models. In this regard, 3D GIS should replicate the same degree of functionality of the 2D GIS. Although 3D functions may be directed to solving the same problems, the addition of the third dimension requires the construction of new algorithms to handle the new possibilities that arise from the greater complexity associated with the 3D space populated by 3D, 2D and 1D objects.

Topology

An inseparable aspect of GIS when it comes to spatial analysis, is the implementation of explicit topological relationships in their models (Figure 1.5), a situation that should also be considered in 3D space. According to (Tanton 2009), “the study of those properties of geometric shapes and surfaces that remain unchanged when the shapes of those objects are distorted by a continuous deformation (such as stretching, shrinking, or twisting) is called topology. Unlike a classical geometer, a topologist is not interested in questions of distances and angles, but is only concerned with the relative positions of points”. The definition in the GIS context is given by Longley et al. (2005): “the science and mathematics of relationships used to validate the geometry of vector entities, and for operations such as network tracing and tests of polygon adjacency”. This definition contains four aspects relevant to GIS: (i) results from the mathematical definition by referring to the relationship between the model objects; (ii) a first utility aspect as support to data validation; (iii) a second utility aspect as support for analysis operations; (iv) the explicit mention of vector data. These aspects show the importance of topology in GIS models and expose the highest capacity of vector data in its definition. In fact, the vector model enables to explicitly store the topological relationships between vector objects in the model structure together with the objects themselves while the matrix model requires that these relationships are inferred from the database.

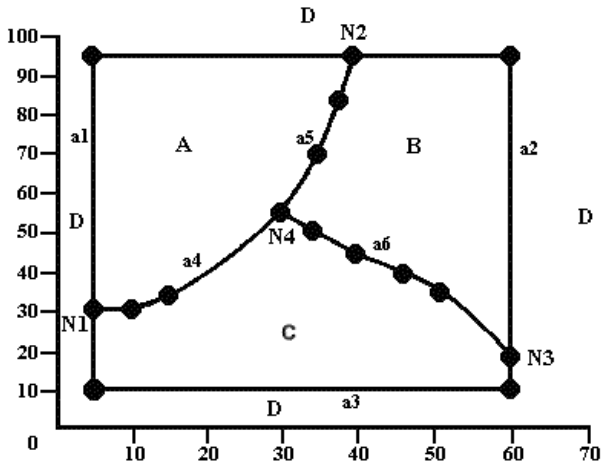

Arc Topology				
Arc	Start Node	End Node	Left Polygon	Right Polygon
a1	N1	N2	D	A
a2	N2	N3	D	B
a3	N3	N1	D	C
a4	N1	N4	A	C
a5	N4	N2	A	B
a6	N3	N4	C	B

Polygon Topology	
Polygon	Arcs
A	a1, a4, a5
B	a2, a5, a6
C	a3, a4, a6
D	outside study area

Node Topology	
Node	Arcs
N1	a1, a3, a4
N2	a1, a2, a5
N3	a2, a3, a6

Figure 1.5 – Vector data topology definition.

Source: http://library.oceanteacher.org/OTMediawiki/index.php/Vector_Data_Topology [Accessed June 9, 2015]

With regard to the topological relationships, the greater number of classes and the dimensional expansion of 3D models compared to 2D models lead to the existence of new relationships between the entities, which causes a greater complexity of the topological model.

The study of topological relationships between model objects can be based on the 4-intersection model (4IM) or on the 9-intersection model (9IM). Currently, this study relies more often on 9IM model (Egenhofer & Herring 1990; Egenhofer & Franzosa 1991; Egenhofer et al. 1993). Following the 9IM model, many other models have been introduced for the same purpose, although the 9IM model continues to be a reference, having been adopted by the Open Geospatial Consortium (OGC). The 4IM and 9IM models build binary matrices of intersections between two objects (the result of each intersection can return the empty or non-empty values).

Each intersection between two objects is seen in the light of invariant topologically properties: the interior and the border in 4IM, and the exterior is added in the 9IM. In the 2D space the possible pairs of objects are: region-region (the region concept refers to a 2D entity without holes), region-line, region-point, line-line, line-point, point-point. For each pair of objects there are $2^4 = 16$ binary matrices for the model 4IM and $2^9 = 512$ for the 9IM model. However, some of these relationships are not

possible, so the actual total number of relationships between the two objects is inferior. For objects with co-dimension = 0 (n-dimensional objects in $\mathbb{R}^n$) both models produce the same results. However, for all the other combinations, with co-dimension> 0 (at least one of the objects has a dimension smaller than the space), the 9IM model allows to distinguish relationships that the 4IM model assumes to be the same (Egenhofer et al. 1993). For two regions in $\mathbb{R}^2$, both models generate eight possible relationships: disjoint, contains, inside, equal, meet, covers, covered by, overlap. The same 8 relationships are found between two lines in $\mathbb{R}$. However, the number of possible relationships between two lines in $\mathbb{R}^2$, detected by the 9IM model, rises to 25, with more 21 relationships in the case of lines with branches.

The change to 3D adds the body object, which allows to create more pairs of intersections: body-body and body with each of the other objects. In addition, the region-region relationships become co-dimension> 0 which allows the 9IM model to produce more possible results than in the $\mathbb{R}^2$ space. The increasing complexity of the topological relationships and resulting difficulties are well patent in Xu & Zlatanova (2013), which state that in 2D models there has been a significant and continuous improvement of the 9IM model implementation, while the development of relationships in the 3D models have been slow. The "Dimensionally Extended 9-Intersection Model" (DE9IM) provides the dimension of the intersections between two spatial objects. Figure 1.6 shows the resulting DE9IM matrix for a particular intersection between a line and a polygon.

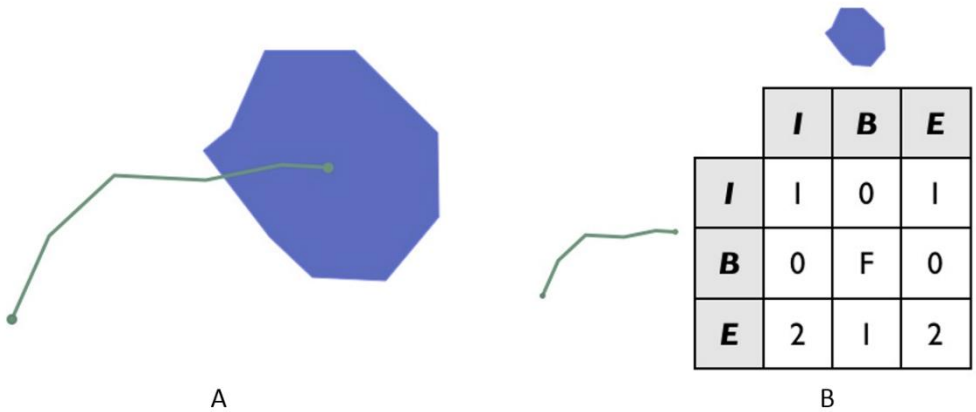

	I	***B***	***E***
I	1	0	1
B	0	F	0
E	2	1	2

Figure 1.6 – DE9IM model.

(A) Linestring intersecting a polygon. (B) DE9IM model for the intersection.

Source: http://suite.opengeo.org/4.1/dataadmin/pgAdvanced/de9im.html [Accessed June 9, 2015]

Surface, Volume and Hybrid Models

The 3D models that have been shown may be classified as geographical, geological or integrated (Wang et al. 2007), or analogously, surface, volume or hybrid models (Schön et al. 2009). Liu et al. (2009) still use the surface data models and solid data models nomenclature. Surface models are often used in the representation of urban areas, with particular emphasis on buildings modeling (Lee & Zlatanova 2008). The volume models are usually employed in the representation of geological structures present in the underground (Wang & Huang 2012). The integrated representation of surface and objects with underground has led to the development of integrated models (Tegtmeier et al. 2014). Given the complexity of reality in 3D, the research in this area has not been directed to develop a global model for 3D. Instead, new models have emerged specifically tailored to the realities they aim to represent. For these reason, there are not satisfactory global 3D models in the known databases (Butwilowski & Breunig 2010).

The 3D Formal Structure Data Model (3DFDS), an extension of the FDS model (Molenaar 1990), exemplifies a topological surface vector model. The fact that it is a surface model, makes it ineffective when it is intended to represent the inside of objects or, in other words, the volume component of the objects. One of the possibilities for the representation of continuous volume in 3D space is the use of raster models constituted by voxel arrays. As models of great simplicity, they become inefficient with respect to the volume of data generated. This difficulty, present in raster models, leads to various forms of structure in order to optimize the amount of data. Thus, the octree model arises by defining a hierarchical tree, in which each voxel can be divided into eight sub-voxels. This makes possible to optimize the volume of model data with the creation of variable-sized voxels. However, despite that raster models materialize more efficiently the field concept than the vector models, the need to perform spatial analysis operations leads to consider the use of the latter (Heywood et al. 2011). Thus, the simultaneous need to establish topological relationships and to represent continuous structures in space involves to the research of 3D vector models that meet these two characteristics. The vector representation of continuous phenomena in 3D space can be achieved with 3D TIN models, also called the tetrahedral network model (TEN) (Figure 1.7).

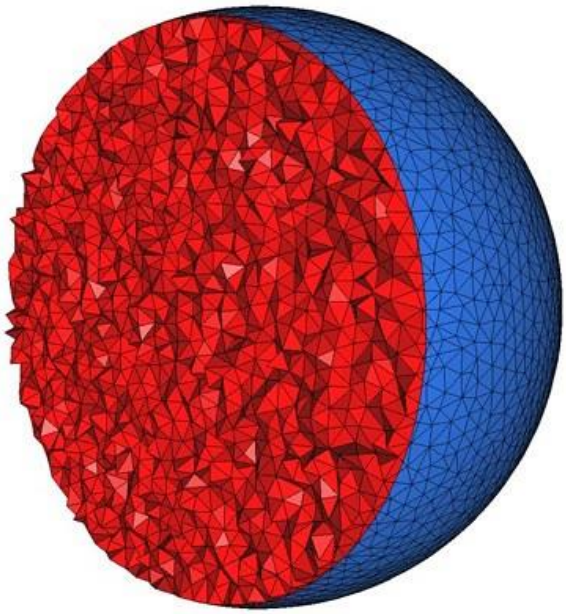

Figure 1.7 - Cut view of a 3D TEN mesh.

Source: http://doc.cgal.org/latest/Mesh_3/ [Accessed June 9, 2015]

This is essentially an extension of the TIN model used in 2D, in which the triangles, 2-simplex, change to tetrahedra, 3-Simplex. Thus, each 3D object is represented by a network of adjacent tetrahedra. TEN is a volume model introduced with the explicit aim to overcome some of the difficulties of 3D FDS model (Wang et al. 2006). The topological relationships in this model are given by adjacency between the spatial objects that constitute it. According to Abdul-Rahman & Pilouk (2008), the TEN model is of remarkable importance since it has been identified as the most appropriate for representations of 3D objects. As the raster model, the TEN model generates data volumes greater than the 3D FDS model. Zlatanova (2006) refers to the limitation of this model in the representation of structures built by man, or in the implementation of surface models since the interior, necessarily filled by tetrahedra, should be omitted in terms of visualization. Currently, 3D GIS models are implemented to represent environments in which there are human constructions and natural objects such as the Earth's surface and the geological structures beneath it.

The model developed by (Wang et al. 2006) exemplifies an integrated representation of the space around the Earth's surface. The region above the surface and the surface itself are represented by TIN models; the representation of geological objects under the earth's surface uses a generalized tri-prism model (GTP), specifically designed to represent geological structures (Figure 1.8). While GTP model is intended to represent volumes, the TIN model represents only the borders of three dimensional objects. A building model, presented by Lee & Zlatanova (2008), is developed with the specific aim to

operationalize emergency plans in urban environments, focusing the interior of buildings. In this model the topological relations are based on network connectivity. Koussa & Koehl (2009) present another 3D topological model designed to represent urban objects, with the ability to dynamically adjust the Level of Detail (LOD) according to the zoom level.

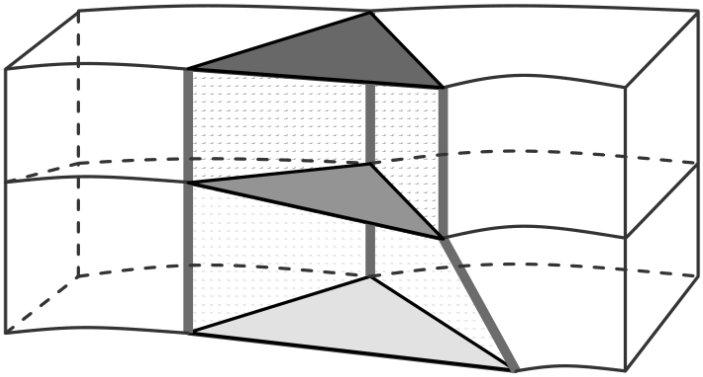

Figure 1.8 - The principle of GTP model based on unparallel drill holes.

Source: Wang (2006).

Yin & Shiode (2014) present a 3D spatial-temporal GIS model of an urban environment. This is a surface model conceived to represent buildings that records data from different times. The graphical user interface (GUI) provides analysis functions and has a time bar that enables the study of the urban landscape at different times. Wang et al. (2014) and Wang et al. (2015) emphasize the importance of 3D models for which are developed methodologies for visualizing and performing spatial analysis in view of the exploration of resources by integrating geological, geophysical and geochemical data. These models consist of 3D matrices with cells of different sizes for various modeled geological entities.

The great diversity of application-based models is reflected in these and other research studies. Such models support the assertion that, contrary to what happens in 2D, it is harder to find a 3D model with global characteristics suitable for the various representations.

1.1.2. Human Body Representation

The non-topological vector models of the human body had their origins in computer aided design (CAD) programs. These models perform representations of the human body by using a set of geometric primitives - triangles (or other geometric shapes), lines and points - and a set of attributes associated

with the geometric components. The information is preferably structured in layers and the use of tools that manipulate the visual parameters allow to get realistic high quality views. These models can be used to develop Atlases dedicated to surface anatomy, however, the representations of the interior of the anatomical structures are not available (CG Studio 2014) (Figure 1.9).

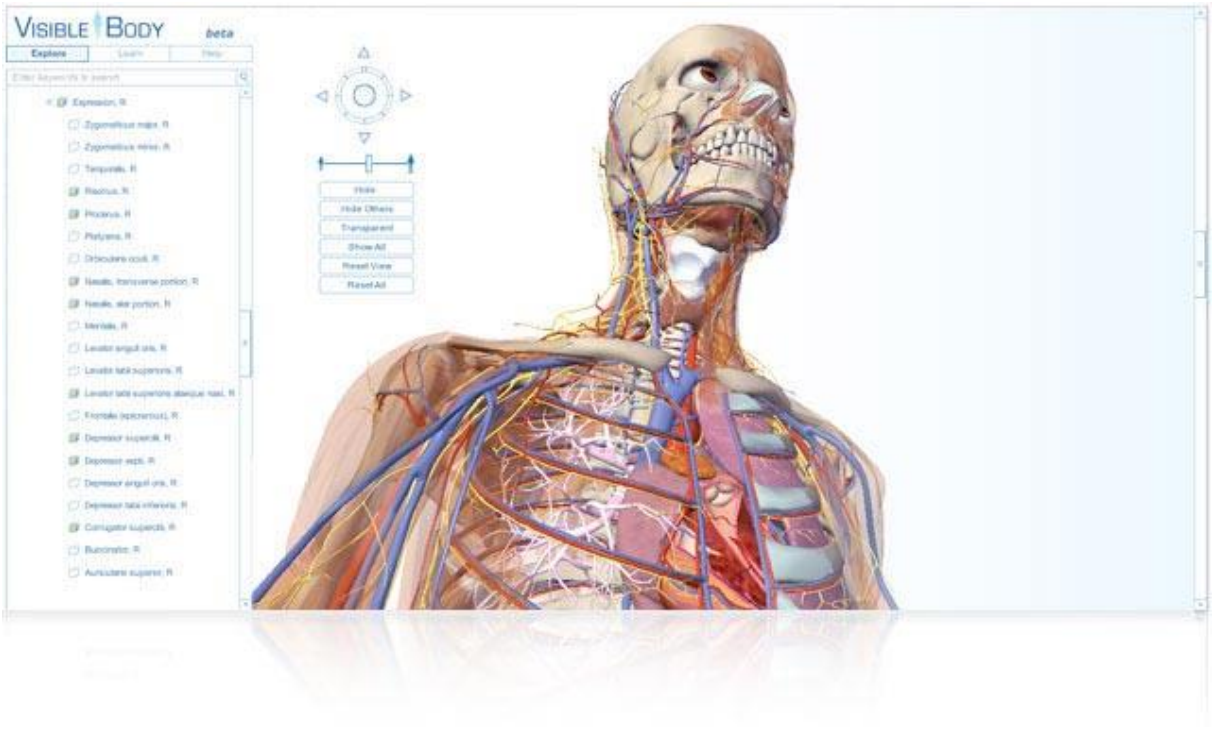

Figure 1.9 – Surface vector model linked to a database.

Source: http://maintenance.visiblebody.com/ [Accessed June 9, 2015]

Unlike the vector surface models, volume models allow to adequately represent the anatomical structures of the interior. The possibility of developing such models is linked to the availability of information about the interior of the human body. Similarly to images of geographical space obtained from satellite RS, medical imaging currently provides large volumes of information about the human body allowing to rebuild volume models contradicting the initial preponderance of surface vector models. However, the large amount of data and the difficulties involved in the visualization of volume models continues to pose challenges to the development of systems using these models.

The images generated by computed tomography (CT) and Magnetic Resonance Imaging (MRI) exemplify types of data that can be used in the reconstruction of volume models. On the other hand, obtaining real sectional images of the inside of the human body has been achieved for the first time

with the Visible Human Project (VHP) (Spitzer et al. 1996). The VHP was conducted by the US National Library of Medicine (NLM) and consisted in obtaining sectional images of the human body. The planning of this project began in 1989. In 1994 the data set for the male model became available and, in the following year, the female model was completed. In addition to the CT and MRI images, 1871 cryosection Red-Green-Blue (RGB) images were collected. These images allow visualizing the interior of the anatomical structures in true color. Two other similar projects followed: the Visible Korean Human (VKH) (Park et al. 2006) and the Virtual Chinese Human (VCH) (Zhang et al. 2006).

These images have been used in many projects that aim at a realistic representation of the human body through the RGB images 3D reconstruction (Figure 1.10) (U.S. National Library of Medicine 2001).

Figure 1.10 – Volume model from the VHP data.

Source: https://www.iai.kit.edu/www-extern/index.php?id=2097 [Accessed June 9, 2015]

any of these systems have been referred in the literature as 3D atlas of the human body such as the system presented by (Kang et al. 2000), a 3D digital muscle-skeletal anatomical atlas. It is an atlas that targets muscles, tendons and bones. It presents interactive capabilities such as navigation, selection, removal of structures, defining degrees of transparency, identification and description of structures. According to these authors, the 3D model view is helpful in understanding the human anatomy. Additionally, they claim that the reconstruction of 3D anatomical models leads to a virtual environment that can support surgical planning, virtual surgery, endoscopy and virtual simulations for training purposes. The Visible Human Projects data are also associated with the development of commercial applications, in particular, the VH Dissector (Spitzer et al. 2004; TolTech 2014) and the Voxel-Man-Man 3D Navigator (Höhne et al. 2000; Höhne & MAN 2009).

The project Digitalized Virtual Chinese Human began in 2001. This project was based on the collection of 8556 sections of the female human body, separated by 0.2 mm. The treatment of data - image registration, background image removal and segmentation - led to a female model called VCH-F1. Yuan et al. (2008) describe the reconstruction phase of the 3D model and the developed applications: VCH Clinics, virtual acupuncture and image guided surgery.

The VCH Clinics is a software that operates on the VCH-F1 model with educational goals. This software contains three modules: 3D anatomical atlas, virtual endoscopy and motion simulation. In the anatomical atlas module one can navigate and interact with the model, set different degrees of transparency and access related extra information including images, movies and introductory texts.

Besides the models and systems developed from VHP data, there are research works that rely exclusively on CT and MRI images from other sources to reconstruct 3D human models (Suri et al. 2002; Dogdas et al. 2005; Jamshidi et al. 2014).

The more elaborated projects, which use sectional images of the human body, develop methodologies aimed at the quality of visualization and its association with alphanumeric information. They can manipulate raster data, produce vector components through segmentation and allow querying. However, the associated models do not sufficiently explore the underlying capabilities of GIS models such as topology and spatial analysis.

Anatomical Atlases

The anatomical atlases are a traditional way of representing the human body (Yuan et al. 2008). In 1543, the Flemish doctor Andreas Vesalius, publishes "De Humani Corporis Fabrica", the first

anatomical text based on direct observation of the human body. In this document, the author introduces the concept of human body atlas, with various graphical representations, of map type, of the human body anatomical structures (Figure 1.11). According to Daintith (2008), although some traditional errors persist, “The work of Vesalius was of considerable significance in marking the departure from ancient concepts. The Fabrica presented in a single, detailed, comprehensive, and accessible work (superbly illustrated, probably at the Titian school in Venice), a basis for following generations of anatomists to compare with their own dissections. It has been said that after Vesalius medicine became a science”.

Figure 1.11 - De Humani Corporis Fabrica.

Source: http://www.metmuseum.org/collection/the-collection-online/search/358129?=&imgno=8&tabname=object-information [Accessed June 9, 2015]

In general, the atlases are characterized by showing pictorial representations of the human body and textual descriptions of the structures depicted. The pictorial representations can be made through drawings and real images involving dissection, which allows viewing the interior of the body, sectional images such as the images taken by CT and MRI and video sequences (Figure 1.12). Lingle (1999), in

reviewing the anatomical atlas of Frank Netter, mentioned its illustrative quality even though there were similar documents, enriched with the addition of information from photography, MRI and CT, exemplifying with the atlases Sobotta et al. (1997) and Abrahams et al. (1998). Using such data would contribute, according to the author, for a better understanding of anatomy, in a clinical perspective, by providing images of greater realism than static illustrations.

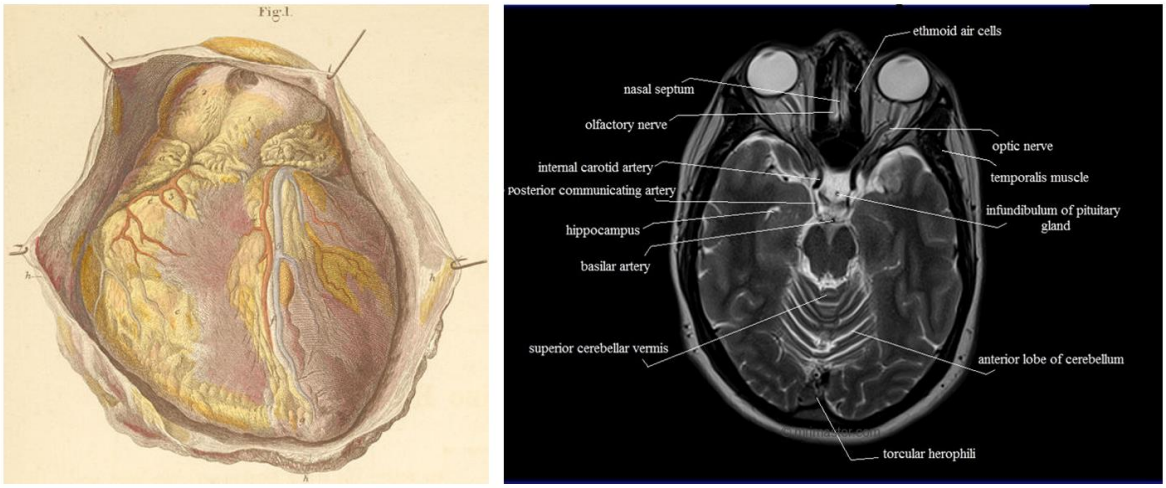

A B

Figure 1.12 - Atlas of Human Anatomy.

(A) The intact heart seen from the anterior surface lying in the opened pericardium.

Source: http://www.anatomyatlases.org/ [Accessed June 9, 2015]

(B) MRI brain cross sectional anatomy.

Source: https://mrimaster.com/anatomy/ [Accessed June 9, 2015]

Presently, the analogic anatomical atlas show a great qualitative evolution with regard to detail, accuracy and visual quality (Agur et al. 2013; Netter 2014; Drake et al. 2014). The advancement of purely analog atlas for 3D digital representations improves educational opportunities and the understanding of human anatomy. Digital systems have as main advantages the possibility to interact with the object represented, the greater realism and detail of anatomical structures, navigation capabilities, including the variation of display scales, and dynamic queries. There are vector systems with these characteristics, including the layer concept and whose geometric component allows a good visualization quality. However, they do not have spatial analysis capabilities based on topology rules. Additionally, they do not allow, in general, the internal representation of the organs.

Currently, the initial tendency to provide 3D digital atlases in optical media has been replaced by providing the same systems through the web (Argosy Publications 2008; Database Center for Life Science 2009; Anatronica 2010; Zygote Body Media 2011; Biodigital Human 2013; Primal Pictures 2014).

1.1.3. Human Body Representation in GIS

According to Bonham-Carter (2014), GIS have as purpose the organization, visualization, spatial query, combination, analysis and prediction, having been provided with tools that allow to perform such functions. In this set of assignments nothing prevents that the information that feeds GIS refers to a broader space than the Earth's surface. Indeed, according to Longley et al. (2005), many of the methods used in GIS are also applicable to other non-geographic spaces, including the surfaces of the cosmos, and the spaces of human body that are captured by medical images. Thus, despite the current 3D systems are developed within specific projects, generally related to the geographic space, its features are a repository of information that can be used in building other systems in other spaces.

The availability of GIS to model the space of the human body is a fundamental aspect of this thesis. Generally, this type of modeling requires 3D GIS developments involving joint representation of the concepts object and field, the development of topological relationships and the creation of functionalities on the 3D models.

Although GIS and systems that represent the human body in 3D models operate with SI, the relationship between GIS and health takes place in a different context. However, the research in this area is substantial, and the importance of GIS in the field of health is recognized (Richardson et al. 2013). The use of GIS occurs in studies where it is necessary to analyze aspects that result of the relationship of certain health issues with the geographic space. One of the health areas with a great deal of research involving GIS is epidemiology. The first study in this area, which involved methods used by current GIS, occurred long before the existence of GIS technology. It is a work done in 1855 to detect the source of a cholera outbreak. In this work, Dr. Snow mapped the spatial pattern of the disease that exposed its origin in a particular pump of a water well (Figure 1.13). According to Ramsay (2006) “He took his findings to the board of governors of the local St. James Parish, and they ordered the removal of the Broad Street pump handle. The epidemic of cholera subsided, but it was already waning. The medical board was not convinced by Snow's evidence, and the pump handle was replaced. For the rest of his life, John Snow continued to argue his theory that ingestion of contaminated water was the cause of cholera. He never succeeded in convincing his peers. It was not until the fourth

cholera outbreak in 1866 that his theory was finally accepted". In Mackenzie (2013), datasets are made available regarding Dr. Snow's map, which can be used to perform a GIS analysis in accordance with the proposed methods and analysis tools such as, for example, the Thiessen polygons.

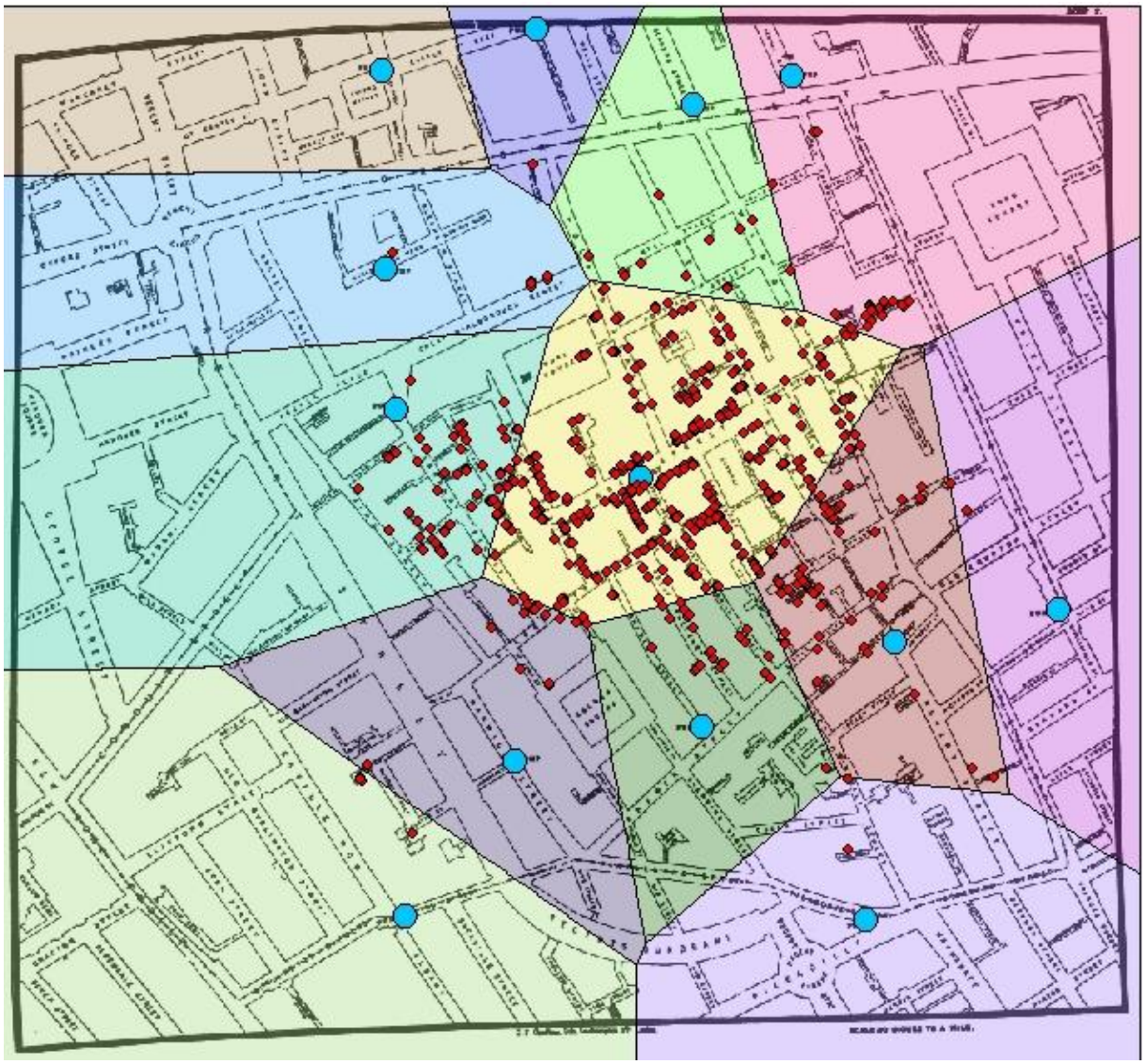

Figure 1.13 – Modern GIS analysis over Dr. Snows cholera map.

Defining zones of cells (Theissen polygons) closest to each water pump.

Source: https://www.udel.edu/johnmack/frec682/cholera/cholera2.html [Accessed June 9, 2015]

Auchincloss et al. (2012) published a study showing a strong growth in spatial epidemiology. In their study, articles published during the decade 2000-2010 in 6 magazines aimed at epidemiologists and one on public health, often read and cited by epidemiologists, were analyzed. The magazines with the

main focus on spatial analysis / health geographics were excluded. The methods of analysis used in the scientific literature were identified as follows: calculations of distances (proximity calculation), estimation of summary measures across pre-specified geographic areas (aggregation methods), assessment of various forms of clustering, spatial smoothing and interpolation methods, and spatial regression.

van Wilgenburg & SPINlab (2013) reported that GIS capabilities facilitate the search for spatial relationships between the physical and social environment and epidemiological factors. These authors highlight data visualization as a positive aspect and mention the costs involving the use of technology, stating that the GIS can be a useful tool in this area.

A large number of maps on various diseases are mentioned by Meade & Emch (2010) which states that "In the GIS era, disease maps often display the results of sophisticated spatial analytical operations performed in a GIS".

The above examples are just a few from the extensive scientific literature that exists on studies linking health areas to GISc. The various international journals whose focus is specifically on the health-geography link is also an indicator of the importance of this association.

Although the approach of GIS to health areas is evident in the context described above, the situation is somewhat different when it moves to the SI regarding the human body. Still, it is not usual to use GIS to make representations of the human body, there have been proposals to develop GIS applications to operate with this type of SI (Suwardhi & Setan 2006; Garb et al. 2007). There are references to the use of GIS as a privileged tool to represent the human body, without this link being effectively implemented. Examples of such approaches are given by Ungar & M'Kirera (2003) which propose the use of GIS techniques to model and study a specific problem of the oral cavity of primates; Rana et al. (2005) presented a model to represent the soft tissues aiming a GIS application for medical purposes; Smith et al. (2005) present the Foundational Model of Anatomy (FMA), a map of the human body which includes a model for relationships between the represented objects whose implementation may occur in a GIS environment. Vongkornvoravej et al. (2006) build a database that receives data from a 3D model based on voxels. Španěl et al. (2007) developed vector segmentation algorithms on the raster component related to the interior of the human body to build 3D vector objects modeling organic structures. This procedure demonstrates also the need of operating with different data models.

In the representations of the human body it is not common to find 3D topological data models specifically designed and tested for the representation of the human body in GIS (Suwardhi & Setan

2006) (Figure 1.14). The implementation of Beylot et al. (1996) is a dynamic model on which was developed explicit topology regarding the links between the anatomical structures that have relative motion. It is a model oriented to dynamic aspects whose topology fits that goal not reproducing the typical forms of topology in GIS.

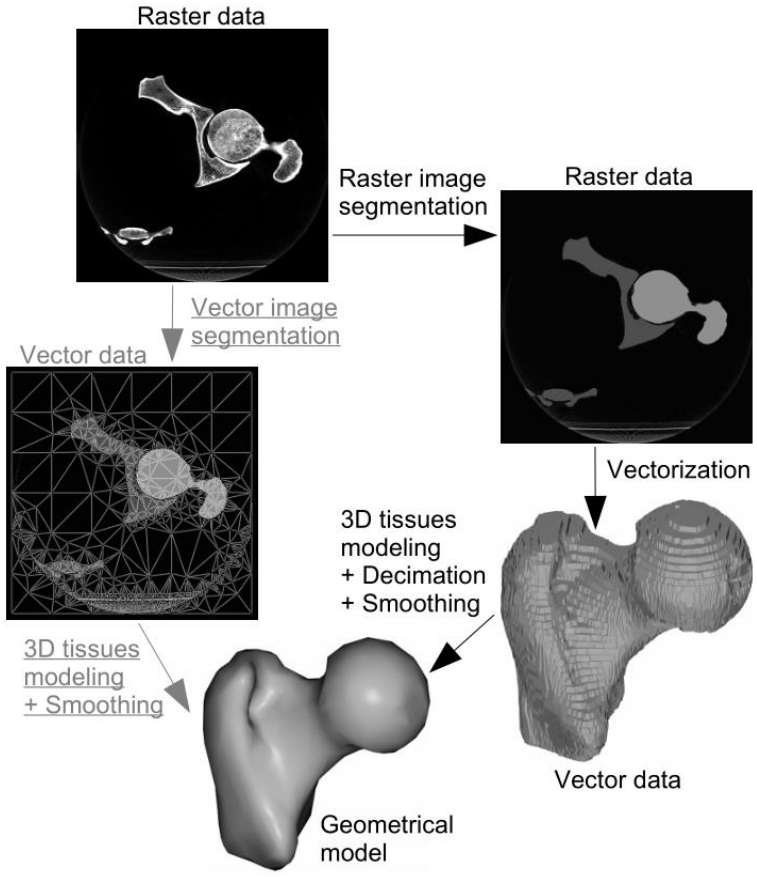

Figure 1.14 – Segmentation and 3D reconstruction of a non-topological model.

Source: Španěl et al. (2007).

Of the various data collection methods in 3D GIS discussed in de By (2004), the use of slices is referred as follows: “the shape of a (sub-)surface object is represented by measuring its shape on a series of regularly spaced planar surfaces that slice through it (…). The associated z-value will correspond to the separation distance between the reference plane and the plane on which the digitized feature has been interpreted”. Transporting this methodology from the geographical space to the space of the human body, we find an interesting indication for data collection to produce a 3D GIS human body

because, on one hand, it is a method identified for collecting data for 3D GIS and, on the other, it uses the same kind of data that are generated by medical imaging techniques.

From the 3D GIS features studied and the system to be developed, whose characteristics must comprise the functionality offered by 3D anatomical atlas and GIS analysis capabilities, the first clues to carry out the GIS-Atlas integration can be found in 3D GIS models that involve both surface and volume representations. This is the case, for example, of the combined representations of objects over the ground (represented by vector surface models) and the geological underground structures (represented by volume models).

Taking as a starting point the integrated models that perform this type of representation as, for example, the model of Wang et al. (2007), the extrapolation to the human body is possible: the surface component would represent the surface, in this case not only the human body but also the various anatomical structures represented, while the volume of component, the GTP structure would be replaced by a geometrical structure more suitable for the representation of the interior of the anatomical structures, since the GTP component is specifically designed to adapt to the geometry of the geological structures.

For GIS-Atlas integration to be advantageous, the conceptualization of an integrated model should take into account the following factors:

- Represent the outer surfaces of anatomical structures;
- Represent the inside of anatomical structures;
- Explicitly define the model's topology;
- Develop functionality;
- Respect the nature of the input data.

The first four points refer to the characteristics of GIS in general and, in particular, of the 3D GIS, which are more directly related to this work. Many of these characteristics, or equivalent, were observed in the studied models. Although they are specifically conceived for applications for which they are designed, certain principles can be used in the reconstruction of a 3D GIS model of the human body, as exemplified with the model of Wang et al. (2007). The last point proves to be very important in this work: the representation of the interior of the anatomical structures must preserve the quality of the

original data, that is, despite the recognized capability of GIS in data conversion between different formats, this type of operation on internal information of the anatomical structures leads to degradation of detail in relation to the original data. This means that, when having a specific format for the input data, it should be part of the model structure without resampling.

According to Goodchild (1992), GIS are sometimes accused of being technology driven, a technology in search of applications. This issue has arisen repeatedly and can be addressed in this work. In this case, it is necessary to verify if the system to be developed is an asset within the anatomical atlases. In this perspective, we will go back to the topic of analytic functions of GIS to determine to what extent they can be used advantageously on a 3D spatial model of the human body.

The measuring tools are usual in GIS. The availability of a 3D spatial model of the human body in a GIS environment could benefit from tools to take measurements of distances, areas and volumes. The distance measurements include simple Cartesian distance between two points and the distance between two points along an element. This second option allows to determine the extent of anatomical structures between two given points. Despite these distance measuring tools are simple to implement, the measurement of distances along an anatomical structure requires a linear, not physical, component that simulates the central axis of this structure. If, moreover, the structure is branched, as in the case of blood vessels, a topological network structure should be built. In this case, the determination of the distance between two points along an anatomical structure consists in solving a problem of network analysis, i.e., the determination of an optimal path between two points.

The layers of information are a concept usually implemented in GIS. If the 3D model of the human body has the geometric components structured in independent layers of information, it is possible to differentiate them and to develop tools to measure areas and volumes. In reality, the surface areas and volumes, being characteristics of these structures, can be determined in the model reconstruction phase and included in the model structure itself.

The interactive queries can be made on the geometric component or on attribute tables. In the first case, structures interacting directly with them are selected and, in the second, records in the table may be selected by identifying, for example, the name of the selected structures. In all cases, the selections are made simultaneously on the geometric component and in the attribute table.

The queries of type "select by attributes" allow to build SQL expressions involving alphanumeric information. The expressions are built by the system after the selection options have been determined by the user in a GUI. An example of such a query is, for example, the determination of all muscles with a volume less than a predetermined value. The queries of type "select by location" use topological

properties to implement the selections: unlike attribute queries that select through a built condition on an alphanumeric value, or a logical combination of attributes, the location-based queries run through spatial criteria, for example, selecting all the objects found within a given distance of the heart.

The classification methods may be used to communicate specific aspects of the data. In the case of a human body GIS, a possible reclassification can be done on a sectional CT, MRI or RGB image, in order to identify all the anatomical structures present, for example, by a color code which will be captioned with the names of the corresponding structures. This type of operation allows to simulate the information contained in a sectional anatomical atlas of the human body (Dixon et al. 2015). Unlike atlases that use a fixed number of images, GIS enables to make this kind of dynamic classification on all images available on the model and on images with other orientations set by the user, obtained by 3D interpolation.

Following the previous example, overlay operations could be used with segmented images defining, interactively, variable degrees of transparency. Thus, it is possible to identify the structures directly on the data. In certain types of applications, databases containing considered healthy structures can be used and overlaid with other images for automatic detection of anomalies.

The neighborhood and network topologies can support some analyzes, for example, in the case of proximity analysis and measurement of lengths along a structure, which have been described.

The example of a 3D spatial analysis problem, which extends the functionality of 2D GIS is the inclusion analysis. In 2D, the point-in-polygon algorithms are used to determine whether a point is inside a polygon. In the 3D space, these become point-in-polyhedron algorithms. This type of analysis can be used, for example, to determine the anatomical structures crossed by a needle inserted at a point of the body with a certain orientation and depth.

GIS, besides providing models of the human body, include tools that allow a detailed and interactive exploration. The fact that they integrate a large number of analysis functions in the same platform constitutes, by itself, an additional advantage compared to the traditional approach of the anatomical atlases.

During this thesis various academic search engines were used to search works related to the study topic. An initial search with an extended search engine, such as Google Scholar, allows to find references on the Internet that are not linked to specific databases. To verify the existence of scientific papers in the area of this thesis, research with two different sets of search keys were carried out: the first set, which used the keys “3D”, “GIS” and “Human Body”, more linked to the theme, and the second with more general keys, “GIS” and “Anatomical Atlas”. The research was subject to the ten most

relevant papers, according to search engine criteria, published in the last five years. Thus, the top twenty links generated in the set of the two surveys were recorded. Of these, only four were clearly related to the development of a human body model by representing anatomical structures. For the first data set, the links found in the study were: An Integrated Model of the Human Body (Barbeito et al. 2014) and Medical information service system based on human 3D anatomical model (Kim & Chung 2013).

For the second set of keys the following results were found: An Integrated Model of the Human Body (Barbeito et al. 2014), Human body modeling in geographic information systems (Barbeito et al. 2011) and Development of anatomical and radiological digital brain maps (Juanes et al. 2012). The first work, which comes in both surveys, corresponds to an article published in the context of the present thesis. The second work of the first search is an information system about anatomical structures, including a 3D model of the human body. This system does not have GIS analysis functions type nor is developed according to this perspective. The second work of the second search is a preliminary study that presents a surface vector model with an analytic point-in-polyhedron function included and was developed by the 3 first authors of the first paper found in the 2 surveys.

Finally, the last work of the second search falls within the scope of this thesis. It is a system that represents the brain structures based on the VHP data and built in Geomedia GIS software. It includes geovisualization, identification and analysis functions. The visualization of the 3D structures is made via the simultaneous representation of transverse, sagittal and coronal planes (Figure 1.15). Thus, the system does not present a truly 3D GIS model. The results of this specific research, according to the established criteria, do not claim to be exhaustive. Still, they seem to confirm, to a first approximation obtained with a broad spectrum search engine, that the scientific literature on GIS-Atlases is not very wide, which has been confirmed throughout this thesis.

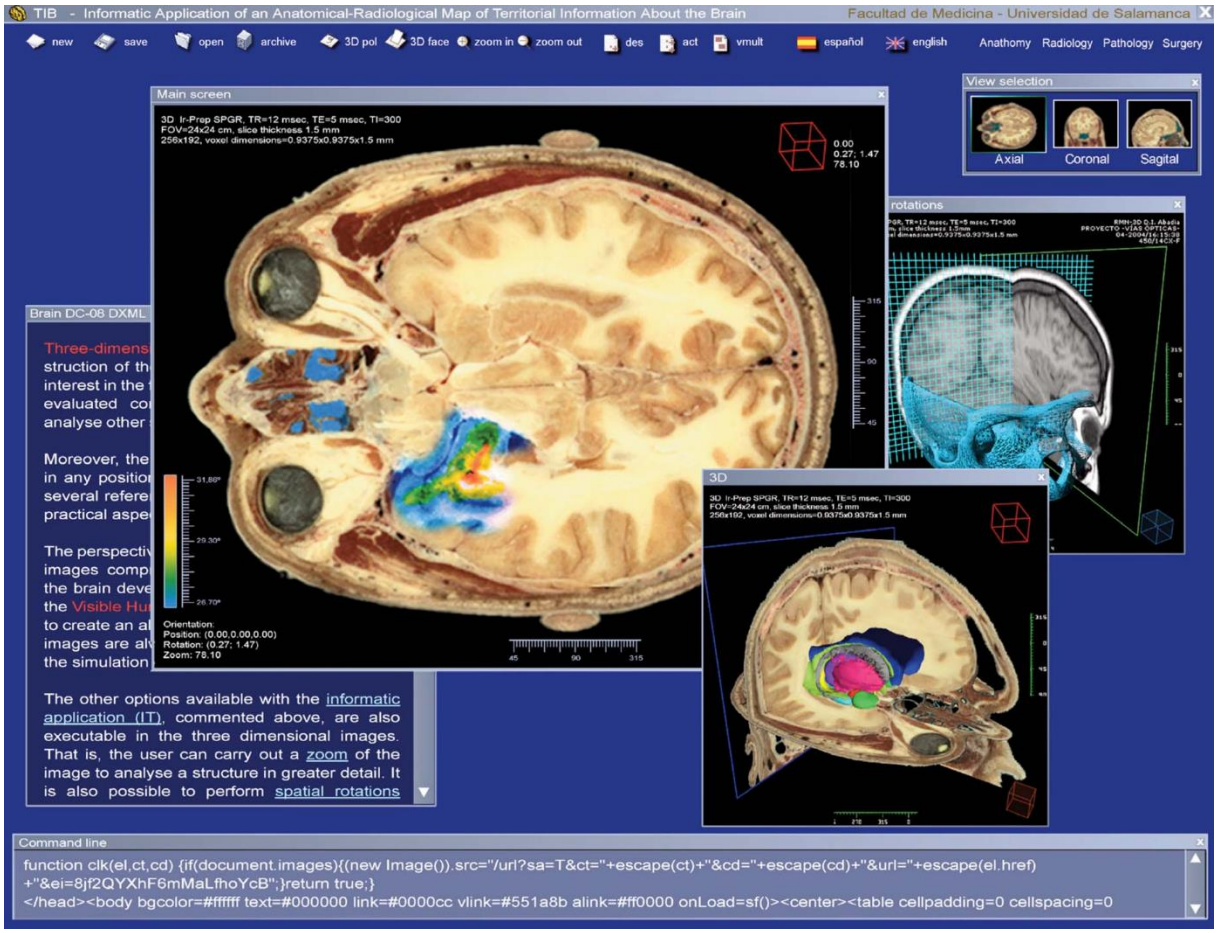

Figure 1.15 – 3D brain model.

Source: Juanes et al. (2012).

1.1.4. Segmentation

The statement that there are no universal GIS 3d models stems from the link between these models and the applications in which they are used. However, the features of the models are also related to the data from which they are constructed. The integrated model developed by Wang et al. (2006) exemplifies this situation: the GTP structure was built to fit the geometric characteristics of the geological structures under the surface.

The construction of human body 3D models, representing the interior and the surface, requires adequate data that can shape the model itself. Currently, medical imaging provides this type of data. The use of sectional images of the human body to reconstruct 3D models involves two steps: (i) The segmentation of the human body and the internal anatomical structures and (ii) the 3D reconstruction based on the data generated in the previous step.

Since the appearance of the Visible Human projects - VHP, VCH and VKH- different approaches have been used in the segmentation of anatomical structures on axial images (Figure 1.16). Leaving aside purely manual operations, the segmentation methods can be classified as semi-automatic or automatic. As semi-automatic methods (Imelińska et al. 2000; Beveridge et al. 2013) require the intervention of an operator, the high volume and complexity of data justify the research works that propose automatic segmentation methods (Li et al. 2014; Xue et al. 2014). However, errors are inherent to segmentation procedures. For example, the algorithm presented by Xue et al. (2014), leads to an overall accuracy of 98.8% CT imaging and 99% for cryosection images. According to Wu et al. (2012), after the primary segmentation, the main errors that are produced include the segmentation error and the segmentation missing. Intra-observer variation between experts is also referred. Thus the complexity and the inevitability of errors in segmentation procedures are clear. Several studies show that automatic procedures cannot be considered when the segmentation needs a high level of detail and non-ambiguity (Schiemann et al. 1997; Beylot et al. 1996; Riemer et al. 2007).

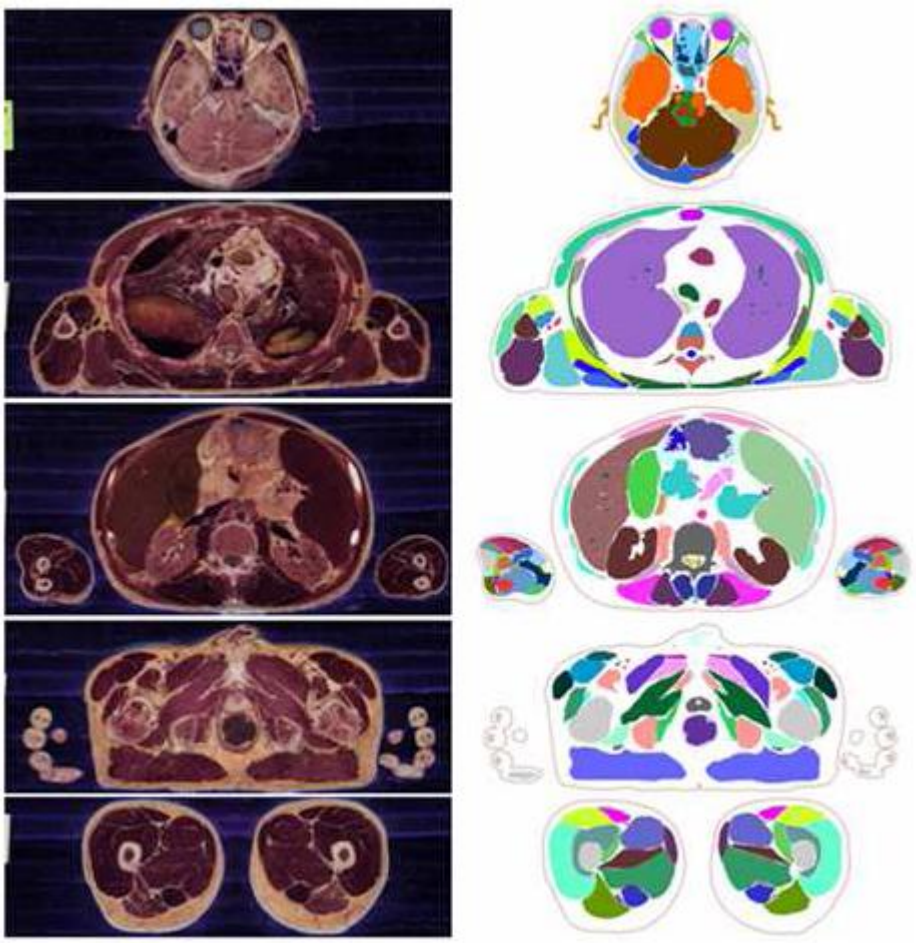

Figure 1.16 – Anatomical structures segmentation.

Source: http://molmed.ajou.ac.kr/faculty/faculty_m14.asp [Accessed June 9, 2015]

The existence of errors, even if they are small, shows that the supervision and human intervention are not negligible. In many cases, the tolerance to segmentation errors can be related to the further use of the obtained results. For example, if the results are used to reconstruct 3D models, a small percentage of wrong pixels outside the segmented structure can lead to a highly deformed anatomical structure. In this particular case, it is absolutely necessary to eliminate such errors. Thus, the necessity to optimize the segmentation methods by minimizing the execution times and controlling the final quality, explains the use of semi-automatic methods. The semi-automatic methods found in literature use the automatic components to facilitate and accelerate the segmentation procedure and the manual intervention to define parameters, correct errors and perform quality control (Schiemann et al. 1997; Takanashi et al. 2002; Imelińska et al. 2000; Beveridge et al. 2013).

Another approach to improve the segmentation quality involves the use of several types of data such as, cryosection images, CT, and MRI: although the segmentation of human body structures with RGB images has been subject of research in several works (Schiemann et al. 1997; Pommert et al. 2001; Flores & Schmitt 2005; Liu et al. 2014), associated with the VHP data, other methods use combinations of different image types, such as cryosection RGB, CT and MRI, included in these projects (Imielinska et al. 2000; Xue et al. 2014). In fact, the joint use of different types of images for segmentation allows to take advantage of each format characteristics and to overcome identified specific limitations. RGB images make available quite realistic information about the visual aspect of anatomical structures and the quantity of stored information, higher than CT and MRI (Takanashi et al. 2002), enable a greater level of discrimination among these structures. However, RGB images present drawbacks as, for example, when it comes to delineate bones in the presence of articulations or tendons. In these cases, CT images are more efficient (Beylot et al. 1996).

1.1.5. 3D Reconstruction

Tao (2004) distinguishes three data acquisition methods in order to reconstruct 3D objects: (i) image-based methods, (ii) map-based methods and (iii) point-clouds-based methods (Figure 1.17). Image-based methods use stereoscopic properties of images allowing to reproduce the desired 3D information. These methods are usually employed in classical photogrammetric surveys to model the terrain, the buildings and other objects on the Earth surface. (Starbuck et al. 2014).

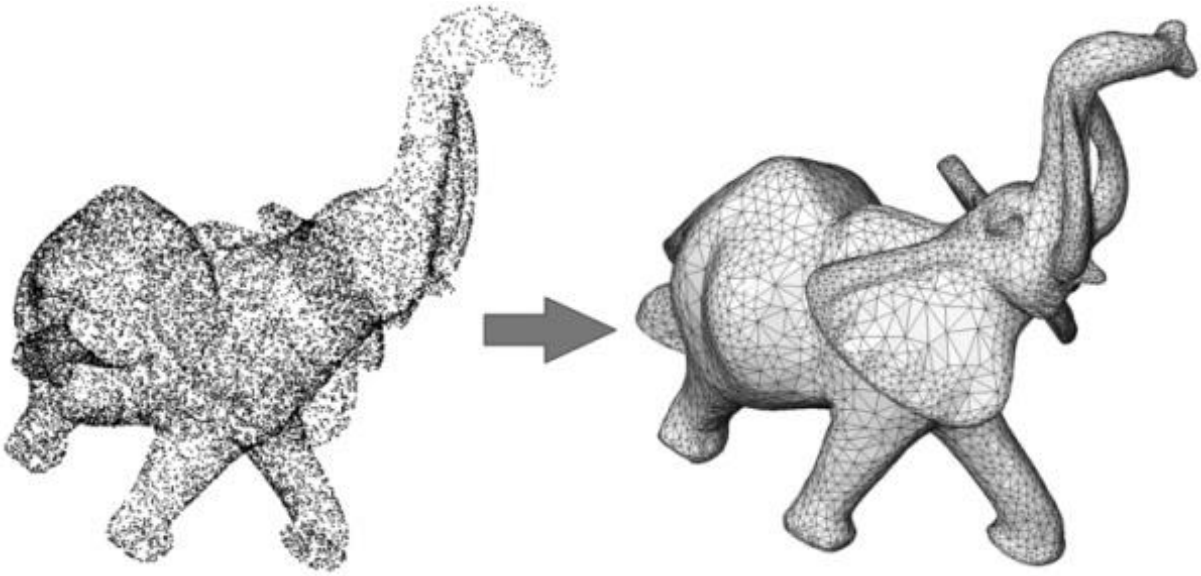

Figure 1.17 - Poisson surface reconstruction from a point-cloud.

Source: http://doc.cgal.org/latest/Surface_reconstruction_points_3/ [Accessed June 9, 2015]

The map based approach uses maps (e.g., 2D GIS maps) and knowledge about the imaging geometry and acquisition parameters, which allows to reduce the complexity of the 3D building reconstruction process (Suveg & Vosselman 2000).

Aggarwal & Xia (2014) state that "Acquiring 3D data from depth sensors is more convenient than estimating it from stereo images or using motion capture systems". Methods using active sensors, for example laser scanning, generate point clouds. These point clouds contain 3D coordinates of points from the object surface. The joint use of sensors and images of the objects allows to texturize the surface of the model with a realistic appearance.

According to Berger et al. (2014) "As the diversity, ease of use, and popularity of 3D acquisition methods continues to increase, so does the need for the development of new surface reconstruction techniques", however, "Acquisition methods tend to produce point clouds containing a variety of properties and imperfections that pose significant challenges for surface reconstruction methods". As the point clouds do not define unique surfaces, the actual algorithms must also deal with its interpretation in order to reproduce adequate surfaces. Berger et al. (2014) identify more than 30 methods, classified in 7 categories, to reconstruct 3D surfaces from point clouds. According to this author, the surface reconstruction problem deals with increasingly sophisticated solvers or richer reconstruction hints that make the problem easier to solve: the availability of oriented normals, for example, complementing the point cloud data, requires only a linear solve through the Poisson

reconstruction approach (Kazhdan & Hoppe 2013), while unoriented normals require solving for a generalized eigenvalue problem (Alliez et al. 2007).

Current surface reconstruction algorithms are tailored to deal with identified characteristics of point clouds, namely, sampling density, noise, outliers, misalignment, and missing data. Different methods treat these features differently. Although it may not be easy to decide if a method is clearly superior to the others, favorable results can be identified for each of these features. Thus, choosing a reconstruction methodology shall take into account the characteristics of the input data – the point cloud – and the geometric characteristics of the objects to be reconstructed. Issues such as execution times and the complexity of the algorithms can also be taken into account.

1.2. OBJECTIVES AND WORKING ASSUMPTIONS

The main objective of this thesis is to create a 3D anatomical atlas in a GIS environment. This objective requires the creation and integration of three distinct components:

- 3D topological model of the human body;
- GUI to allow user access to the model;
- Functions implemented in the interface for exploring the model.

These three points highlight the creation of an application to interact with a 3D representation of the human body. In detailing each of the points, we find the characteristics related to the intended GIS approach.

The model to be developed must have geometric characteristics allowing to represent the entire human body. This means that, in addition to the morphological representation of anatomical structures, i.e., the representation of its outer surface, the model should contain information about the interior of these structures and allow its visualization.

The first point refers to the development of a topological model. This goal follows a typical GIS approach that usually presents models with topological characteristics. One of the advantages of incorporating topology in the models is to facilitate the development of spatial analysis functions which contribute to enhance the system capacity.

The design of the GUI must also include GIS features: indeed, it is intended to obtain an interface where the information, organized in layers, can be managed by a table of contents (TOC), beside which shall be presented the geometric component of the model.

Regarding the functions to implement in the system, which can be accessed through the interface and allow to operate on the model, they have as main objective to extract as much information as possible from the model. To achieve this goal, it is not necessary to think first about the functions of GIS and transport them to the system to be developed. In fact, first we looked to the anatomical atlases to find what kind of information they provide. The first functions were built using this perspective. After replicating the level of information provided by the anatomical atlases, we checked for the GIS functions which could expand the system's capabilities constituting thus a real added value. The set of functions that should incorporate the GUI in the GIS prototype, analyzed in the anatomical atlases and GIS, were defined as the following:

- Navigation;
- Visualization of the interior and exterior of the model;
- Information management through layers;
- Identification;
- Measurement of distances, lengths along anatomical structures (which requires a network/connectivity topology), areas and volumes;
- Neighborhood spatial analysis;
- Inclusion analysis (e.g., simulation of inserting needles into the human body)

The objectives put forward in this thesis assume a set of assumptions that must be demonstrated during this study.

The first question has to do with the feasibility of developing such a system, that is, we should check if it is possible to develop a spatial model of the human body in the desired conditions, include it in a GUI and assess the required degree of functionality. There are several problems involved in this question, such as, which 3D GIS model to represent the human body: vector (3DFDS, TEN), raster, or integrated? The proposal of a 3D model should arise in the current context of GIS: a broadly developed technology in the 2D version but that remains at the expense of prototypes specifically developed for

3D applications. The fact that there are several 3D models that are suited to specific problems, but they are not suitable for a wider use, requires the consideration of a specific solution to be studied, that may be based on the features of existing models.

Initially, the possibilities of using a raster or a vector model should be considered. Given that the representation of volume is desired, the vector surface models can be discarded, leaving the decision between a raster and a TEN model. Since topology is also a requirement, the raster approach presents difficulties. The use of a TEN model, according to the data available, requires its resampling, which necessarily results into a poorer information input, even before the model is used. Besides the option of choosing only a vector or raster model, there is still the possibility of considering an integrated model. The development of an integrated vector-raster model could be justified by the following aspects: (i) the volume component (raster or TEN) allows to make the representation of a continuous space, which fits the inside of the anatomical structures. The choice between the raster or TEN approach should take into account the intrinsic characteristics of the two representations, for example, topological features and the nature of the data (raster type); (ii) the use of a vector surface component to define the anatomical structures is, on the one hand, suitable to the development of topology while, on the other, it allows to load the GUI of the system with only vector information without volume data, much lighter than 3D voxel matrices. Thus, the interface would receive raster information only when and where is visualized the inside of anatomical structures.

The answer to the question of the viability of the model was found as the work progressed by studying the literature on the development of GIS to model 3D spaces and after the first experiences with models that have been modified and improved until a stable model was reached that took into account its intended purpose and, largely, the type of data used.

A second issue had to do with the opportunity, that is, is it useful and advantageous to undertake such work knowing beforehand, for example, that there are other systems specifically designed to study the human anatomy? To answer this question it is necessary to situate it in the proper context in which it is intended that the prototype should emulate specifically a 3D anatomical atlas, maximizing the levels of interactivity and functionality. Thus, from the perspective of anatomical atlases, it should be verified if the final prototype meets the requirements of such representations and, in addition, if the taken approach contributes with added-value.

The simple construction of anatomical atlases in a GIS environment would not provide a clear advantage over the representations currently provided by digital atlases, given its ascertained visual quality, the extent of databases and, thus, the study possibilities associated with such systems. In addition, the inclusion of artistic components in analogical representations that enable,

simultaneously, a very informative overview of the various anatomical structures, is difficult to translate into a GIS. There are, however, some typical characteristics of GIS, which could be an asset when it comes to modeling, analyses and study the human body:

- Ability to interact, navigate, visualize and query the model;
- Ability to integrate data from different sources. If, in the first generations, this integration was not a trivial matter, it is currently possible to combine raster and vector data and carry out mutual conversions. Thus, a GIS can import data from different sources and integrate them in the same environment of representation and analysis;
- Possibility of analysis arising from the existence of topological data models. Current anatomical atlases allow to extract information through database query but, contrary to GIS, have difficulties in producing new information from criteria based on spatial relationships;
- Possibility to develop applications for various specific purposes in the same environment from the available set of spatial data.

The above points let foresee that a 3D GIS equipped with a 3D topological data model, specifically suited to modeling the human body allows, effectively, to take advantage of features that enhance the analysis capabilities of the anatomic structures. To do this, it is necessary to develop a prototype which implements the required functionalities.

While the first assumption is achieved with the completion of this work, the second should be verified by carrying out tests on the final prototype to assess the degree of usability, functionality and accuracy of the final system.

The possible demonstration of the premises of this work does not prevent to question beyond the initial goals. Therefore, it is valid to question whether such models can be applied in a wider context than the constitution of anatomical atlas with a pre-established model. Indeed, if the opportunity of the model is validated, it would be interesting to question its expansion and application into other contexts, such as, (i) its composition and use with real time data, (ii) its use not only as a source for collecting information but as simulator of medical interventions, (iii) its use with the development of dynamic capabilities, including the observation of the internal anatomical structures in motion situations defined by the user or in the functioning of the human body and its systems. Although there are apparently numerous possibilities for such systems, the study elaborated along this thesis was

focused on the implementation of a 3D anatomical atlas from a GIS approach that allow to confirm the feasibility and opportunity premises.

1.3. THESIS ORGANIZATION

This thesis consists of six chapters: Introduction (the present chapter), Data and methods, Results, Discussion, Conclusions and References. The content of these chapters follows the course of the research that has elapsed since the proposal of an initial model to the final prototype, which includes a 3D topological model, the GUI and the GIS functions.

The Data and methods chapter present the input data and the methodologies involved in the study. After describing the characteristics of the input images obtained from VHP, the conceptual model, that is intended to meet the requirements defined in the study, is presented. The first operational task is to segment the human body, i.e., extract it from the surrounding area that is composed of a blue gel. The segmentation process follows with the focus on the anatomical structures. Here, a semi-automated method is presented. This method works first with the RGB images and, in certain circumstances, the CT images are also used. The final step consists of an interactive procedure that allows to integrate the results of the segmentations performed in the RGB and CT images.

After the segmentation step, 3D reconstruction methods are tested in order to obtain a 3D surface model of the human body. After choosing a particular algorithm the resulting surface model was validated. The reconstruction method is then applied to the various segmented anatomical structures.

In this stage, the geometric components of the model are constituted by the voxels and the surface vector. A methodology for the development of the last geometric component of the model is then presented. This component consists of an axial structure that evolves along the central axis of the anatomical structures that have linear characteristics and, on which, length measurements can be performed.

With all geometric components of the model presented, the topological relationships contained in the model are described along with the procedures to implement them in the model structure.

The last development on the model relates to its dimensions. Once it is intended to perform measurements on the model, a system of real coordinates is defined.

After the presentation of the methodologies used in the model building, the GUI and the functions embedded become the focus of this chapter. Thus, the hierarchical classification method used to implement the multilayer management system in the TOC is described.

A first function of the prototype that consists in exploring directly the input data is presented. The geovisualization is another relevant issue concerning the presentation of the information given that GIS must produce maps to communicate specific messages. Thus, several geovisualization possibilities are presented allowing to show different perspectives for the included information.

Several identification functions are also proposed to read information about selected structures and to link them with documents or web pages.

The development of the measurement functions is described as well as the link between the length measurement along an anatomical structure and the connectivity topology.

The description of the methods ends with the analysis functions, namely, the inclusion analysis, based on the containment topology, and the neighborhood analysis, based on the same type of topology.

The Results chapter presents all the results that are obtained throughout the study. Intermediate results, tests that justify certain options and final results are presented. All the topics included in this chapter are considered and discussed in the Discussion chapter. The Conclusions chapter gathers all the produced material in order to end the study with a global view on the several tasks that constitute the thesis.

Finally, the last chapter of the thesis lists the references on which the study is based.

2. DATA AND METHODS

2.1. DATA

The development of a 3D model can be based on a virtual reconstruction or use real data. In the latter case, the reconstruction of a model containing information about the interior of the human body, requires data collection techniques beyond the scanning of the external surface. The model presented in this study was based in real data that depicts the internal anatomical structures. These internal data were created under the VHP.

The VHP is conducted by the U.S. NLM and implemented at the University of Colorado's Health Sciences Center. It contains sequences of digital images of human bodies (male and female) obtained through MRI, CT, and anatomic cryosection imaging in true color, RGB bands. The MRI data of the male consists of axial images of the head and neck at intervals of 4 mm, and longitudinal sections of the remaining body, also at intervals of 4 mm. The resolution is 256x256 pixels, each pixel 12-bit grayscale. The CT data are formed by axial images of the whole body at intervals of 1 mm and 512x512 pixels, each pixel 12-bit grayscale. The axial cryosection images have intervals of 1 mm, 2048x1216 pixels, each pixel with 0.33mm and 24-bit color. The planes of the anatomical images and of the CT images are coincident. There are 1871 sections for each of these modes. Later on, the film of the anatomical images was scanned with a resolution of 4069x2700 pixels and 24 bit color depth (Spitzer et al. 1996).

The direct reconstruction of a 3D model from this type of data consists of repositioning the transverse planes formed by the input images along the vertical Z axis. In this case, non-cubic voxels are built since the spacing between consecutive planes is different from the linear dimensions of the pixels in the images.

Data from female have the same characteristics, with the only difference that the axial planes are distant from 0.33mm. This difference makes the model to consist of 5000 axial images allowing to build a 3D model with cubic voxels.

The data used in this study are a subset of the data from the VHP, namely 1871 cryosections axial images of the male, representing the entire human body, and the corresponding CT images (Figure 2.1).

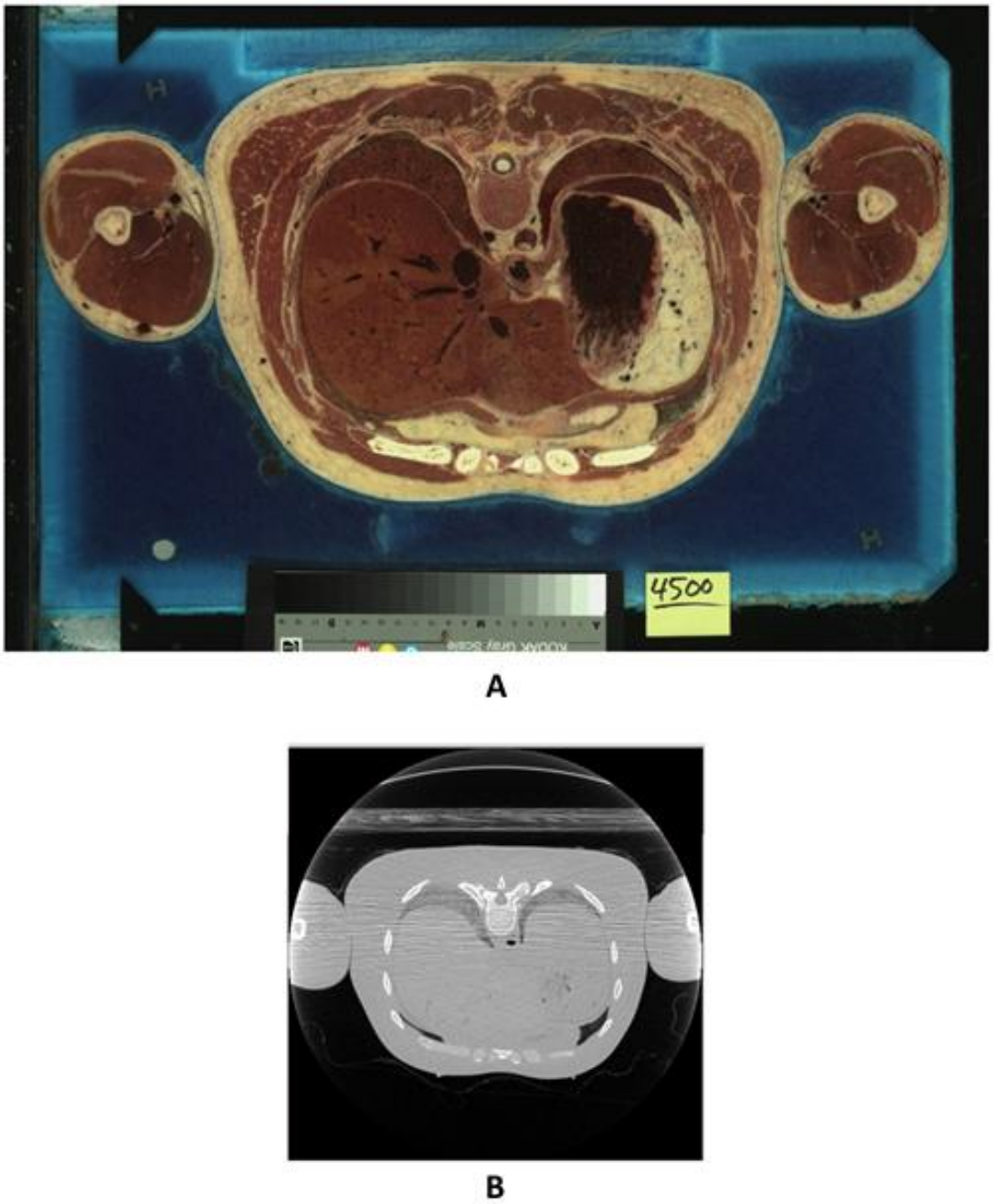

Figure 2.1 - Data from the VHP.

(A) Cryosection anatomical RGB image. (B) CT image.

2.2. CONCEPTUAL MODEL

The conceptualization of a human body model according to the defined objectives shall take into account the nature of the input data. In the context of the present work, the model building process will use the VHP input images without degrading their original quality. The images will be used to represent and visualize the internal anatomical structures and also to build the vector surface

components. The requirements proposed for the model in the section 1.1.3 will guide the construction of the conceptual model:

- Represent the outer surfaces of anatomical structures;
- Represent the inside of anatomical structures;
- Explicitly define the model's topology;
- Develop functionality;
- Respect the nature of the input data.

The first point of the requirements list states that the surfaces encompassing the anatomical structures should be based on surface models. Furthermore, they are external surfaces that shall establish topological relations between neighboring objects. These two aspects highlight the choice of a surface vector model to represent the boundaries of anatomical structures, including the surface of the human body itself. The choice of a surface vector model can be based on TIN models. Instead of using triangle meshes, surfaces may use other geometric shapes that could be better adapted to different representations. However, such solution would lead to increased complexity in terms of model structure and its manipulation. For these reasons, a TIN model adapted to the representation of closed surfaces was chosen (Barbeito et al. 2014).

The representation of the interior of the human body should be based on appropriate volume models to show the spatial evolution of anatomical structures. In this case, the choice would fall on 3D raster models, formed by voxels, or TEN vector models, formed by tetrahedra meshes. From the topological point of view, TEN vector models are preferable, however, data quality preservation is best achieved with 3D raster models in case the data is also in raster format. Effectively, the use of a TEN model involves the resampling of a regular grid to feed the tetrahedra centroids. The interpolation procedure used in this resampling necessarily leads to a degradation of the input data. This factor, associated with the fact that the construction of topological relations can be left to the surface vector component, led to the direct use of the raster structure to represent the internal volume of the model.

The use of two different types of structures involves the construction of an integrated model. Thus, the connection between raster and vector components must also be defined. The conceptual model to be developed is directed to the representation of the anatomical structures, whose surfaces are defined by a vector model, whereby, the vector-raster connection must be implemented at the level

of these structures. To do so, the model should contain a structure that associates the voxel matrix to the vector surface for each segmented anatomical structure. This structure was defined with a 3D matrix that reproduces, for each voxel corresponding to the input data, a unique identifier for each anatomical structure, which, in turn, is associated with the respective vector surface component. This structure, referred to as Layer Matrix (LM) has the same dimension as the matrix of input data apart from the dimensionality of the RGB bands. These options allow defining the first three model structures:

- 3D imagery: 3D matrix of voxels that contain the RGB intensity values of the pixels on the original images. Each voxel has 0.33 mm along the horizontal axes (pixel dimensions on the original images) and 1 mm along the vertical axis (distance between two successive images);
- 3D LM: 3D matrix were the voxels assume the unique identifier (ID) values corresponding to the respective anatomical structures;
- Surface Vector Model: the surface of the anatomical structures formed by triangles.

The construction of these three objects is based on five main functions (Figure 2.2):

- $(x,y)_{binary} = F_1(x,y)_{RGB}$: Converts each original image into a 2D binary mask;
- $(x,y,z)_{binary} = F_2(x,y)_{binary}$: Aggregates the binary masks constituting the LM;
- $(x,y,z)_{vector} = F_3(x,y,z)_{binary}$: Performs a 3D raster-vector conversion;
- $(x,y,z)_{RGB} = F_4(x,y)_{RGB}$: Aggregates the original images in 3D voxel matrices;
- $(x,y,z)_{binary}^{vector} = F_5((x,y,z)_{vector},(x,y,z)_{binary})$: Aggregates the raster and vector domains composing an integrated volume model.

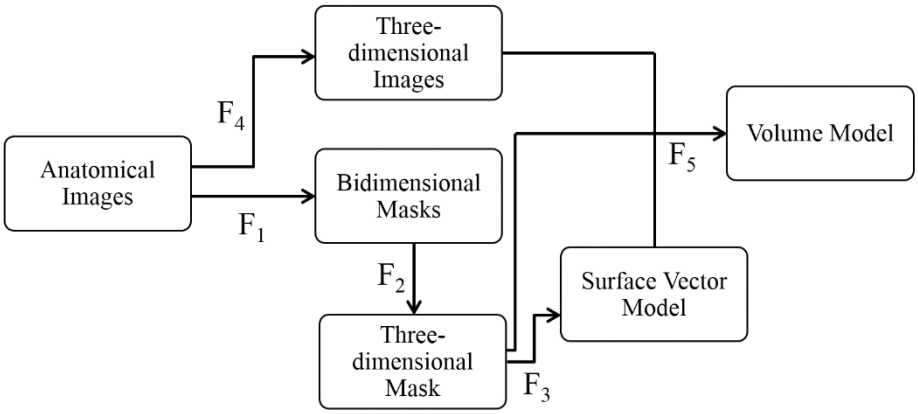

Figure 2.2 - Functions used in the volume model building.

The defined components can be used to define containment and neighborhood topology. On the one hand, the vector surface component can be used to introduce topological neighborhood relations and, on the other hand, the LM matrix contains itself topological containment information. Although the information in the LM is not identical to the explicit containment relations between model objects, as defined in GIS, they can be used to perform inclusion analysis or to develop these relations explicitly. From a GIS point of view, the model lacks a structure that contains connectivity topology. Beyond the GIS perspective, it must be determined whether this type of topology is necessary for the model. The answer to this question can be found with the development of a type of measurement tools. As mentioned, the prototype should contain several measuring tools, including the measurement of lengths along an anatomical structure. However, this type of measure cannot be achieved by simply measuring the Euclidean distance between two points. To perform this type of measure, the model should be complemented with additional components.

Traditionally, GIS models contain the central axis of the roads and topological tables with the respective graphs and traveling costs. The measures are carried out by using these components and an algorithm that calculates the traveling cost between 2 points on a branched network (Kennedy et al. 2013). The travel cost can be measured in time or distance units. This problem, well known in GIS, allows to determine the shortest path between the two points. Thus, the implementation of this approach to a model of the human body, involves the creation of (i) central axes for the anatomical structures, (ii) topological tables of arc-node type and (iii) shortest path algorithms for measuring distances in branched linear structures. This means that, in addition to the previously defined geometric components, the model should include this new geometric structure and the respective topological table.

Beyond the geometric components and the structure that connects them, the model should also record alphanumeric information, which will contribute to the desired functionality (Figure 2.3):

- Attribute tables associate alphanumeric information with anatomical structures, namely, designation, descriptive information and links to documents or web pages;
- Color tables allow to operate with the model in three different modes by selecting (i) simulated color for groups of structures, (ii) segmentation color for each structure and (iii) true color from the RGB input images;
- Neighborhood tables allow to determine the neighboring structures of a predetermined structure (or part of it);
- Arc-node tables contain graphs of the central axes of anatomical structures in which it is possible to make length measurements. They provide connectivity topology to the model.

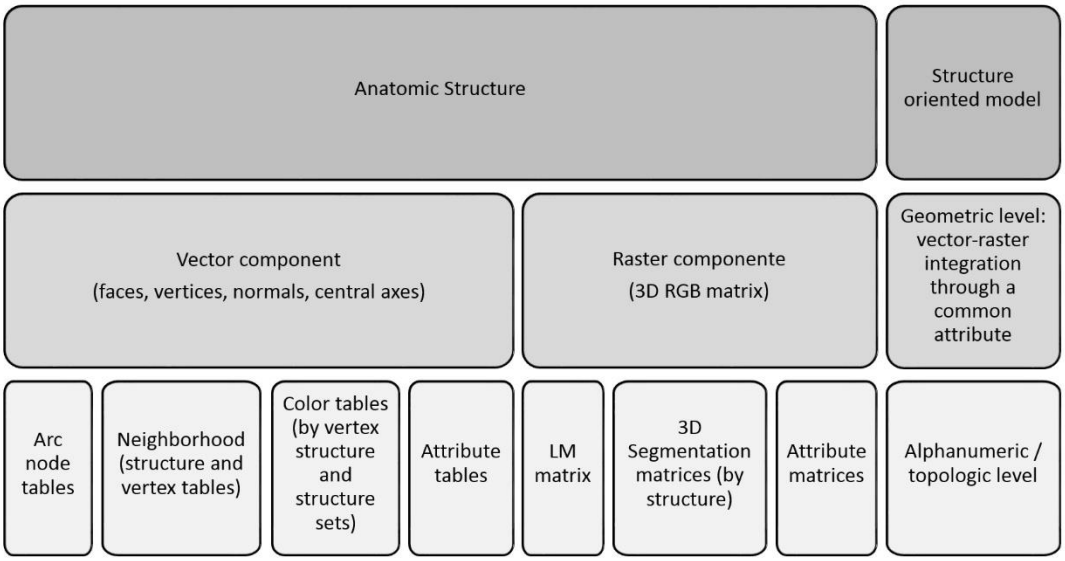

Figure 2.3 – Model components.

The flow diagram in Figure 2.4 provides an overview of the sequence of procedures that allow to obtain the final model from the data. The descriptions in the following sections refer to each of these processes.

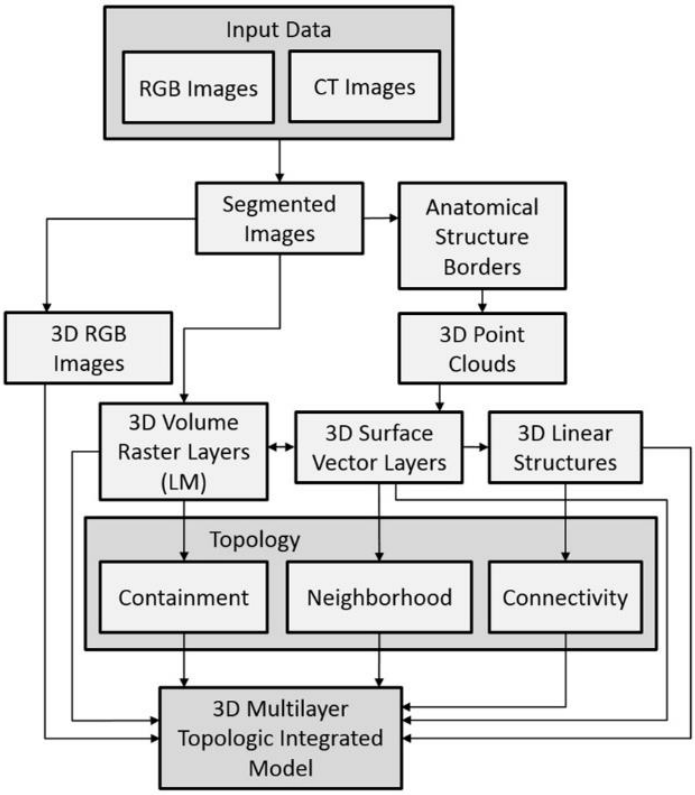

Figure 2.4 - Flow chart of the conceptual model.

2.3. HUMAN BODY SEGMENTATION

The segmentation process is crucial for the reconstruction of the 3D model, being particularly involved in providing information to implement the surface vector component.

The segmentation procedures of the anatomical structures and the model itself have common features. However, the latter is simpler given the RGB characteristics of the surrounding gel. Effectively, the use of a blue gel facilitates the segmentation procedure since it provides a high degree of contrast with the body region. The main difficulties in this procedure are caused by some characteristics of the input data, namely, the occurrence of noise (e.g., invasion of the body by blue gel), the existence of some planes without information (black images) and the displacement of some images in the XY plane (Chang 1996) (Figure 2.5). This factor, though not impeding each of the segmentations, prevents the correct 3D reconstruction since the segmented areas are moved from the correct position. To correct this deviation a preprocessing phase was implemented. This correction takes place by adjusting the fiducial marks contained in the images.

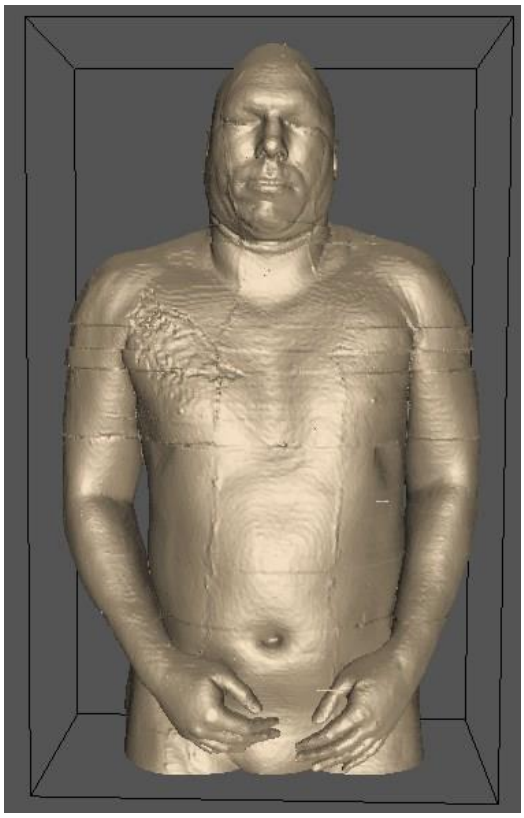

Figure 2.5 – Reconstruction of the VHP model.

The horizontal displacements caused by the data can be observed around the arms and chest.

Source: http://www.cs.carleton.edu/cs_comps/0405/shape/ [Accessed June 2, 2015]

The body segmentation is the first step of the process that culminates with the 3D reconstruction of the surface. This procedure uses only the RGB images since their characteristics were found to be sufficient to achieve the desired results. The first analysis is to separately evaluate the intensities of each color. In case there are distinct intensity intervals, inside and outside, the segmentation procedure can be performed simply by applying a threshold whose value lies between the two intensity ranges. Since it is important to define as accurately as possible the peripheral area of the body, it may be advantageous to define the threshold value in the range corresponding to the intensities within the body. This approach can, on the one hand, create gaps inside the body but, on the other hand, may define more precisely the edge of the body and minimize the occurrence of noise in this region and in the outside. Furthermore, the inner gaps are easily filled.

Another feature that can be investigated in the study of RGB intensities is the ratio between different colors. The inversion of R-G or R-B pairs in the interior and exterior regions could be used in the segmentation. It is expected that the pair R-B presents a higher degree of discrimination due the color

of the surrounding gel. The choice of the segmentation technique can be based in this relation or in the application of a threshold value or in a combination of the two, depending on the image characteristics, which includes the occurrence of noise.

The occurrence of persistent noise after the segmentation will be treated with appropriate filtering techniques. Some of the additional adjustments made to deal with specific errors or noise in input data include: (i) eliminating noise (spots / islands) outside the body area; (ii) filling holes inside the body; (iii) applying morphological close operations (a dilation followed by an erosion); (iv) smoothing the external border of the body (Table 2.1)

Operation	Cases in which the operation can be applied
Rule: R > FACTOR * B	Almost all images
Threshold	Several images, e.g., invasion of the blue gel over the image
Delete islands	All images
Fill holes	All images
Morphological close	Small gaps in the borders
Smoothing borders	All images

Table 2.1 - Operations used in the segmentation procedure.

2.4. ANATOMICAL STRUCTURES SEGMENTATION WITH RGB IMAGES

The segmentation of the internal structures is more complex than the segmentation of the body. To make these segmentations two approaches were used involving, respectively, the cryosection and the CT images. This section addresses the methodology used in the segmentation of RGB images.

The segmentation of RGB images relies on a semi-automatic procedure. In this method, the automatic component allows accelerating the segmentation while the manual component is targeted at correcting the segmentation errors and to control its quality.

The input images, which represent horizontal sections of the human body, are separated by a distance of 1mm and, therefore, exhibit many similarities. The segmentation method uses this information through the image segmentation made in the previous images. Techniques involving the determination of statistical parameters, manual intervention, and image matching are used. The similarities between images are used in two ways: (i) by applying to each new image the statistical parameters and the sequence of operations performed in the previous images, and (ii) by using and

adjusting a previous segmentation polygon trough image matching. This is a semi-automatic method that allows a continuous control of the segmented anatomical structures since the manual and automatic components are available at each step of the procedure. In these circumstances, there is a high degree of dependence between the final quality of the segmentation of each structure and the knowledge of its morphology by the operator. As mentioned above, this knowledge is essential because the subsequent 3D reconstruction of structures cannot depend on wrong delimitations. With the segmentations, the LM is expanded with the morphology of the anatomical structures, which allows to generate 3D representations of individual anatomic structures.

The segmentation of a given structure begins with the manual definition of a Region Of Interest (ROI) in which the training data is selected (Canty 2014). An optional second step consists in defining a bounding polygon that encloses the area to be segmented. This polygon can be useful, for example, to isolate this area from other regions with similar RGB properties. In the next step, an RGB ellipsoid (Pommert et al. 2001) is built from the parameters calculated in the ROI; the center and the axes of the ellipsoid correspond to the average and the standard deviation of the three RGB colors, respectively. The segmentation region results from the adjustment of the standard deviations through the interactive application of a scale factor. Once obtained the initial segmented area, several operations can be applied depending on the characteristics of the image, including: filling holes, morphological dilation or erosion, eliminating noise outside de segmented area, and smoothing borders. Finally, the segmentation polygon may be manually adjusted by creating, deleting, or moving vertices.

After validating a segmented area, the algorithm reaches the next image. The parameters and the operations applied to the previous image can be reproduced and the segmentation polygon can be adjusted. In the case of adjustment an image matching technique was used.

For each point of the segmentation polygon a template image around the point is built. The image matching technique consists of positioning the template image in the subsequent image. To perform this operation the convolution between the new image and the template image rotated 180 degrees was calculated. The resulting matrix is the cross-correlation, since the convolution performed in this way corresponds to the correlation operation (Smith 1997). The maximum value in the cross-correlation matrix corresponds to the position of best fit between each template image and the new image. From this position it is possible to extract the coordinates of the segmentation polygon in the new image which may be, however, manually adjusted.

The convolution between the two images was done through the Fast Fourier Transform implementation (Frigo & Johnson 2014) of the Discrete Fourier Transform. By applying the convolution

theorem (Bracewell 2000), the convolution of the two images is converted into a multiplication operation of the respective Fourier transforms. The Inverse Discrete Fourier Transform is then applied to obtain the desired result. Expression (1) refers to the convolution between images, x and y, using the Discrete Fourier Transform (DFT) and the Inverse Discrete Fourier Transform (DFT^{-1}):

$$x * y = DFT^{-1}[DFT\{x\}.DFT\{y\}] \qquad (1)$$

To reduce the possibility to produce false positives in the cross-correlation matrix, the complete image is reproduced only in the neighborhood of the starting point, being represented by zeros in the remaining points.

Once covered all images, the voxels corresponding to the segmented structure are encoded with an ID in the LM. Table 2.2 shows automatic and manual features that are included in the segmentation method.

Manual functionalities	**Automatic functionalities**
ROI drawing	Creation of the segmented region by applying the statistical parameters of the RGB ellipsoid
Boundary polygon drawing	Segmentation polygon drawing
Segmentation polygon manipulation: creation, deletion and displacement of vertices	Recording of segmented structures
Choice of scale factors to be applied to standard deviation values of the RGB ellipsoid	Segmentation polygon adjustment by image matching
Parameter Setting: size of the moving average, multiple of sigma, neighborhood 4/8, size of error spots, size of dilation and erosion	Morphological operations: Dilation, erosion
	Fill Holes
	Delete islands
	Edge smoothing with moving average filter
	Navigation tools: zoom and pan

Table 2.2 - Automatic and manual features of the segmentation method.

The degree of automation of the method may vary from manual to automatic after setting the ROI. The quality of the segmentation depends on the quality of the input data and the capabilities of the operator with regard to the correct identification of the anatomical structures.

Before applying the segmentation method, and noting that the similarity between consecutive images is a premise for the segmentation method, a quantitative parameter is calculated to evaluate the level of similarity between the consecutive and the non-consecutive images. The quantitative parameter, Dif_{abs}, measures the percentage of absolute difference of the RGB values per pixel in the two images through the expression (2):

$$Dif_{abs} = 100 \times \frac{\sum_{i=1}^{n} |R_1 - R_2|_i + |G_1 - G_2|_i + |B_1 - B_2|_i}{3n} \qquad (2)$$

where R_k, G_k, B_k values correspond, respectively, to the values of *R*, *G*, and *B* in the image *k*; *n* is the number of pixels used in the calculation process. The differences are calculated only in the pixels in which there is information in both images, i.e., nonzero pixels.

Figure 2.6 presents a flowchart with possible operations for use in RGB image segmentation.

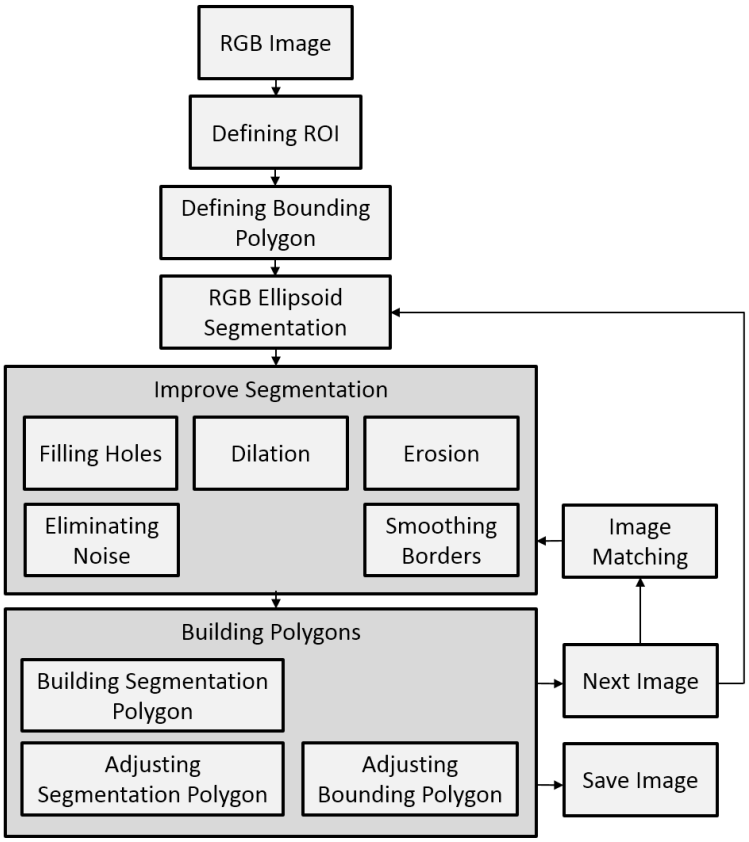

Figure 2.6 - RGB image segmentation procedure.

2.5. ANATOMICAL STRUCTURES SEGMENTATION WITH CT IMAGES

In the semi-automatic segmentation, one aspect which requires a manual intervention and hence a greater expenditure of time, is the segmentation of hard tissue in the neighborhood of other structures with similar RGB values, such as tendons. In these cases, the segmentation algorithm presents difficulties in discriminating the two structures. Solutions to mitigate such problems can be found through the use of additional data such as CT images (Beylot et al. 1996). Thus, to improve the segmentation application functioning and minimize the segmentation time, routines that operate and integrate the CT images on the application were developed. The segmentation of structures with CT images starts with the interactive setting of a threshold value over the target image. After initial segmentation, the program evolves through the image sequence maintaining the threshold value that can be interactively adjusted.

Once again, in the cases, in which there is the presence of noise, filters are provided to correct the segmentation areas. The procedure comprises applying the threshold value, filling gaps within the target area, eliminating islands whose size can be adjusted and smoothing of boundaries. The

smoothing of the segmentation boundaries aims at minimizing the pixelization effect that occurs in the reconstruction of the final 3D model (Figure 2.7).

Since the RGB and CT images have different sizes and resolution, their adjustment is made through an interactive definition of translation parameters and a scale factor. These parameters are determined to convert the CT images to the RGB images coordinate system. Through an interface where the images are overlaid, the visual validation of the CT image segmentation on the RGB image is carried out interactively.

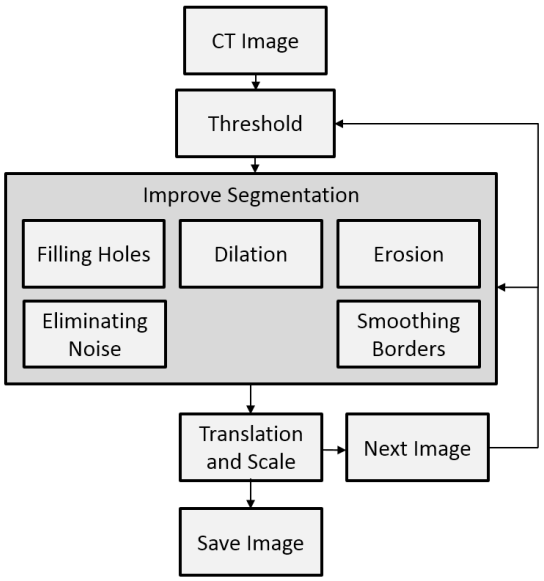

Figure 2.7 - CT image segmentation procedure.

2.6. 3D RECONSTRUCTION

After the segmentation step, a 3D voxel structure is built from the segmented slices in order to obtain the 3D Mask matrix. From this matrix a point cloud is obtained by extracting the border voxels. More precisely, a file with the 3D coordinates of these voxels is produced. This file constitutes the input data for the 3D reconstruction process that leads to the final vector model.

The vector surface consists of a mesh of triangles obtained by a 3D reconstruction Poisson algorithm. A particular screened Poisson reconstruction developed by Kazhdan & Hoppe (2013), which incorporates the surface points as interpolation constraints, is used. These authors show that the screened Poisson technique improves fit accuracy and sharpens the reconstruction without amplifying noise.

The Poisson reconstruction algorithm needs oriented points as input, that is, beyond the point cloud, normal directions are required. First of all, a horizontal normal vector is determined for each point in each horizontal plane. The direction of the vectors corresponds to the composition of the normal directions to the segments joining the actual point to its neighbors on either side. In a second phase, each point is joined to its nearest upper and lower neighbors, which determines the vertical direction by composing the vertical components of the normal vectors. The final direction at each point is the combination between the horizontal and vertical directions. The value of the point weight, requested in the screened Poisson algorithm, was determined on a recursive empirical basis (Figure 2.8).

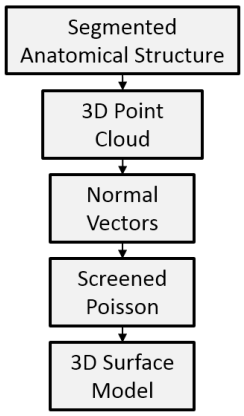

Figure 2.8 - Anatomical structures 3D reconstruction.

2.7. VALIDATION OF THE 3D RECONSTRUCTION

The 3D reconstruction involves the application of several tools which, from the initial masks, produce a final vector model. To assess the compliance of the vector reconstruction with the input data, a procedure was developed to validate the methodology and apply it to the various segmented anatomical structures. The validation process was performed on the vector model corresponding to the outer surface of the human body.

This process determines a parameter that measures the gap between the peripheral region of the body in axial images and the corresponding vector model obtained by the 3D reconstruction. The parameter used was the Root Mean Squared Error (RMSE) which provides a measure of the difference between the two entities and by comparing the value obtained with reference values. Thus, it is possible to assess the positional quality of the vector model with regard to the input data.

The determination of RMSE value is based on the calculation of distances, d_i, between the points of the vector component, (x_i^v, y_i^v), and the corresponding points on the border of the LM, (x_i^r, y_i^r). The

centroids of the triangles were considered for the points of the vector component. The dots at the border of the LM were calculated by linear interpolation to obtain the voxel coordinates that should be at the same level of the considered Z centroid.

Since the original data are images composed of pixels, the deviations of the vector model were evaluated in terms of the size of such data. In this case, as there is a 3D model, the comparison was made in terms of the voxel size. However, as the resulting voxels of the input data are not cubic, three different dimensions were considered to generate values for comparison with RMSE: the length side of the voxel in the XY plane, the length side of the voxel in the direction Z and the length of the side of a conceptual cubic voxel with the same volume of the original voxel. Given the values of the dimensions considered, the pixel side in the XY plane, being the smallest of the three, leads to a more demanding comparison based on the RMSE. The reference value to validate the vector model was 1.00 in terms of the voxel size (Pouncey et al. 1999). The final comparison is made between this reference value and the value obtained for the RMSE divided by each of the dimensions considered.

2.8. CENTRAL AXES

The linear structures implemented in the model do not have physical correspondence with the anatomical structures of the human body. These representations are common in GIS and are associated with objects that evolve linearly in space. These structures enable length measurements and network analysis operations, such as determining optimal paths. In the model, the structures that evolve linearly, such as blood vessels have a center line corresponding to the central axis of the structure in 3D space. The branches of the structure are linked by nodes.

The creation of central axis uses a 3D Skeletonization operation through the repulsive potential method (Cornea et al. 2007). After obtaining the axes, the points are filtered and reconstructed to have a homogeneous distance and a comparable size to the resolution of the input data (VHP images).

Once the central axis is created, the topological component associated with this structure is defined explicitly in the model through arc-node tables, in which each record contains the start and end nodes and the impedance - in this case, the length - of each arc that composes the central axis. These tables define the associations between arcs and nodes, representing the graphs corresponding to the respective geometric structures (Figure 2.9).

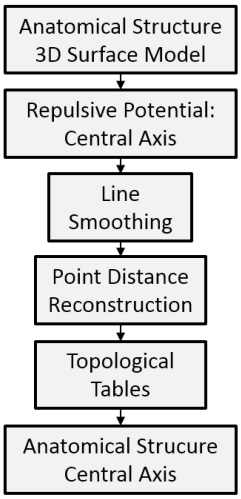

Figure 2.9 - Central axis building from surface models.

The procedure followed for the blood vessels is not always efficient. This is also the case of the intestines, which are structures that fold over themselves and have large compression zones. Thus, the vector surface structure does not represent the whole anatomical surface, being the determination of the central axis affected by a structure which does not correspond exactly to reality. In this case, it is developed a manual module that allows the user to position the points of the central axis in images using different perspectives: the original axial images and the front vertical images. Thus, it is possible to reconstruct the sequence of points corresponding to the central axis. With the last point, the sequence is closed, enabling the reconstruction of the central axis structure.

2.9. TOPOLOGY

The conceptual model contains 3 types of topologic information: containment, neighborhood and connectivity. The containment topological information results from the partition of space by the LM voxels. This information remains available in the model after the segmentation procedure and the construction of the LM structure.

The second type of topological structure of the model is based in neighborhood relationships at the level of the surface vector components. To this end, all the surrounding structures were identified for each frame. The decision on whether two structures are neighbors take into account the size of the voxels of the input data: for each structure are considered the points that form the vertices of the triangles of the vector component. For each vertex are detected the points that are at a distance comparable to the voxel size and do not belong to the same structure. These points are considered neighbors and, for each of them, is registered the neighboring structure. After checking all points of a

given structure, a list is saved without repetitions of the surrounding structures. The procedure is performed for all the structures and the information is explicitly described in the model by associating each ID of the structure to the ID of the neighboring structures.

The neighborhood topological component of the input model solves problems involving the determination of the neighboring structures of a pre-selected structure. This type of analysis is based on the reading of the neighborhood topological information which describes the neighboring structures of each structure in the model. Also regarding the neighborhood topology, another structure was implemented in the model. This topological component consists in tabular information with the neighboring anatomical structures for each vertex of the vector component for each structure of the model. This increase of information solves neighborhood analysis problems regarding a sub-region of an anatomical structure and not necessarily of the whole structure. The determination of this information consists in assessing, for all vertices of the vector component of each structure, the vertices of the structures with a different ID, located at a distance equal to the largest dimension of the raster data component, i.e., of the voxel. The results - IDs of neighboring structures - are listed in the model structure after eliminating repeated values.

The connectivity topological component is associated with the axes structures. This component is defined explicitly in the model through arc-node tables, in which each record contains the start and end nodes and the impedance - in this case, the length (in meters) - of each arc that composes the central axis. These tables define the associations between arcs and nodes translating the graphs corresponding to the represented geometric structures (Figure 2.10).

Arc	Impedance	From	To
1	3.31	1	2
2	3.46	2	3
3	2.89	3	4
4	3.11	4	5
5	3.02	3	6
6	2.98	6	7
7	3.24	7	8

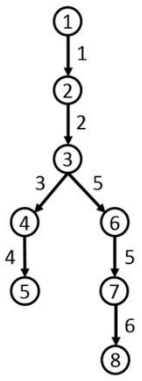

Figure 2.10 - Connectivity topology. Arc-node table and respective graph.

2.10. COORDINATE REFERENCE SYSTEM

Without an adequate coordinate system, the model and the respective interface cannot provide measurement capabilities. In fact, in such interface the reference system and the model dimensions may not correspond to the actual dimensions. With the inclusion of measurement tools in the prototype, it became necessary to assign the actual dimensions. To this end, the coordinates of the original image data were converted into real coordinates in the final model. The vector surface of the body was used to determine the 3D coordinate system: the system origin was the centroid of all vertices coordinates of this component.

The horizontal coordinates were determined as function of the horizontal resolution of the images, i.e., 0:33 mm per pixel in X and Y. The vertical coordinates took into account the distance of 1 mm between every two successive images. The system orientation was defined according to the sagittal, coronal and axial planes, as is usual in human body representations. The definition of a direct coordinate system with the Z axis increasing in the caudal-cranial direction is achieved by reverting the direction of Y and Z axes in relation to input images (Figure 2.11).

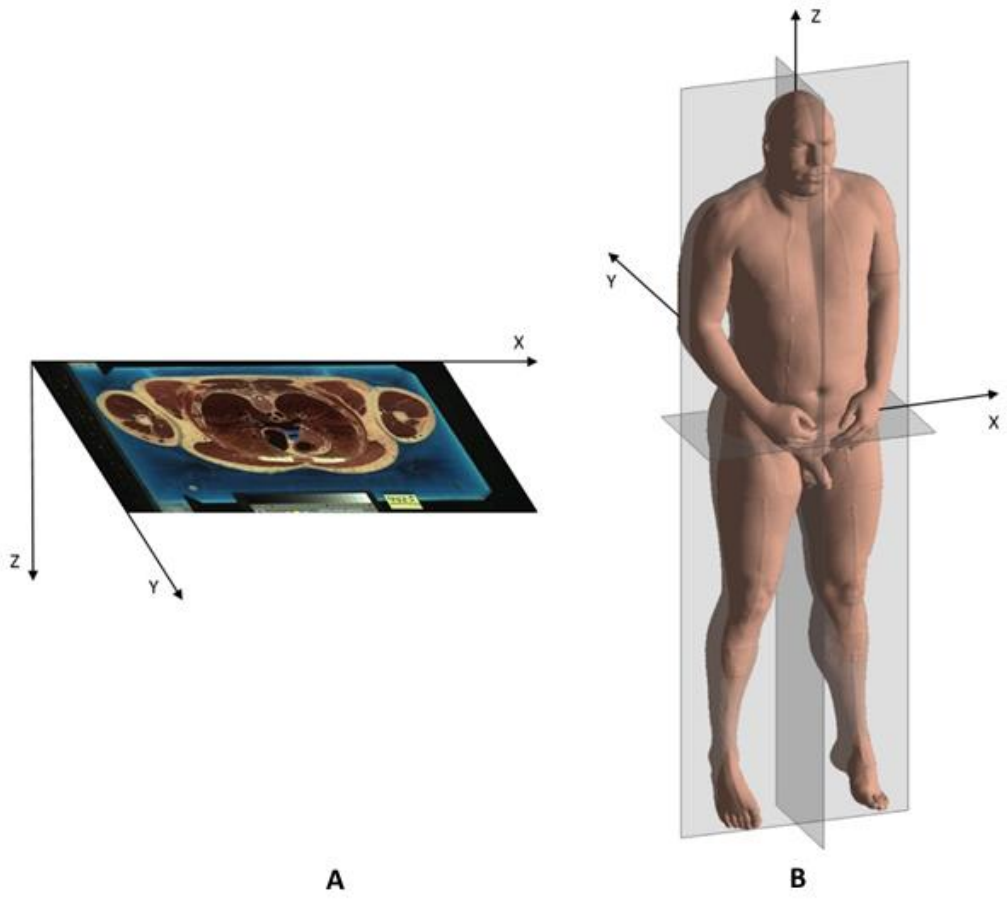

Figure 2.11 - Coordinate systems.

(A) Coordinates of input image data. (B) 3D coordinates defined using the vector model of the human body surface.

2.11. CLASSIFICATION OF ANATOMICAL STRUCTURES AND MULTILAYER MANAGEMENT

After developing the model, the 3DBodyGIS prototype was built. The prototype includes a graphical environment in which the model is embedded as well as functions developed to operate and test the model. The GI consists of two main zones: the TOC, where the layers are handled, and the graphical area, where the model is displayed. The management of the layers on the TOC is common in GIS applications. This manipulation consists of enabling / disabling the anatomical structures contained in a hierarchical list. The hierarchical list of anatomical structures reproduces typical classifications in anatomical atlases. The three hierarchical classification systems implemented in the TOC are based on regions, tissues and systems, having been designed according to the classifications in TolTech (2014). The classification systems, thoroughly described in spreadsheets, were converted into binary files and imported into the file structure of the prototype, being implemented in the TOC of the GUI whenever the application runs.

2.12. EXPLORATION OF THE INPUT DATA AND GEOVISUALIZATION

An application was developed within the prototype to explore directly the input RGB images. This application enables to position axial, coronal or sagittal planes and, simultaneously, show the respective RGB images. The images can be displayed statically or as a video sequence. An identification function on the raster component is implemented in this module.

One of the fundamental functions of the prototype consists in the visualization of internal anatomical structures activated by interactive definition of cutting planes. The definition of cutting plans is based on the following steps:

- Interactive identification of three non-coplanar points on the body surface so as to define a cutting plane;
- Elimination of the triangles that are strictly above the plane
- Identification of the triangles of the vector model involved in intersection with the cutting plane;
- Definition of the cut lines in the triangles involved;
- Elimination of the geometric figures above the cut line;
- Readjustment / reconstruction of new triangles: when the shape below the intersection line is a quadrilateral, two triangles are built instead.
- Placing the cutting plane on a temporary model;
- Rendering of the cutting plane by interpolating the 3D RGB matrix;

To render the cutting plane, RGB values of sampling points are obtained by interpolation from the 3D RGB matrix that contains the information of the input images. The interpolation can be carried out through 3 alternative methods: nearest neighbor, linear and cubic.

The definition of cutting planes can be carried out by simulating the insertion of a needle into the body surface. This feature uses the multilayer characteristics to implement the definition of cutting planes from the insertion of a needle in different anatomical structures, or on the body surface. The definition of a cutting plane started with a given point on a structure which is simultaneously identified. The orientation of the needle will define the cutting plane on the identified structure. Then, the algorithm which makes the detection is applied, cutting and reshaping of the triangles of the vector component as well as the rendering of the cutting plane with raster information representative of the internal

structures. Another possibility to define cutting planes is to use three points on the surface of the structure to be cut.

Through the visualization procedure, initiated by defining a cutting plane, raster-vector integration, which occurred at the level of the data structure of the model, also occurs at the visual level. This means that only the raster portion corresponding to a possible cutting plane is placed on the visual interface, which allows to reduce the weight of the data in this interface.

The input model enables the display of the raster and vector components in different color records. The raster component - showing the internal structures through cutting planes - can be viewed in true color through the RGB images of the original data or by the segmentation color defined in the LM which assigns each segmented anatomical structure to a single color. This component can also be displayed after 3D reconstruction of voxels with true color information (Conti 2004; Woodford 2011).

The 3D visualization of segmented structures through the vector surface components can use the segmentation color of the LM or another false color similar to the one of the represented structures. This color aggregates groups of structures, for example, a color for all the muscles and another one for all the bones. To introduce true color information in the vector component of the model, the following procedure was developed: for each vertex of the vector components, the RGB value of the nearest voxel is recorded. This record is stored in the model structure being associated to the corresponding anatomical structure and is a texture map that will be used to render the surface vector component with true color information. In reality the true color information is approximate because the RGB values used to render the faces of the vector components do not necessarily correspond to the boundary voxels of the corresponding structures. However, the rendering of the vector component with the resulting color information allows to visualize the anatomical structures with a more realistic appearance when compared with false color.

2.13. VECTOR-RASTER INTEGRATION

The visualization of anatomical structures is based on the definition of cutting planes. The application of a cutting plane to an anatomical structure requires cutting the surface vector component of the model and resampling the RGB values of the raster component on the cutting plane. Thus, the cutting procedure uses the two integrated components of the model. Although the integration of model components occurs at the level of their structure, the same cannot be said in terms of visualization, if the two components are directly depicted in the GUI. To eliminate the visual gaps between the raster and vector components, a triangulation was built on the cutting plane. To perform this triangulation

two sets of points are generated: (i) a regular grid on the plane and (ii) a reconstruction of border points so that its distance is of the order of the pixel resolution. It is important to ensure that the distance between the points does not exceed a predetermined value to apply the alpha-shape method of triangulation (Akkiraju et al. 1995), which allows to create a triangulation on a non-convex polygonal region. To perform the triangulation, the method is calibrated with a radius parameter greater than the pixel resolution, which ensures the inexistence of non-connected border points. Once built the triangle mesh on the cutting plane, the color information contained in the raster component is then resampled at the centroids of the triangles.

The method for obtaining the color in each triangle can be based simply on the nearest neighbor interpolation, or use any other interpolation methods which uses of the 1st law of geography, which states that objects that are closer are more similar than the ones that are farther: this can be translated into an interpolation method which gives a greater weight to the voxels that are closest to the centroid of the triangle to render.

With this procedure, the cut of an anatomical structure consists in showing, in the GUI, two integrated vector components: the surface component of the model and the new component built on the cutting plane.

2.14. IDENTIFICATION AND EDITING

The identification function provides the names of the anatomical structures at the internal and surface component levels. After the interactive selection of a point on the model, its coordinates are determined for identifying the anatomical structure to which it belongs. In this way, a point selected interactively returns a label with the name of the respective structure. The labels are created directly from the names in the TOC.

The current prototype contains two features associated with the identification of sub-regions in the surface vector component of an anatomical structure. The first functionality corresponds to the edition mode. When activated, it assigns a given name to a region drawn in the surface.

Once this level of information is created, the second functionality, the identification function, allows to extract this information and display it in the same way as the first level identification function.

Besides the identification of anatomical structures, which information is contained in the model attribute tables, identification functions also include the ability to link to external information, including documents in the computer or internet pages. In terms of operation, these functions are

identical to the above: after selecting a structure, the linked information is accessed by opening a specific page of a document or a web page.

2.15. MEASUREMENT TOOLS

Once implemented a coordinate system with actual dimensions, four measurement functions have been developed: area, volume, length between two points and length between two points along a structure. The construction of these operations benefits from the features of the integrated topological model. In this sense, it becomes possible to simplify certain measuring algorithms using the available information in the model: (i) measuring areas consists in determining the surface area of a given anatomical structure. This operation is associated with the vector component surface, being the calculation made from the sum of the areas of the triangles that form the surface of the structure; (ii) measuring volume uses the raster component and consists in counting the voxels of the anatomical structure. The conversion to volume is based on multiplying the number of voxels by its known volume (1x0.33x0.33 mm^3); (iii) measuring lengths along an anatomical structure is based on the topological connectivity information of the linear component of the model. To perform this type of measurement, the points among which is intended to measure the length of the anatomical structure are selected. After selecting the points, situated on the component of the central axis of the structure, the reading of the topological component described in arc-node table allows to calculate the total impedance - the desired distance - using the Dijkstra's algorithm (Dijkstra 1959; Jasika et al. 2012); (iv) measuring lengths between two points *p* and *q*, with 3D p_i , q_i coordinates, consists in calculating the Euclidean distance in the three dimensional space (3):

$$d_{p,q} = \sqrt{\sum_{i=1}^{3}(q_i - p_i)^2} \qquad (3)$$

This distance depends exclusively on the coordinates of the two given points and does not use the characteristics of any of the components of the model.

The four developed measurement functionalities are available in the GUI and work interactively with the placement of measurement points on the structures.

2.16. SPATIAL ANALYSIS

The GIS environment is built by incorporating the segmented model in the GUI where several tools are implemented, namely, navigation, visualization, identification, and analysis functions.

By using the raster component that partitions the space it is possible to determine whether a given point is contained within the model, and if so, what anatomical structure contains it. The inclusion function that performs this kind of analysis can simulate, for instance, the insertion of a needle in a given point of the body surface. This function is implemented by defining five parameters (Figure 2.12): (1) the insertion position on the surface of the body *P*; (2) the length of the needle, *L*; (3) the depth of needle insertion, *D*, and (4) the horizontal and vertical angles that define the orientation of the needle, $\vec{V}$. Based on these parameters, the extreme points of the needle, P_i and P_f, are determined. Then, the needle body is materialized by a set of points spaced 0.33 mm by default. The analysis result, read in LM, is displayed by coding the needle points with different colors according to the crossed structures, whose identification is described in a map legend.

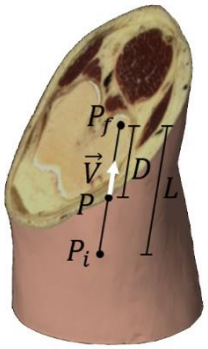

Figure 2.12 - Insertion parameters of a needle into the human body.

The spatial neighborhood analysis function determines the neighboring structures of a pre-determined structure. To implement this function, the structure whose neighborhood is to be determined is identified. It is also possible to further select a subset of structures inside of which must be evaluated the surrounding structures. The result of this analysis is obtained by the intersection of this set with the set of the neighboring structures which, in turn, is read in the table that contains information about the neighborhood. Alternatively, given the way the model defines neighborhood topology, it is possible to determine the surrounding structures of only a part of a given structure.

3. RESULTS

3.1. BODY SEGMENTATION

The segmentation of the body consists of extracting binary masks from the RGB images. The input data (Figure 2.1) suggests the importance of blue color in obtaining the intended masks. To analyze the intensity levels of each color, which may vary from 0 to 255, different paths are chosen on the images, inside and outside the body. For a selected path $\overline{P_0P_1}$, (Figure 3.1) which contains regions outside the body and various inner anatomical structures, the corresponding RGB intensity graphic is drawn (Figure 3.2). The graph shows that the intensity of blue has a wide range of common values inside and outside the body. So, it is not possible to define the mask using the elimination of this color based on a simple threshold value. The green and red colors, especially the red, show differences between the outside and the border area of the body. In this case a threshold value should be tested. Additionally, the same graph shows another behavior: there is an inversion of the intensity values red-blue, inside and outside the body. This behavior is extensive to all the images. Despite this behavior also occurs at red-green intensities, the magnitude of the difference is much smaller. Thus the rule “red greater than blue” (R> B) should be more efficient than the rule “red greater than green” (R> G) to separate the body from the surrounding area.

Figure 3.1 - Definition of $\overline{P_0P_1}$ path to study the RGB intensity profiles.

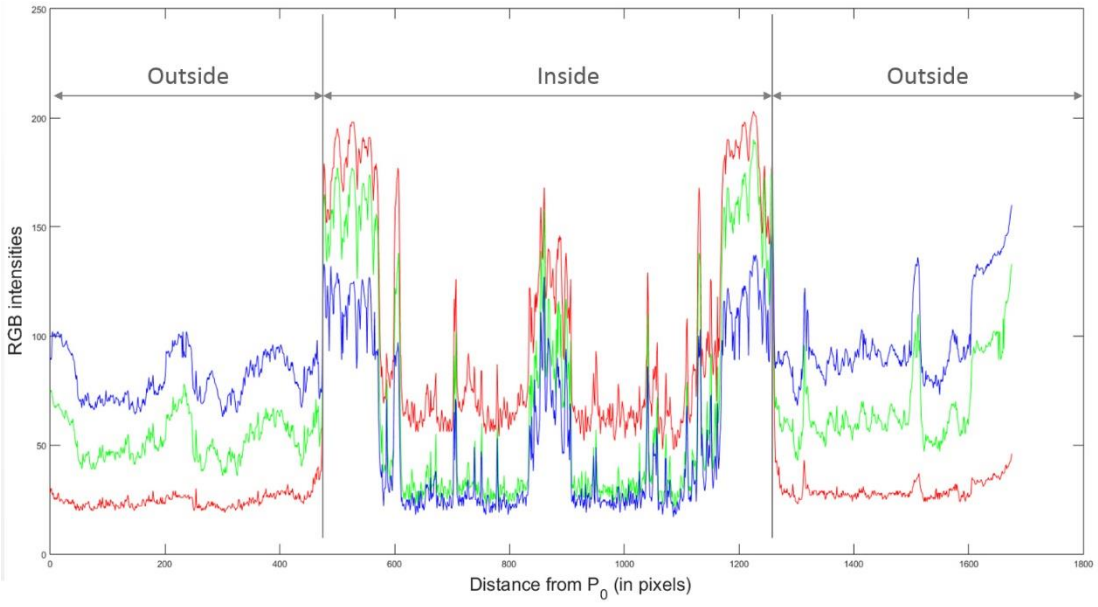

Figure 3.2 - RGB levels measured along $\overline{P_0P_1}$.

The path along which RGB intensities were measured, starts outside the body, crosses various structures within the body and ends again at the outside. The inner and outer regions were delimited by vertical lines in the graph.

Figure 3.3 shows tests with threshold values for the 3 colors and the application of the R>G and R>B rules. As expected, the threshold with blue fails to discriminate the border of the body from the blue gel. The same technique applied to green and red colors improves the results, especially with the red color. The rules R>G and R>B show a more robust behavior. Although the results depicted in the images look the same, the rule R > B is more efficient than the rule R>G.

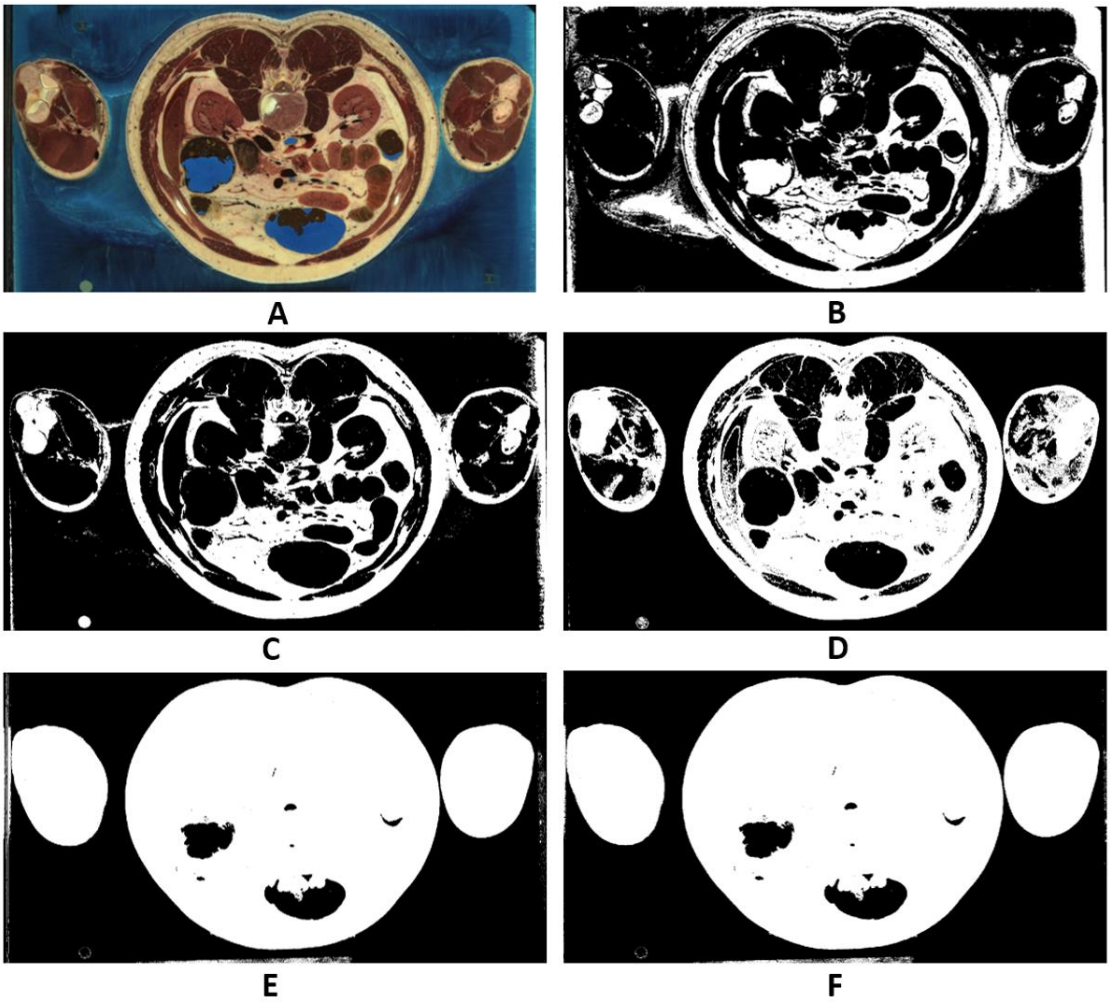

Figure 3.3 - Segmentation of the body.

(A) Input image. (B) Threshold with blue color (100). (C) Threshold with green color (100). (D) Threshold with red color (100). (E) Rule R>G (R > 0.9 x G). (F) Rule R>B (R > 1.1 x B).

The segmentation rule R> B is not free from noise, since: (i) areas with value 1 persist outside the body (islands), (ii) areas with value 0 persist inside the body (holes) and (iii) deformations along the border are also present. These behaviors are due to the interaction between the body and the material that surrounds it and should be corrected (Figure 3.4):

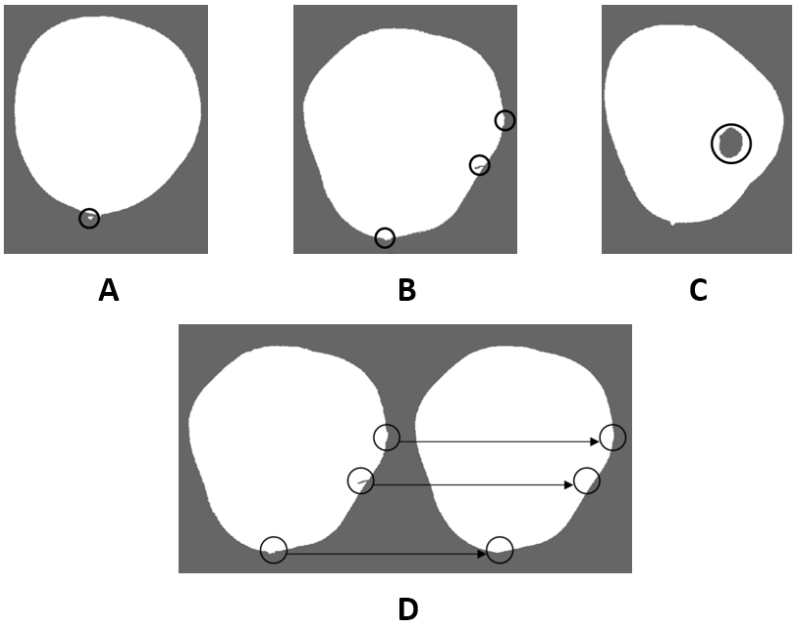

Figure 3.4 - Masks obtained through rule R > B, showing the existence of noise.

The circles indicate regions where noise occurs: (A) Islands. (B) Deformations along the border and (C) Holes. (D) The effect of applying a moving average filter on the boundary positions of the mask.

The result of a segmented slice is shown in Figure 3.5. This is a case were no relevant noise occurs, so that, segmentation was carried out with the common operations: Rule R > B; Delete islands; Fill holes; Smoothing borders.

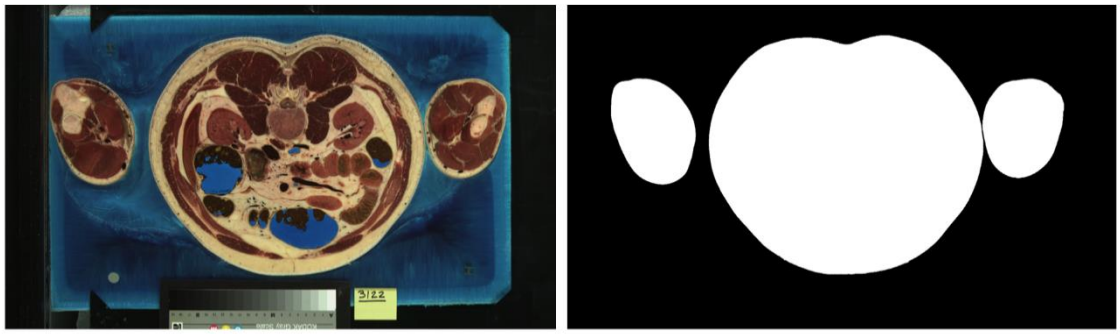

Figure 3.5 - The segmentation process of the human body.

Input data and the respective mask.

Figure 3.6 shows an example where a threshold value was applied to deal with noise caused by the blue gel over the body region. Once the blue color invades the body and the relation with the red was affected, the threshold was applied with the green color.

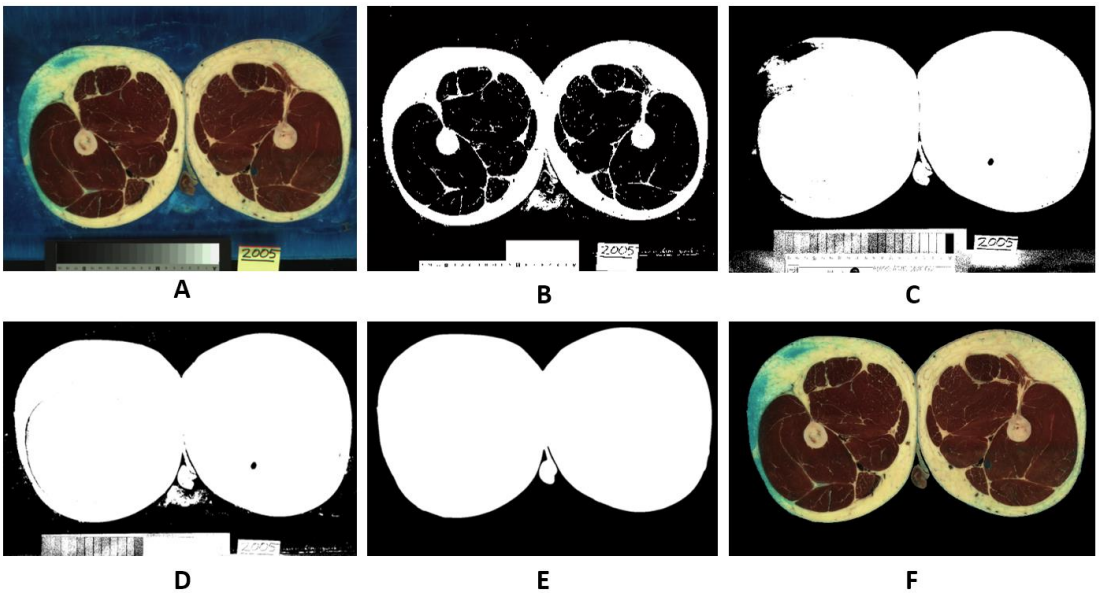

Figure 3.6 - Segmentation of the body with an additional threshold to correct noise.

(A) Input image with noise (invasion of the body with the surrounding blue gel). (B) Threshold with green color. (C) Rule R>B. (D) Logical "OR" between the two previous procedures. (E) Final filters: delete islands, fill holes and smoothing borders. (F) Application of the final mask to the input image.

3.2. Segmentation of the Internal Structures with RGB Images

The image matching technique implemented in the segmentation of the internal anatomical structures depends on the similarity between the input images. To evaluate the level of similarity three different comparisons were carried out (Figure 3.7): (i) between images whose RGB values are randomly generated; (ii) between consecutive RGB images; and (iii) between non-consecutive RGB images. In each case, the absolute differences were calculated. In the case of similarity between the input images, it is expected that the difference obtained in the first case should be considerably greater than in the other two cases. Furthermore, the difference in the second case should also be lower than in the third case. If so, the similarity between the input images can be used by the image matching technique.

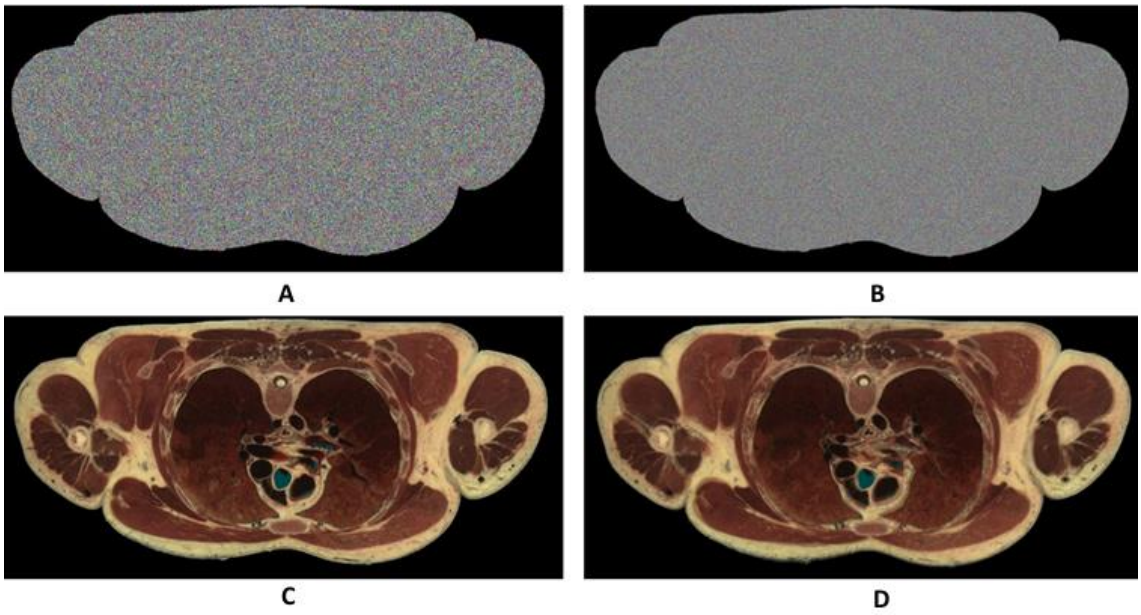

Figure 3.7 - Evaluating the similarity between the cryosection anatomical images.

(A) Random image. (B) Overlapping random images. (C) Overlapping consecutive RGB images. (D) Overlapping non-consecutive RGB images.

The absolute differences were calculated for 600 pairs of images. The average values for random, consecutive and non-consecutive images are shown in Table 3.1. These results show that the consecutive images have a high degree of similarity and superior to non-consecutive images. Nevertheless, it should be noted that the segmentation does not necessarily depends of the image matching algorithm. In fact, this technique proposes the segmented area in each new image but the final segmentation is validated by the user. Thus, the proposed segmented areas can be accepted or not, and corrections can be made if they are found necessary.

Relative position of the images	**Absolute difference per pixel (percentage average)**
Consecutive images	1.8
Non-consecutive images	2.5
Random images	19.8

Table 3.1 - Absolute differences per pixel between two images (percentage averages).

The segmentation method was applied on the cryosection anatomical images in which 211 structures were segmented totaling 39660 segmentations: the bones and the muscles of the lower limb and various organs of the abdominal and thoracic regions (heart, lungs, liver, stomach, small intestine, large

intestine and skin). Figure 3.8 shows some of the techniques included in the segmentation module such as: (i) using the RGB ellipsoid after setting the ROI; (ii) correcting errors (filling holes inside and eliminating spots outside); (iii) smoothing the border of the segmentation area; (iii) using the bounding polygon; and (iv) using the image matching technique to update the segmentation polygon.

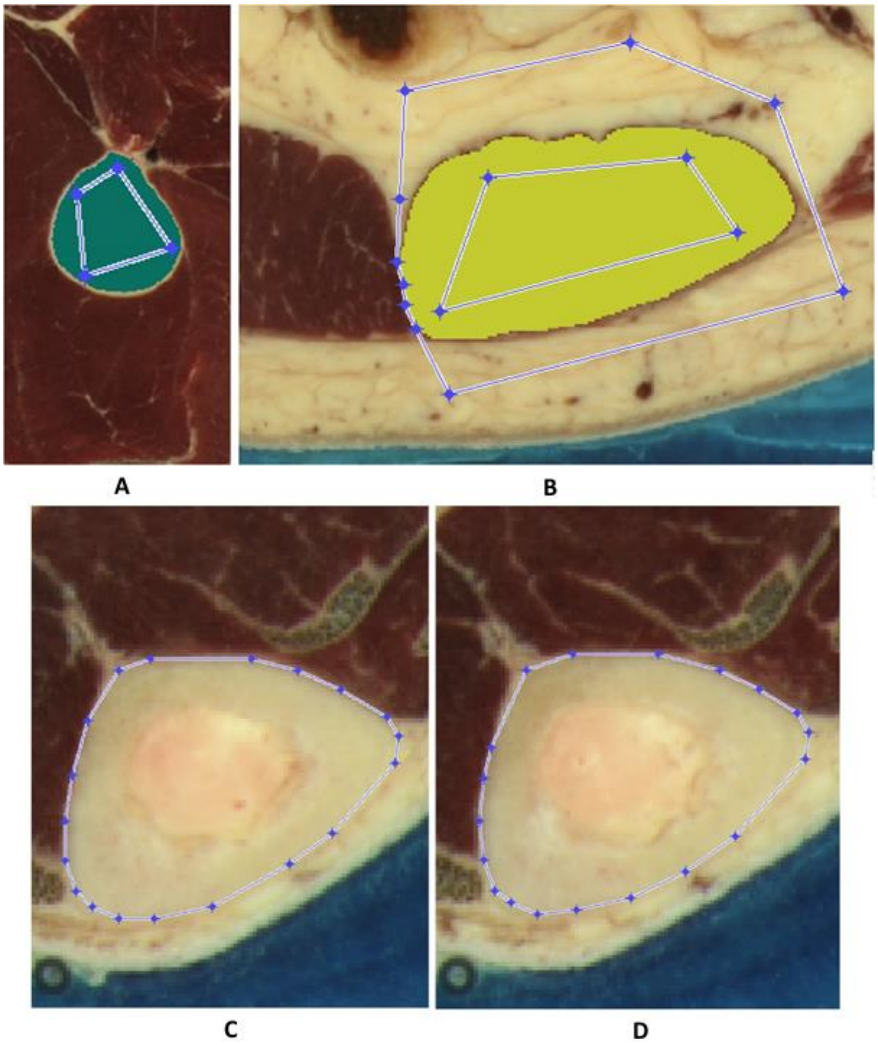

Figure 3.8 - Segmentation of anatomical structures.

(A) ROI definition and segmentation of the femur without the bounding polygon. (B) ROI and bounding polygon definition and segmentation of the left rectus abdominis muscle. (C) and (D) evolution of the tibial segmentation from image 2611 to image 2616 with the image matching technique.

After the segmentation stage, the segmented structures are coded in the LM, carrying out the desired model expansion (relatively to the initial body segmentation). The LM updating enhances the

containment information of the model. In fact, with this new information the identification and the analysis functions provide a more detailed and correct response to requests made by the users.

The final results of segmentations are voxel clusters in a 3D space. These voxels allow to generate 3D views of the segmented structures (Figure 3.9). By inspecting the 3D structures it is possible to evaluate the quality of the segmentation. From the user point of view, the reconstructed 3D structures allow to have a more realistic idea of its morphology, which is not so evident from the direct inspection of the input data.

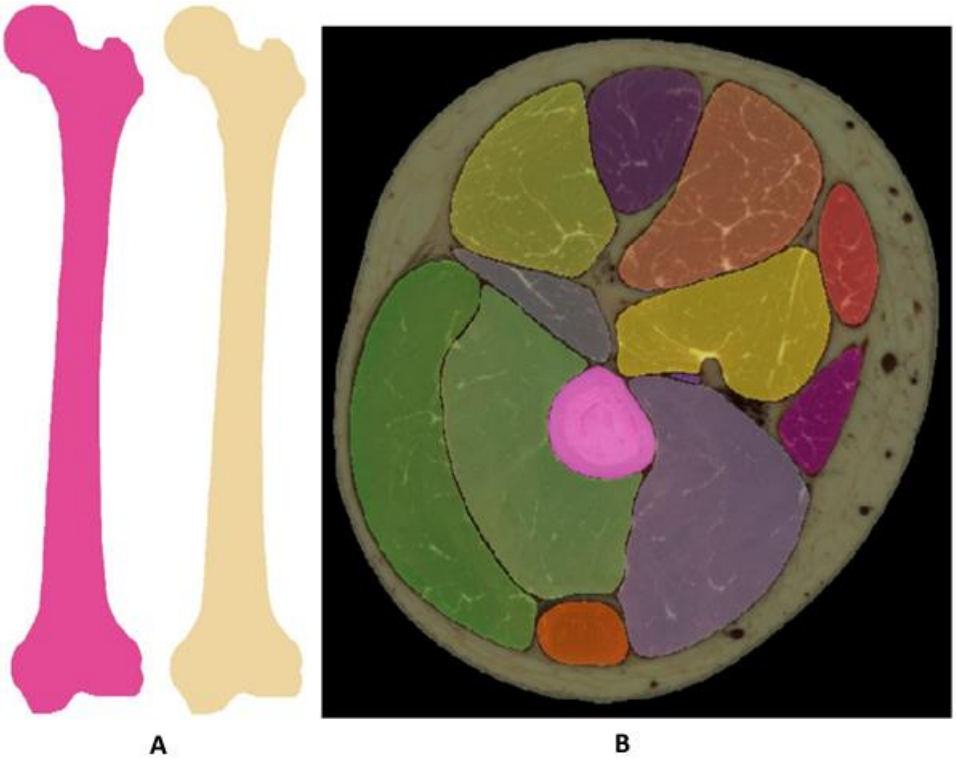

Figure 3.9 - Visualization of the segmented structures with the LM.

(A) 3D reconstruction of voxels representative of the left femur with segmentation color (one color for each structure) and with the color assigned to all the skeletal system; (B) RGB image overlaid with the corresponding LM plane.

3.3. SEGMENTATION OF THE INTERNAL STRUCTURES WITH CT IMAGES

CT image segmentation is based essentially in applying a threshold value to highlight the hard tissues. This type of segmentation has been implemented to complement the segmentation module that operates on RGB images. The segmentation principle through threshold application is complemented with other procedures to further improve the final result. In Figure 3.10 is shown an axial section in

which the noise becomes quite noticeable after the initial application of the threshold. Because of such recurrent situations in the input data, the segmentation module has been equipped with additional functions to eliminate noise.

The noise shown in Figure 3.10 results from the image acquisition process. Its elimination consists in detecting and eliminating the horizontal segments. The filter that eliminates these segments detects the image pixels containing the value 1 and which have the value 0 in the lines immediately above and below, and replaces them by 0. The remaining noise outside the segmentation area, and the occurrence of spots, is eliminated by a filter that detects voxel clusters smaller than a predefined size. Then, the filling of gaps within the segmented regions is carried out and, finally, its boundaries are smoothed.

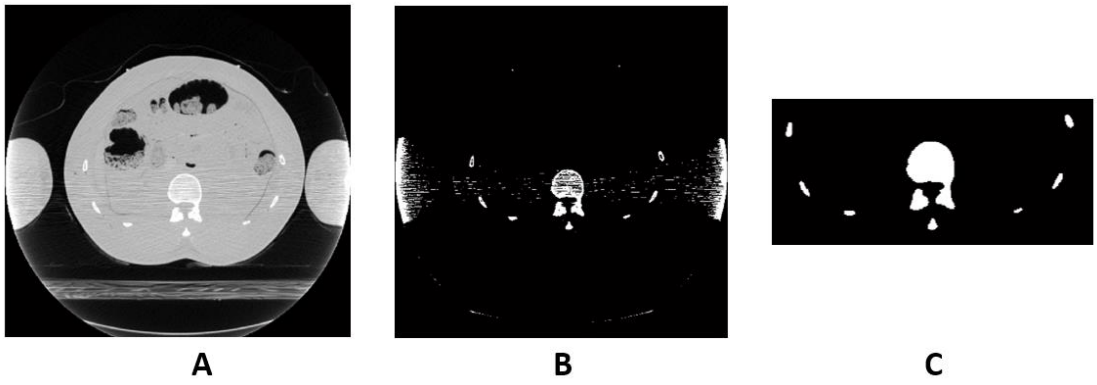

Figure 3.10 - Segmentation on CT image with noise.

(A) Original image. (B) Application of a threshold value. (C) Final filtering with horizontal noise removal, filling holes, deleting islands, and smoothing borders.

3.4. INTEGRATION OF RGB AND CT IMAGES

Once performed the segmentation of a CT image, the result will be transformed into a coordinate system common to the RGB images. The option to transform the coordinate system of the CT images to the RGB images, has to do with the fact that the latter is already integrated with the application. The transformation parameters are determined interactively by translations in the X and Y directions and a scale factor. Figure 3.11 shows the result of a segmentation overlaid with the respective RGB image. In the first case, the two images are shown in their original coordinate systems. In the second case, the CT image coordinate system of coordinates was converted to the RGB image coordinate system.

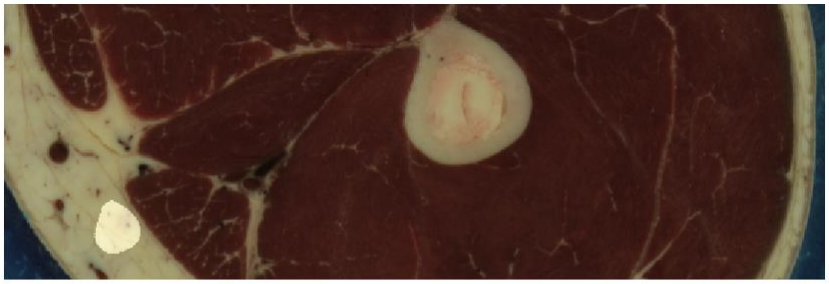

A

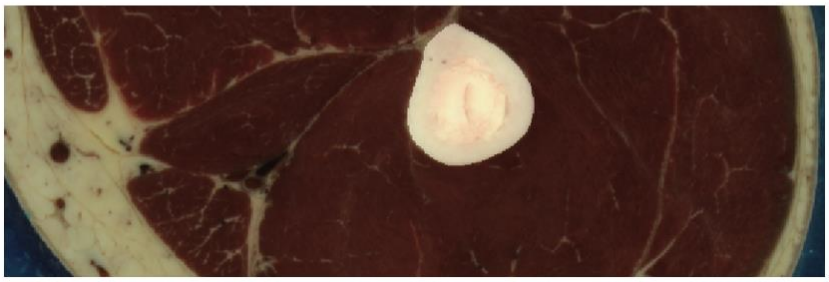

B

Figure 3.11 – Conversion between coordinate systems.

Transformation of CT segmentation to the cryosection image coordinate system.

(A) Initial overlap of CT segmentation with the cryosection image without coordinate transformation. (B) Transforming the CT image coordinate system to the cryosection image.

The combined use of CT and RGB images aimed to have the advantageous features of each of them, using in the segmentation process the one that leads to better results. Figure 3.12 shows a typical situation where the segmentation on a RGB image requires manual intervention due to the difficulty in distinguishing between two different structures, one being a bone structure. In such situations, the segmentation of CT images helps to eliminate the difficulties, correctly classifying the hard tissue. In this figure, it is apparent that the automatic component of the right tibia on the RGB image segmentation is not able to distinguish this structure from some neighboring regions. In this case, manual intervention is used to draw a bounding polygon that restricts the segmented area. An alternative way of proceeding consists in the use of CT images. In this case, the bone structure is easily discriminated by applying a threshold value. After determining this parameter and adjusting the two images, the segmentation is defined.

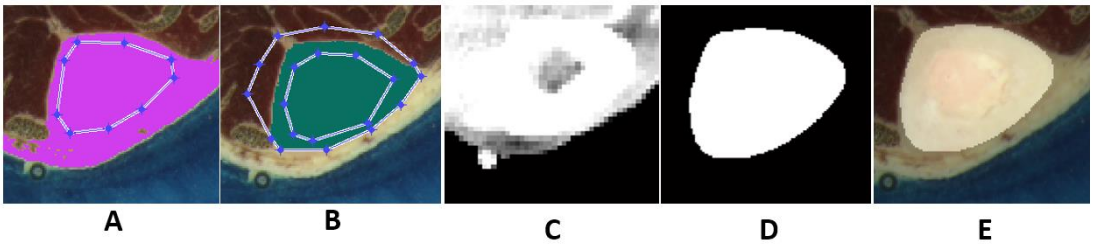

Figure 3.12 - . Integration of CT and cryosection images.

(A) A cryosection image segmentation in which the segmentation area is bordered with similar areas in terms of RGB characteristics. (B) The difficulties of segmentation of cryosection images can be supported with manual intervention - in this case it was used an external enclosing polygon. (C) Use of CT image. (D) CT image segmentation with threshold application. (E) Integration of cryosection and CT images in the cryosection image coordinate system.

3.5. 3D Reconstruction and Validation

The bi-dimensional masks are aggregated in the LM. To produce the surface vector model, the coordinates of the centroids of the border voxels in this 3D matrix – a non-uniform point cloud - are used to generate the surface of the body. The final surface was obtained after tests made in order to find an adequate reconstruction method. The use of α – shape concept, for example, is viable in areas with evenly spaced points, however fails when it is applied to the complete model (Figure 3.13).

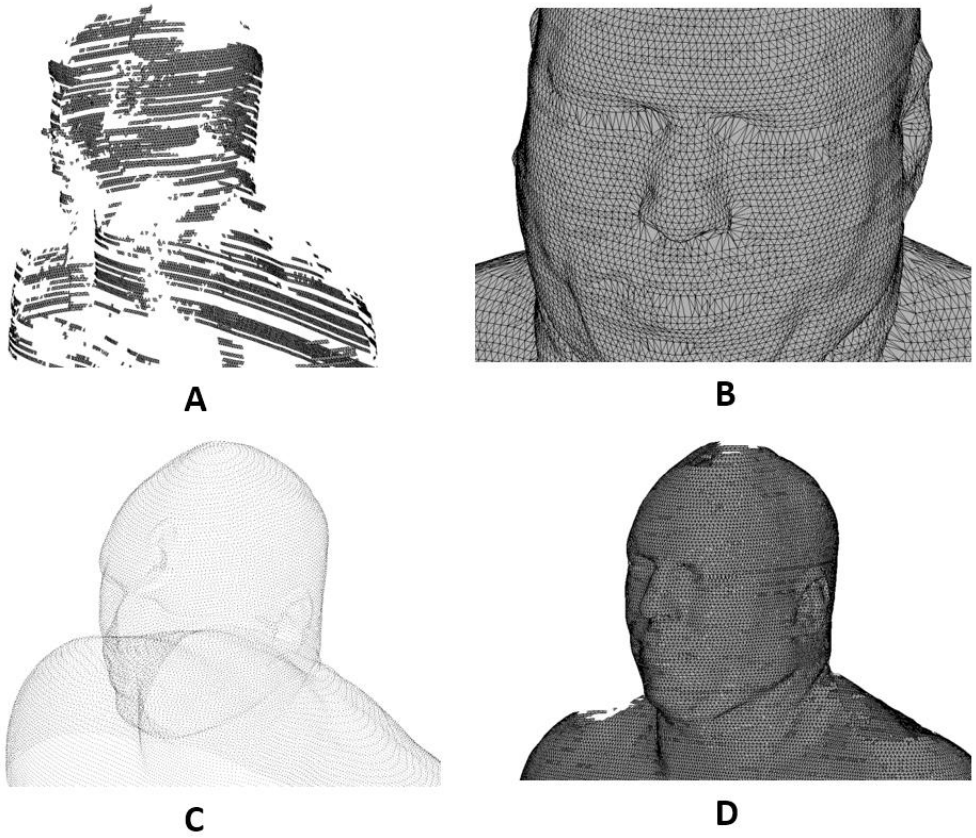

Figure 3.13 - Surface reconstruction with α-shapes.

(A) A small α may drop points of the original cloud and produce holes. (B) An high α may cause loss of detail. (C) Considering the complete model, non-uniform sample data is found (particularly visible on the shoulders and the top of the head). (D) To fill the holes in the surface, the choice of α leads to loss of detail. In the picture it can be seen that, despite the loss of detail, some holes in the surface still remain.

Using the point coordinates and the corresponding estimated normal vectors, it is possible to apply the Poisson method. The reproduction of the body surface is depicted in Figure 3.14. The tests carried out with this method were intended to smooth the surface without losing essential detail. In fact, the screened Poisson method, used in the reconstruction procedure, allows to assign weights to the points so that the surface can be more or less smoothed.

Figure 3.14 - 3D body surface reconstruction with the screened Poisson algorithm.

The 3D surface, reconstructed by applying the screened Poisson algorithm, is composed by a vector triangle mesh representing the outer surface of the human body. The approach of this vector component to the input data was evaluated by the RMSE parameter. The calculation of the RMSE involved 14,389 centroids of the triangles that make up the vector component of the human body surface. The obtained value was 0.18mm. Table 3.2 shows the correlation of this value with the three reference values used.

Reference	Ratio RMSE / Reference
Side of original voxel along Z axis	0.180
Side of cubic voxel	0.375
Side of original voxel on the XY plane	0.545

Table 3.2 - Root Mean Squared Error value assessment measured between the vector surface and the boundary of the respective raster component.

As shown in Table 3.2, the ratio between the RMSE value and the various raster sizes is significantly less than 1.00, the benchmark used to perform this validation, even in the most unfavorable situation – the comparison of the RMSE value with the pixel size in the XY plane. This means that the vector

component surface has a suitable geometric adjustment to the original raster. This result is achieved on a model that was obtained after applying the screened Poisson and filtering methods. The filtering is intended to smooth the final surface which allows to mitigate the pixelization effect. The use of filtering enables also to validate the model from the visual point of view. This validation is important because if the smoothing of vector surface were not performed, the result of the RMSE value would be smaller but the surface would present a pixelated clearly unrealistic appearance. The use of filtering enables also to validate the model from the visual point of view. Thus, it is desirable to balance the realistic aspect with the quantitative quality of the model.

To mitigate the possible pixelated aspect of the vector surface, the original triangles can be replaced by larger triangles, with no perceptible loss of detail. The reduction of the number of triangles allows also decrease the data volume of the vector component. The combination of this reduction with the smoothing filters applied to de boundary points gives a more realistic appearance to the model (Figure 3.15).

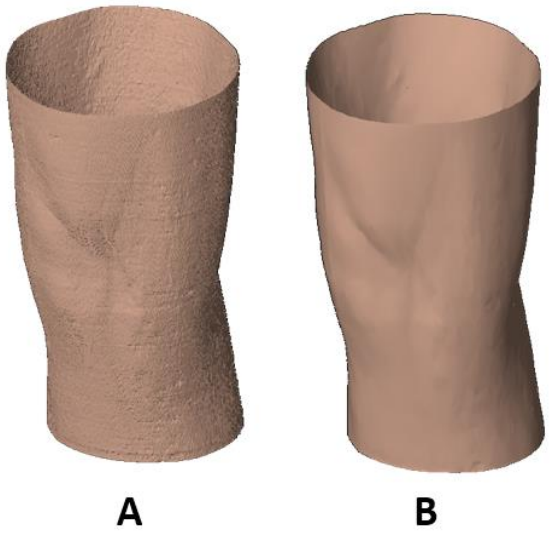

Figure 3.15 - The effect of smoothing border points and reducing the number of triangles.

(A) Surface without smoothing/ reducing. (B) Surface with smoothing / reducing.

Once reconstructed and validated the surface vector components of the body, the technique was applied to the segmented anatomical structures, which are stored in the model structure together with the corresponding ID entered in the LM as well as the assigned color information. Figure 3.16 shows the resulting mesh of triangles reconstruction of the left femur and the colors stored in the

model: the false color that mimics the structure of bone (one color for all bones) and the segmentation color of the left femur.

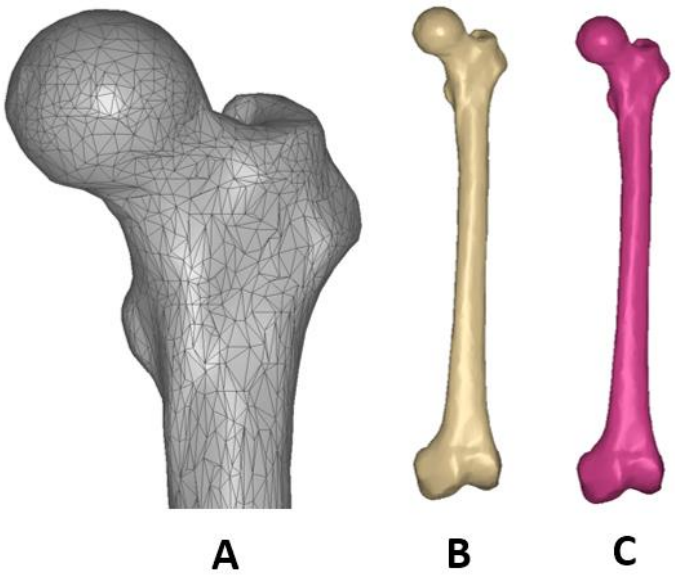

Figure 3.16 - Reconstruction of the vector surface component of the left femur.

(A) Triangle mesh that materializes the geometrical component. (B) False color assigned to the bones. (C) Color assigned to the segmentation of the left femur.

3.6. CENTRAL AXIS

The implementation of the connectivity topology is associated with the inclusion of central axes in some anatomical structures. The definition of the axes, made via an interactive application, generates three different views of the input data: (i) the original axial images; (ii) front vertical images of the same data; (iii) a 3D image which enables the visualization of the voxels of the anatomical structure with a degree of transparency dynamically defined by the user (Figure 3.17). In both the input images, the cursor must be positioned in the center of the structure. The cursor appears in the 3D image being possible to confirm the position within the structure. After determining all the positions, the central axis is defined and registered in the model structure by creating the topology arc-node table that is associated with the ID of the corresponding anatomical structure.

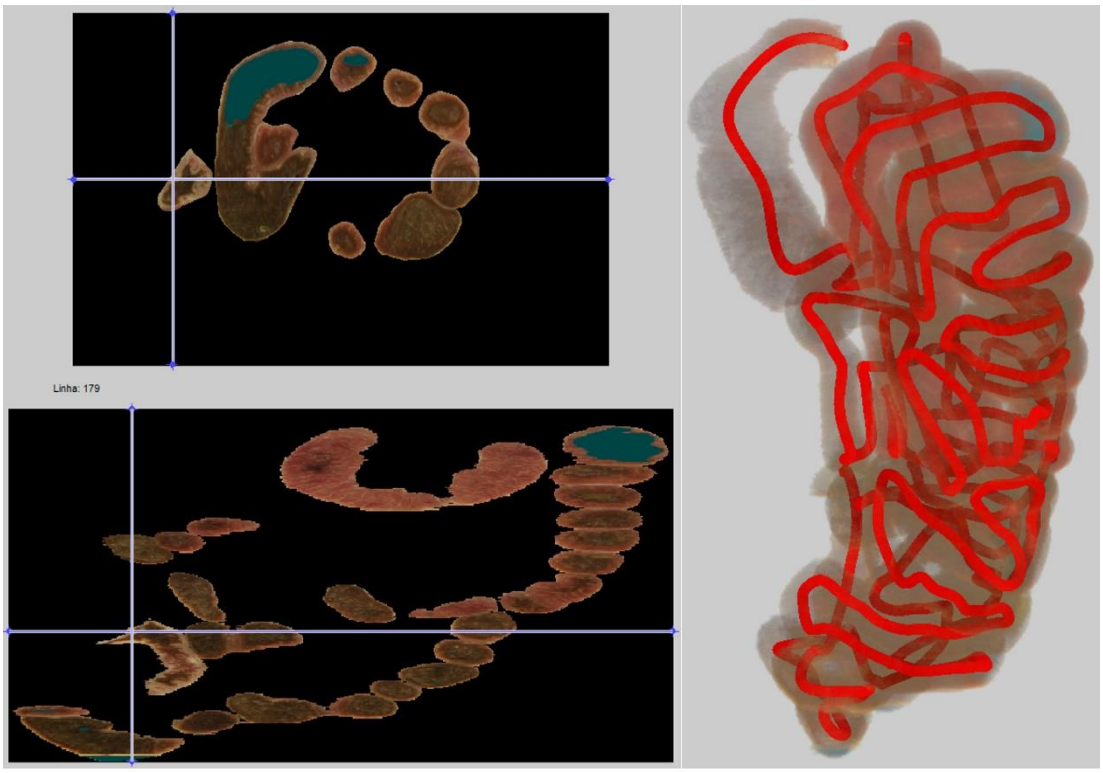

Figure 3.17 - Defining the central axes of the anatomical structures: interactive interface.

3.7. CLASSIFICATION OF ANATOMICAL STRUCTURES AND MULTILAYER MANAGEMENT

The management of the layers is made through the TOC. The alphabetical listing of anatomical structures in the TOC is not the most efficient way to manage the information layers. An alternative way of presenting the TOC consists of classifying the anatomical structures as is usual in the anatomical atlases. In this way, a more efficient organization scheme and a faster access to each structure or groups of structures is obtained. To implement classification systems in the GUI, three different hierarchical forms were added to the TOC that enable the organization of the anatomical structures in regions, tissues or systems. The different classifications are exclusive and when one of the classifications is selected, the TOC is filled with the corresponding hierarchical tree (Figure 3.18).

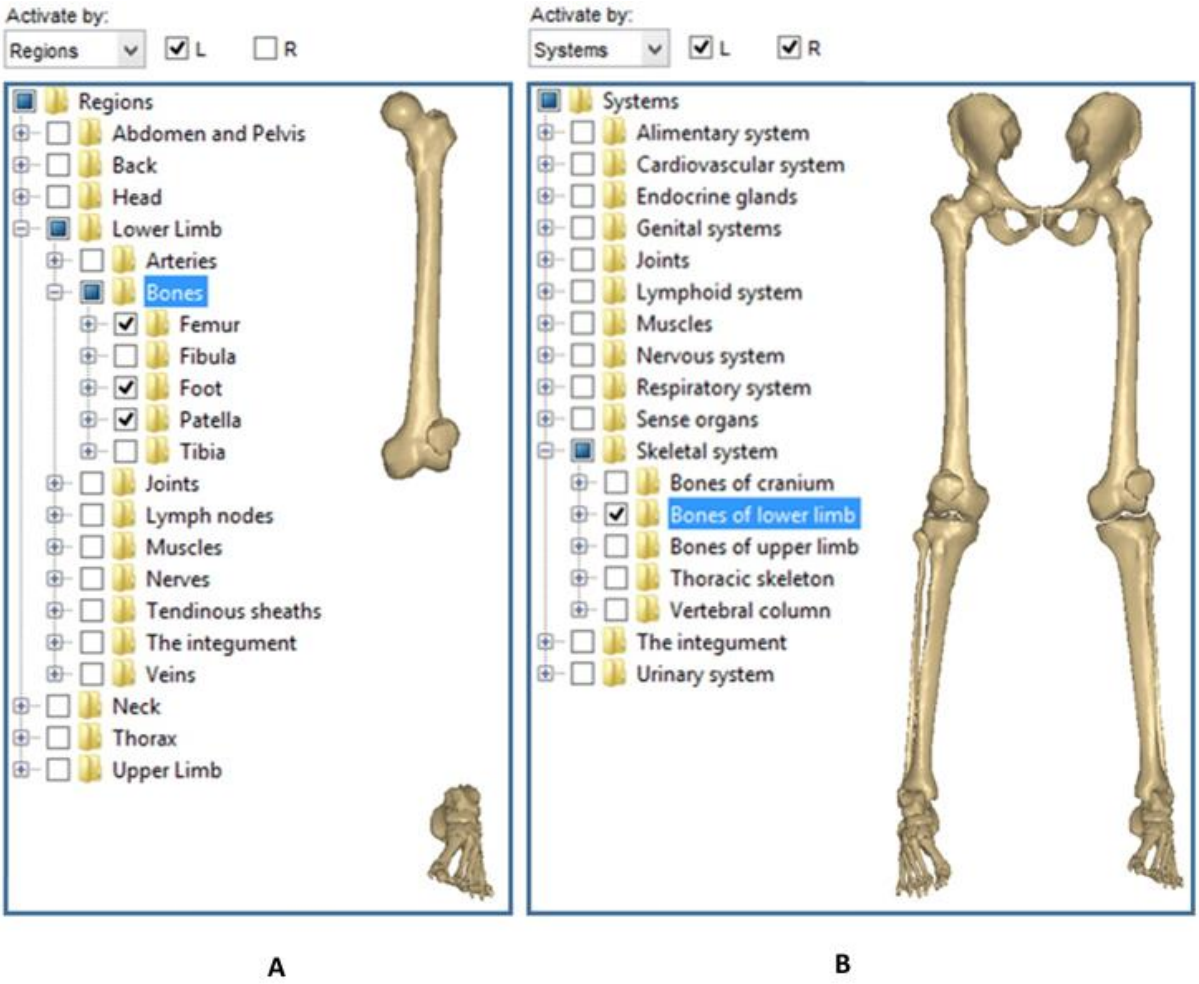

Figure 3.18 - Hierarchical classification systems implemented in the TOC.

(A) Classification by regions; (B) Classification by systems.

3.8. EXPLORATION OF THE INPUT DATA AND GEOVISUALIZATION

In the 3DBodyGIS, most direct access to data is done through a module whose graphical representation consists of the images of the transverse (input data), coronal and sagittal planes. The module provides three functions that operate on the three planes: (i) Navigate through successive images; (ii) identify anatomical structures on the images; (iii) Go to an anatomical structure selected from a list. (Figure 3.19).

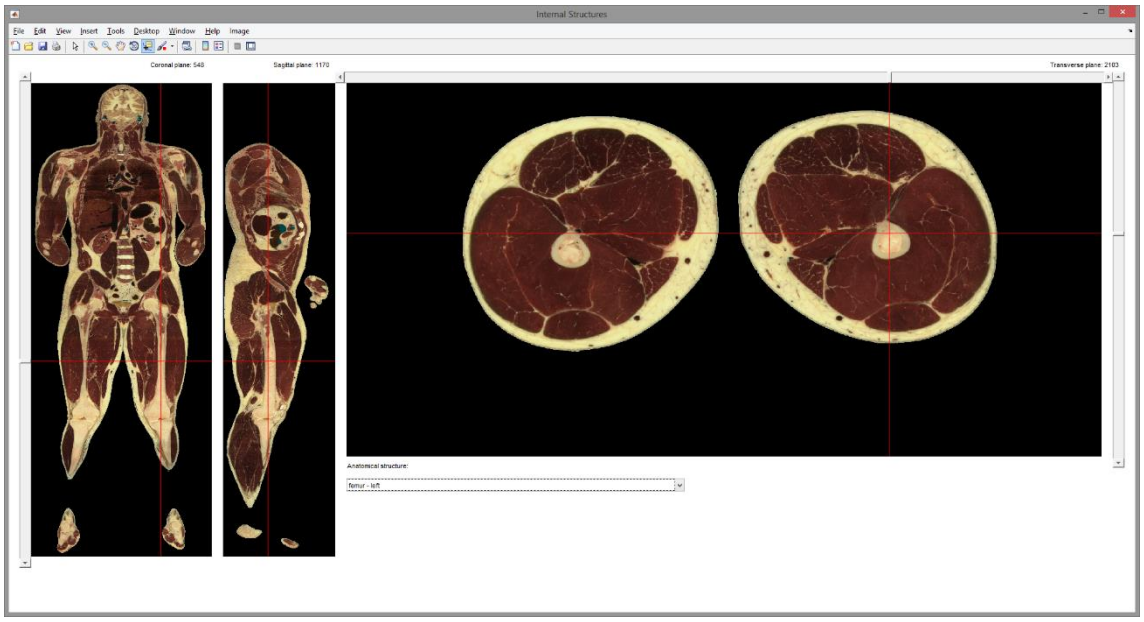

Figure 3.19 - Input data direct exploration and identification function.

The visualization of the interior of the body is achieved by defining a cutting plane through a needle insertion or by placing three points on the surface. The algorithm produces a temporary visual model (Figure 3.20). This model is constituted by the vector surface component that remains after the cut and by the cutting plane rendered with the true color information provided by the RGB input data. This temporary model intends to minimize data volume in the GUI allowing faster interaction with the model.

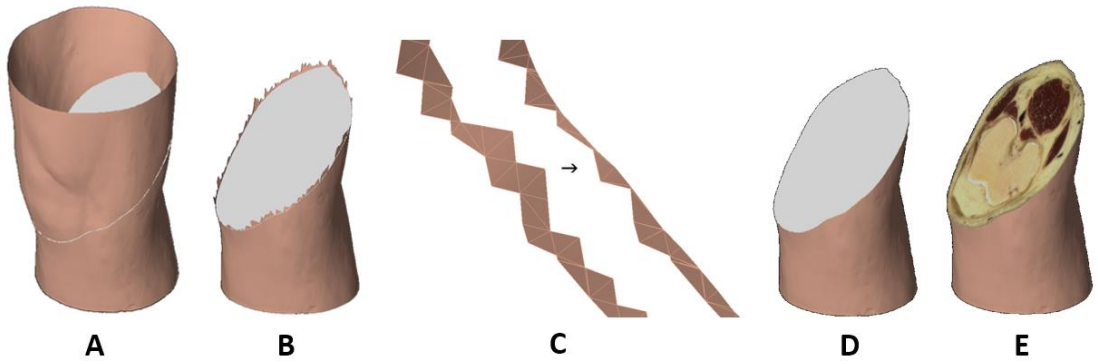

Figure 3.20 - Visualization of internal structures by defining a cutting plane.

(A) Definition of the cutting plane. (B) Eliminating triangles. (C) Adjusting the triangles that are involved in the cutting region. (D) Building the visual model. (E) Rendering cutting plane.

To render the cutting plane, three interpolation methods are tested: Nearest neighbor, linear and cubic. Although the three methods are available, the tests show that the nearest neighbor method presents a banding effect noticed in some interpolations. Due to the high density of the interpolating 3D RGB matrix, the other two methods lead to similar results, therefore the linear interpolation was implemented by default since it is less computationally demanding than the cubic interpolation.

The multilayer system makes the current model allows obtaining 3D representations and define cutting planes not only on the body surface but also at each anatomical structure. This feature deepens the ability of the 3DBodyGIS to explore the human body. Without this characteristic, when defining a cutting plane, it is not possible to have the perception of the 3D morphology of the internal structures. This lack of perception can be minimized by performing cutting plans for this structure with different perspectives. However, the existence of a surface vector component for each structure and the multilayer system allows, beyond the cross-sectional information, the actual 3D reconstruction and visualization of anatomical structures, i.e., it is possible to directly observe its true shape. Figure 3.21 shows the application of different cutting planes, uncut structures and the use of transparency.

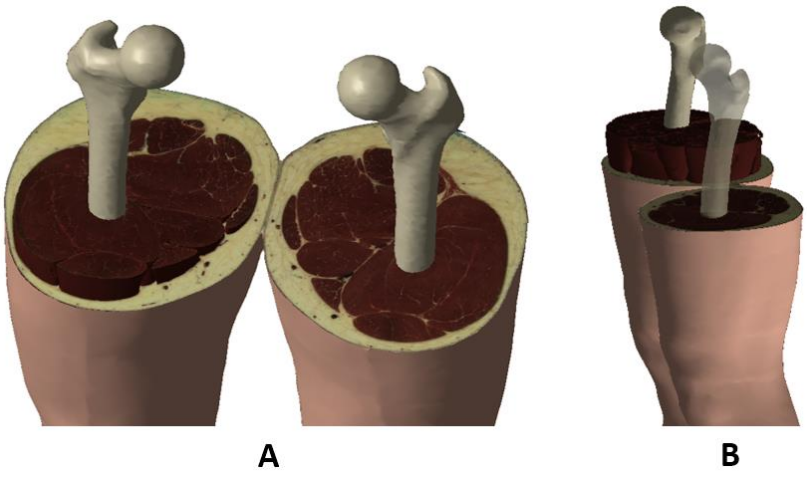

Figure 3.21 - 3D Visualization of anatomical structures.

(A) Defining different cutting planes and representing 3D anatomical structures. (B) Assigning different properties to preselected structures such as setting the degree of transparency.

When defining a cutting plane through the insertion of a needle, the user sets interactively the insertion point, the direction and the depth. Then, the resulting cutting plane corresponds to the plane whose line of maximum gradient coincides with the insertion point and needle direction (Figure 3.22).

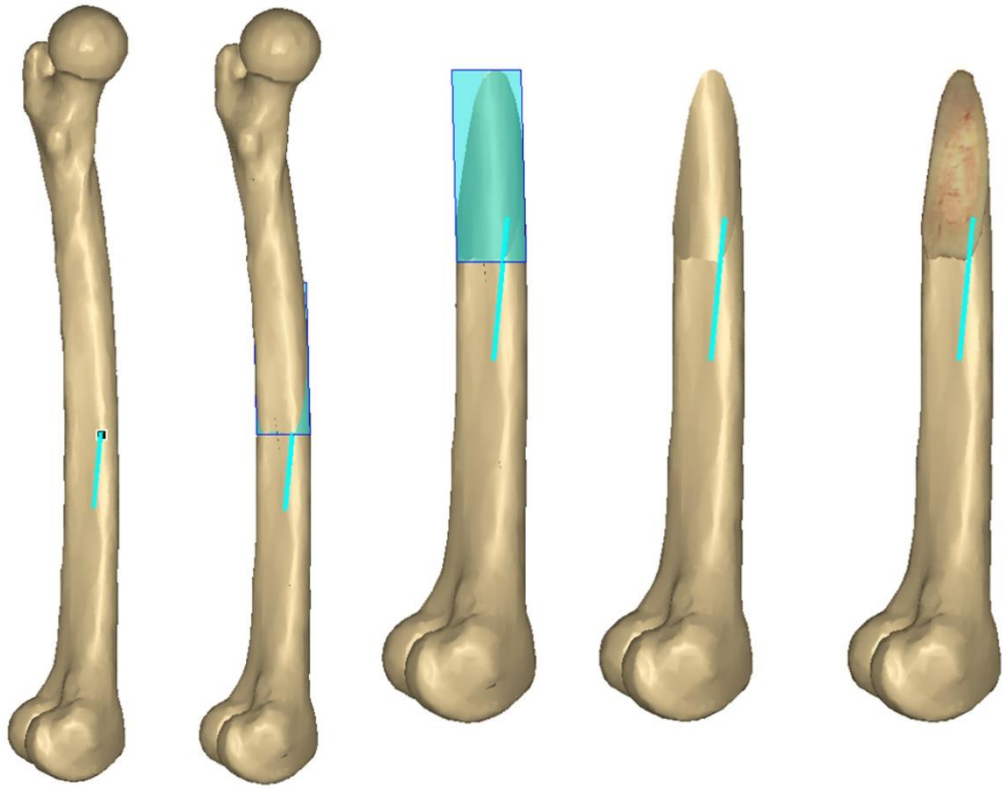

Figure 3.22 - Application of a cutting plane from the interactive insertion of a needle.

GIS depict 2D or 3D maps in their GUI. In the present system, a model of the human body is mapped in a three dimensional space. The forms of visualization of this map are relevant aspects because the adequate communication of information relies on them. To this end, different types of visualization aiming to communicate different aspects of information were implemented, namely, (i) the visualization of internal component with true color (the color in the RGB input images); (ii) the visualization of the internal component with the segmentation color (linked to LM matrix); (iii) the visualization of the vector component with false color (a simulated color for a group of structures, for example, one color for bones and another color for muscles); (iv) the visualization of the surface component with the segmentation color (a color for each segmented structure); (v) the surface texturing component with true color information, and (vi) the display of 3D raster structures in voxel format. Figure 3.23 illustrates some of these visualization methods.

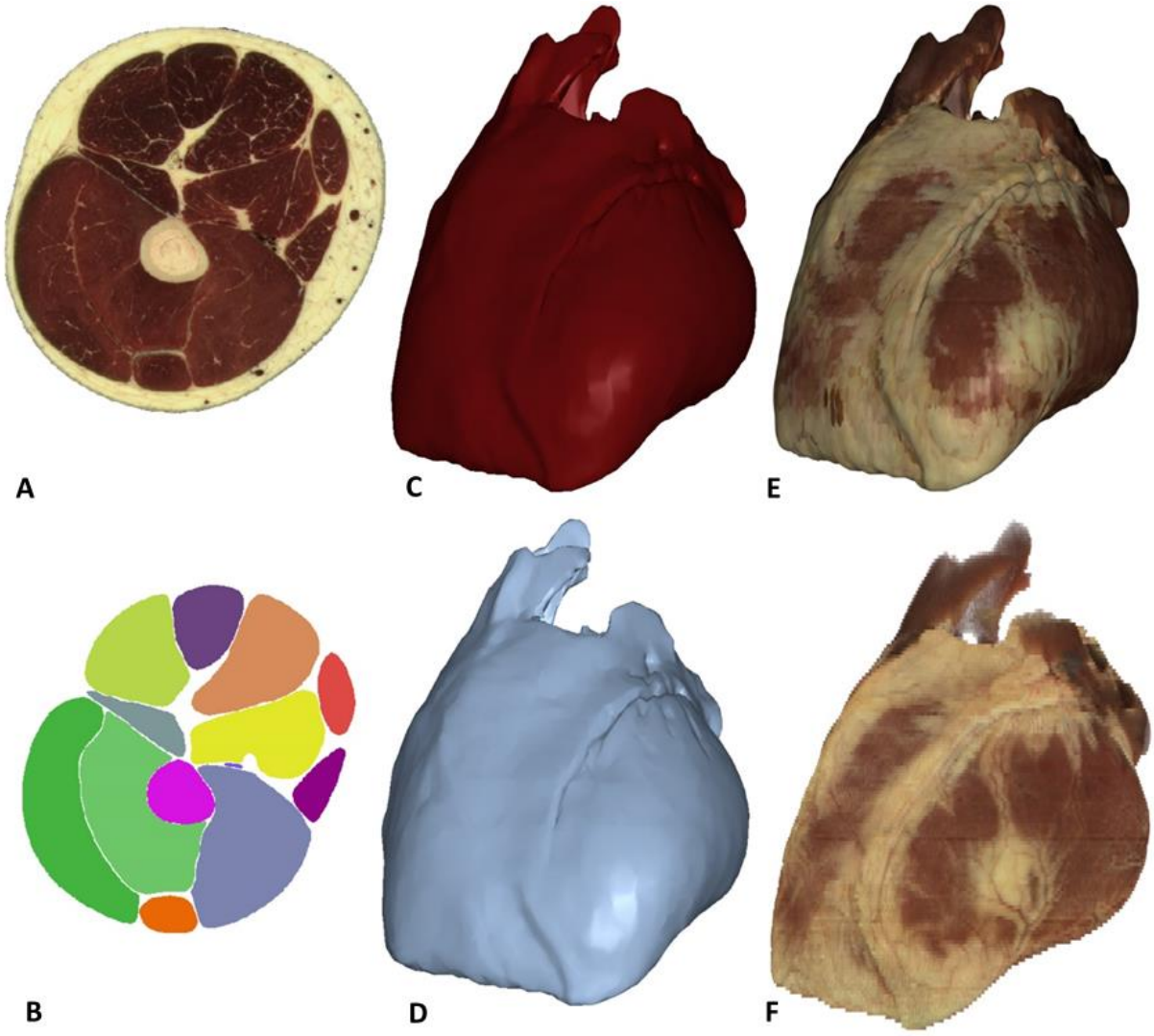

Figure 3.23 - Geovisualization modes available in the prototype.

(A) True color on the raster component. (B) Segmentation color on the raster component. (C) False color on the vector component. (D) Segmentation color on the vector component. (E) Color obtained by texturing the vector component. (F) Voxel component with true color.

3.9. VECTOR-RASTER INTEGRATION

When cutting an anatomical structure, direct visualization of the raster and vector components creates gaps at the periphery of cutting plane. As shown in Figure 3.24 this problem is solved by converting the raster component in a triangle mesh designed to be integrated with the surface component. This vector-raster integration allows to load the GUI only with vector components.

It should be noted that the resampling of the raster component causes some degradation compared to the original data. However, this resampling is required to create the proper color information on

the cutting plane, either using the raster component directly either with the visual integration of the proposed method.

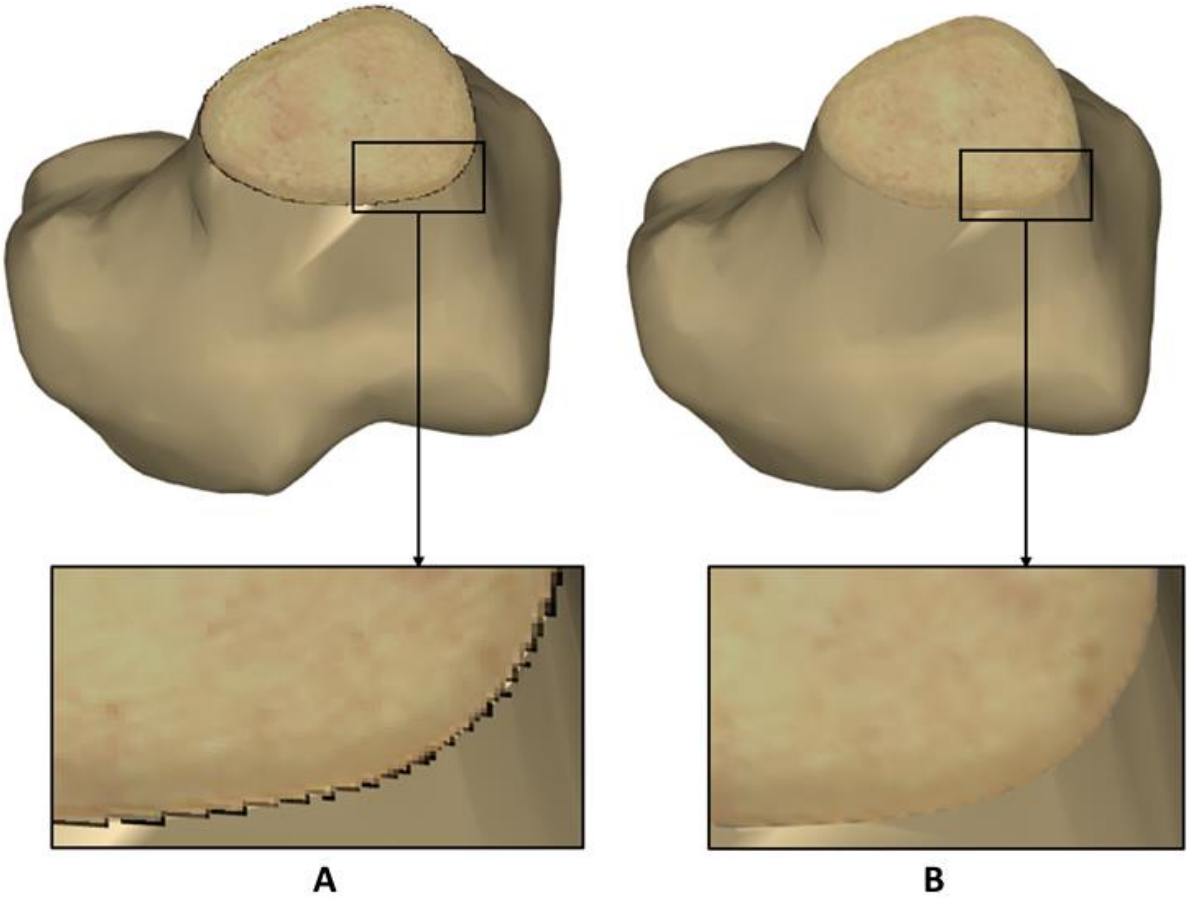

Figure 3.24. Vector-raster visual integration after defining a cutting plane.

(A) Direct visualization of raster and vector components (the mismatch between the two components in the peripheral region is visible). (B) Vector-raster integration by resampling the raster component in the triangulated cutting plane.

3.10. IDENTIFICATION AND EDITING

The functions that act on the model allow to extract information on the surface and within the anatomical structures. Some gaps of information found in the dataset may imply limitations in the developed functions. Chang (1996) describes several errors related with the VHP image collection procedure, including, for example, images without information (totally black images). Another example relates to the collapse of some smaller structures, whereby, they do not appear in the original dataset. It is therefore not possible to obtain adequate information from these structures. To produce

a complete model of the body, these gaps must be corrected. One possibility to overcome this problem is to fill the gaps with simulated information.

GIS connects SI with alphanumeric attributes. Once established the connection, it is possible to retrieve alphanumeric information by identifying the geometric component. In the present work two distinct identification functions were locally built. The first function connects the LM and the vector surface components with the name/description of the corresponding structures. The second function connects the same geometric components to specific hyperlinks, so that, pointing a geometric structure causes a document or web page opening.

The identification function that allows to obtain, at the voxel level, the name of each selected structure, works on the 3D representation. After defining a cutting plane, the identification of the structures can be showed on the RGB or the LM data. In any case, an identification label is generated on the required structures (Figure 3.25) (this function is available on any cutting plane defined by the user).

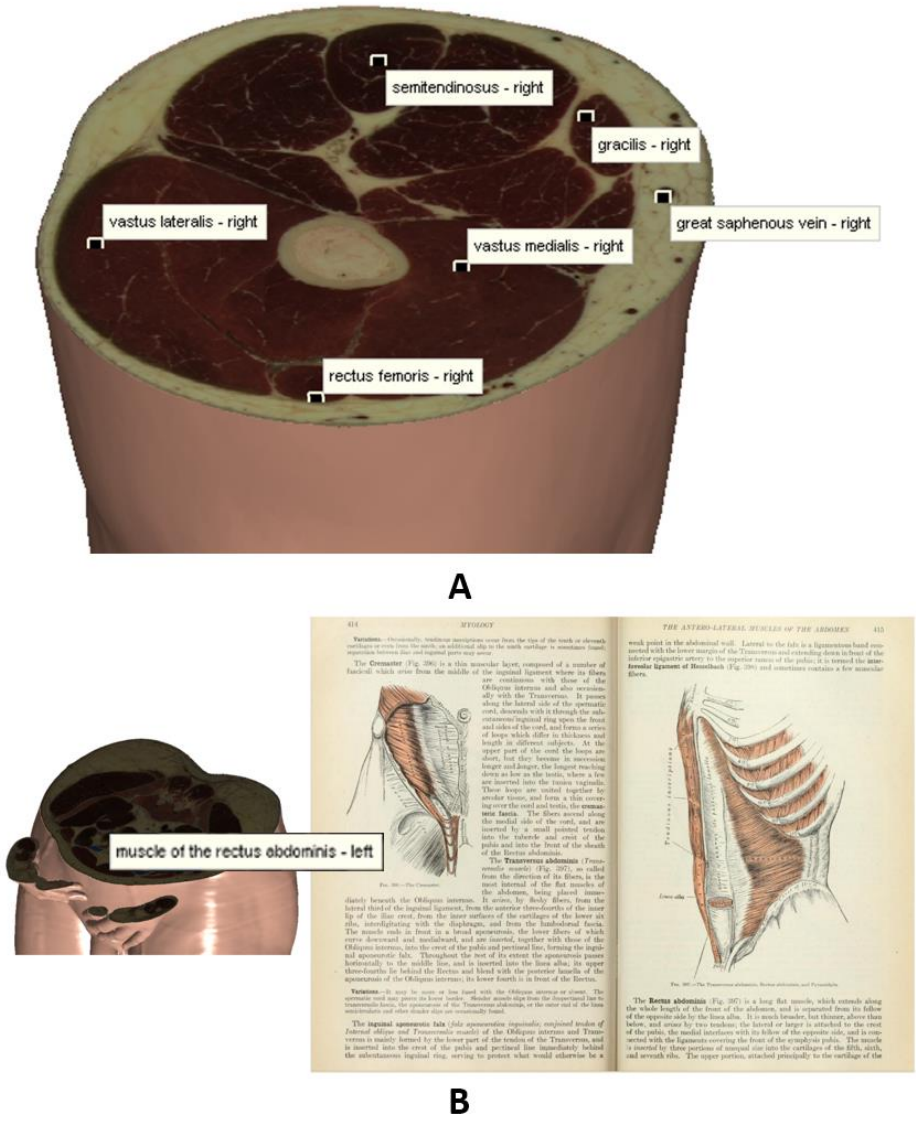

Figure 3.25 - Identification function.

(A) Identification on the RGB image that renders the cutting plane.

(B) Connection to an external document in Open Library web page.

Source: Swartz (2006).

The interactive editing function enables the association of sub-regions on the surface of an anatomical structure with their identification. This functionality is used to produce detailed information for the identification function. By expanding the identification function with this information, it is possible to identify not only an anatomical structure but also the selected sub-region.

The editing functionality begins with the assignment of the region name, followed by its definition on the 3D geometric component through a painting tool. Once accepted the delineated region, the information becomes available in the detailed identification function (Figure 3.26).

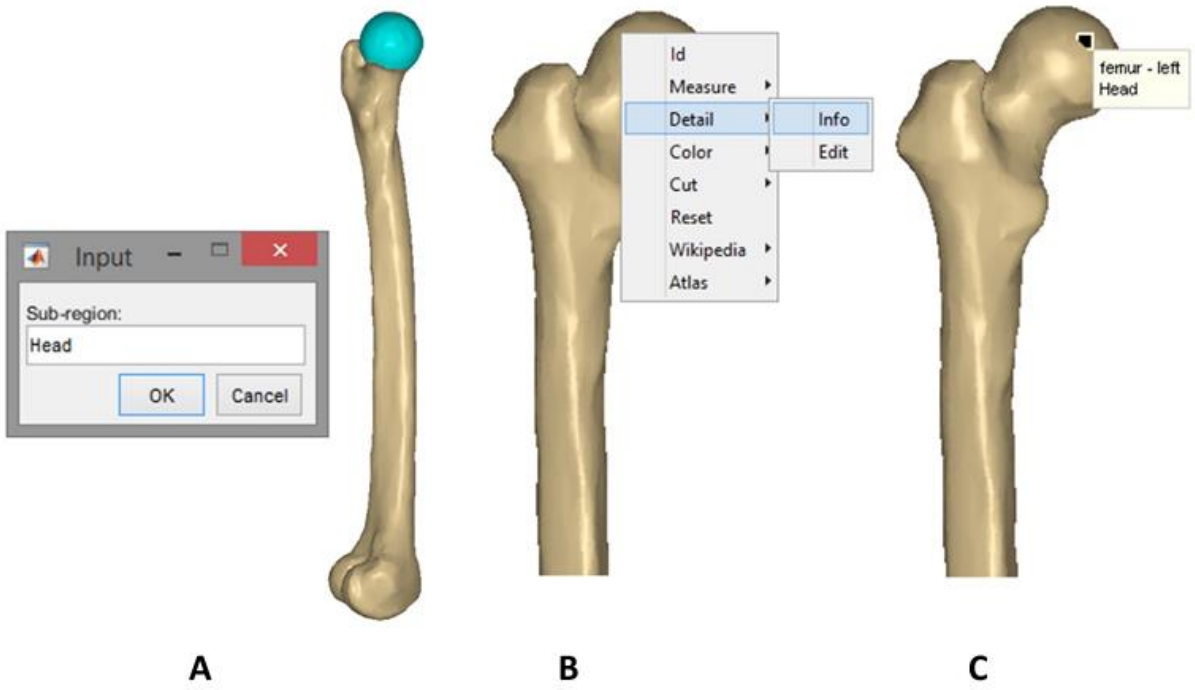

Figure 3.26 - Editing function and detail identification.

(A) Creation of a sub-region in an anatomical structure. (B) Enabling the detail identification function. (C) Applying the detailed identification.

3.11. MEASUREMENT TOOLS

The vector-raster integrated 3D model, with topological capabilities and real dimensions, allows the implementation and application of measurement tools. The functions implemented in the prototype were assessed by comparing results of measurements with reference values available in scientific studies. These tests cannot assess rigorously the precision of the tools, however, they are a good indicator if they are consistent with the values reported in the literature. For the VHP male model, height and weight are, respectively, 186 cm and 104 kg (Caon 2004). Both the height and weight are measures usually used in the calculation of common ratios in anthropometry works and will be used in some of the checks made. These values can be used to calculate the body mass index (BMI) with the following expression (4):

$$BMI = Weight / Height^2 \ (Kg/m^2) \qquad (4)$$

The BMI values can be grouped into four main categories depicted in Table 3.3 (World Health Organization 2013). According to the expression (4) and Table 3.3, the VHP model has a BMI value of 30.1 kg / m^2, which corresponds to an obese condition.

Group	**BMI Interval (Kg/m^2)**
Underwieght	< 18.5
Normal	18.5 a 24.9
Overweight	25 a 29.9
Obese	$\geq$ 30

Table 3.3 - BMI classification.

Of all the measurement tools used (Figure 3.27), measuring the distance between two points, is the only one that does not use model-specific features. This measurement was tested over the left femur and compared with reference values. The length obtained on the model was 48.3 cm. In the study presented by Feldesman et al. (1990), carried out on a sample of 13149 individuals, consisting of 51 populations from different geographic areas, the mean value obtained for the ratio femur/height was 26.74%. Thus, the following formula which relates the length of the femur with height of an individual is proposed (5):

$$Height = femur\ length / 0.2674 \ (cm) \qquad (5)$$

The height calculated by this expression, from the femur length of the value obtained on the model, is approximately 181 cm, which corresponds to a deviation of less than 3% of the actual height of the model. In the study of Strecker et al. (1997) the tibiofemoral relationship is evaluated. In 378 measurements a ratio of 1 to 1.26 ± 0.1 was obtained. The measurement of the left tibia in the model was 40.19 cm, resulting in a ratio of 1 to 1.2, a value that falls within the reference range.

The liver and stomach volumes were determined using the model. The measurement of liver volume was 1720 ml, being the ratio weight / volume liver (kg/l) equal to 60.5 Kg/l. In the study of Kan &

Hopkins (1979), with 22 volunteers without clinical or laboratory evidence of liver disease, estimates were obtained from images generated by single-photon emission computed tomography (SPECT) for this ratio. The average value was 42 kg/l with a standard deviation of 4.91 kg/l.

For the stomach, the references to its volume have a large variability indicating a maximum value of 400 ml (Curtis & Barnes 1994; Rinehart et al. 1998; Wenzel et al. 1998). The measurement performed on the model resulted in a value of 465 ml.

Attending to the obese condition of the model and that this condition was not referred in these studies, it is not possible to conclude about the accuracy / inaccuracy of the volume measurement tools.

To evaluate the area measurement tool, the body surface area (BSA) was determined on the model. The value obtained was 2.13 m2. This value was compared with the values obtained by three expressions which were introduced on separate occasions. The three expressions use the height (cm) and the weight (kg) of the body and return the value in m^2:

Du Bois (Hoppe et al. 1992): $BSA = 0.007184 \times Weight^{0.425} \times Height^{0.725}$ (6)

Mosteller (Mosteller 1987): $BSA = \sqrt{\frac{Weight \times Hight}{3600}}$ (7)

Schlich (for male) (Schlich et al. 2010): $0.000579479 \times Weight^{0.38} \times Height^{1.24}$ (8)

The BSA values obtained for the VHP model according to the expressions (6), (7) and (8) were, respectively, 2.72 m^2, 3.02 m^2 and 1.92 m^2. Beyond these empirical expressions that lead to a wide range of values, we used another study as reference, Verbraecken et al. (2006), which gives intervals around the mean BSA values. This study is based on 1868 patients which were classified into three groups, considering the BMI values: (i) normal group 23 ± 1 kg / m^2; (ii) overweight group, 27 ± 1 kg / m^2; (iii) obese group, 36 ± 6 kg / m^2. The BSA global value was 2.04 ± 0.24 m^2 with 1.81 ± 0.19 m^2 in the normal group, 1.99 ± 0.16 m^2 in the overweight group and 2.21 ± 0.22 m^2 in the obese group. Comparing the measured value with the global values of the study and with the obese group, there is a correspondence between the measurement and the study values.

The measurement along a branched structure allows to validate not only the measurement tools but also the connectivity topological component. Figure 3.28 shows a measurement performed on a set of arteries, which have a branch at the abdominal aorta and the common iliac arteries level. The

application of Dijkstra's algorithm based on the arc-node table that represents these structures, allows finding the path between the two points and determining the total length between them.

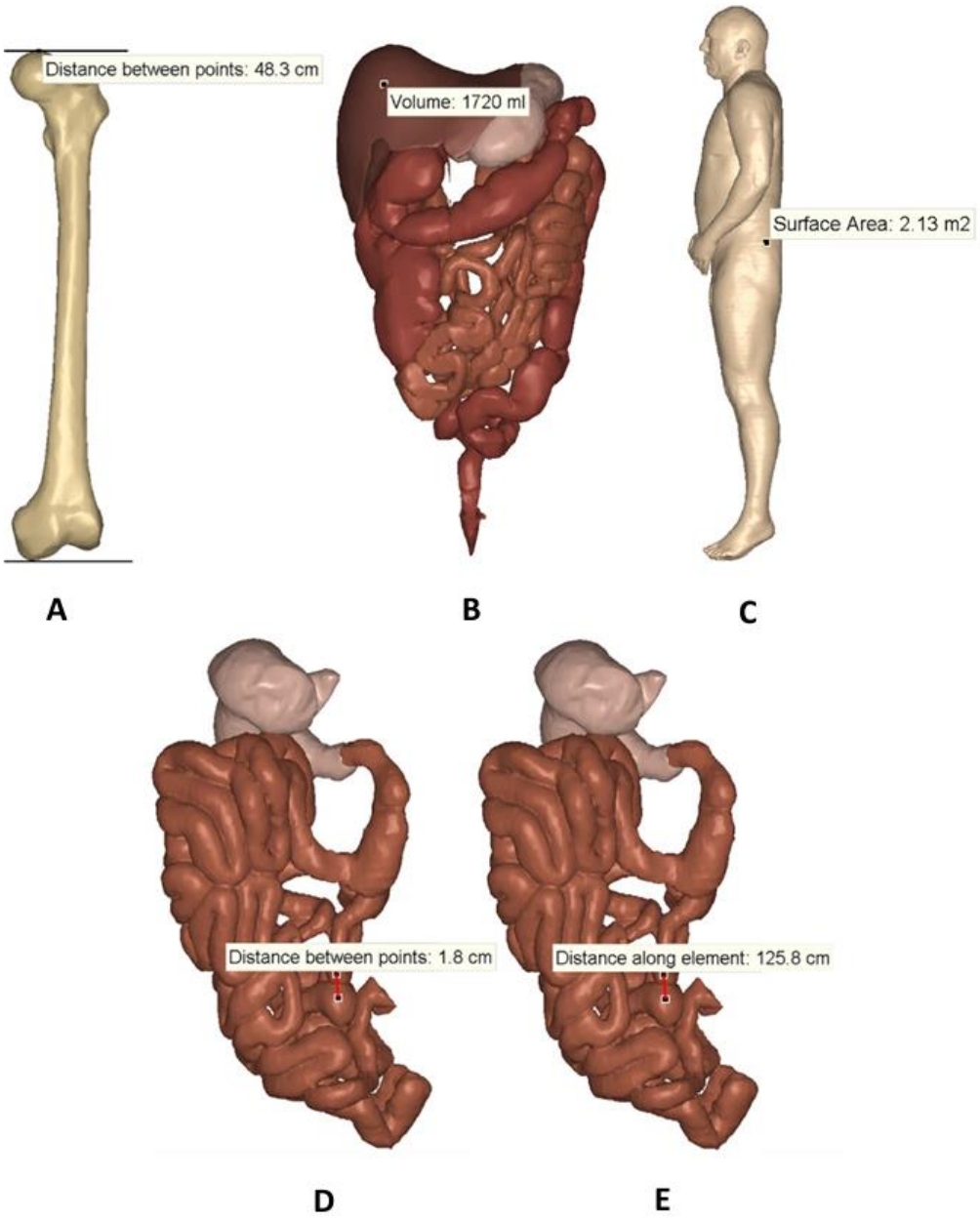

Figure 3.27 - Measurements of anatomical structures.

(A) Measuring the distance between two points. (B) Determination of the liver volume. (C) Measurement of the surface area of the human body. (D) Measuring the distance between two points in the small intestine. (E) Measurement of the distance between two points along the small intestine.

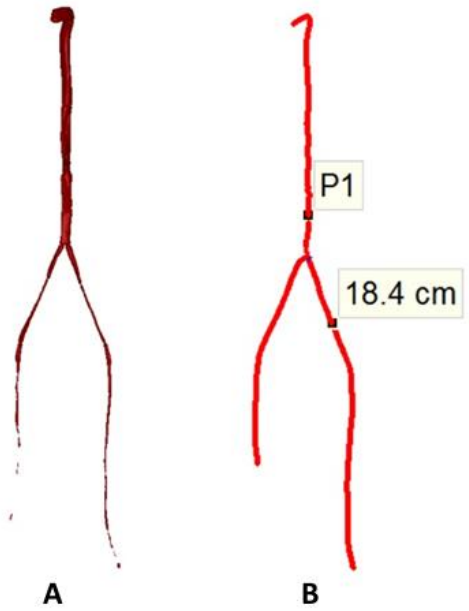

Figure 3.28 - Measurement of length between two points on a set of arteries.

(A) Arteries view (aortic arch, thoracic aorta, abdominal aorta, common iliac artery, external iliac artery, femoral artery). (B) Central axis of a set of arteries represented with a measurement.

3.12. SPATIAL ANALYSIS

Like the identification function, the inclusion function uses the information contained in the LM. This function is designed to simulate a needle insertion into the human body. Once identified the parameters of the needle insertion, the positions of the points along the needle are calculated. Each point is then coded by the value of the surrounding voxel. When all points are coded, the corresponding legend is generated. Figure 3.29 depicts results of the inclusion analysis function, highlighting the discrimination capability of the model.

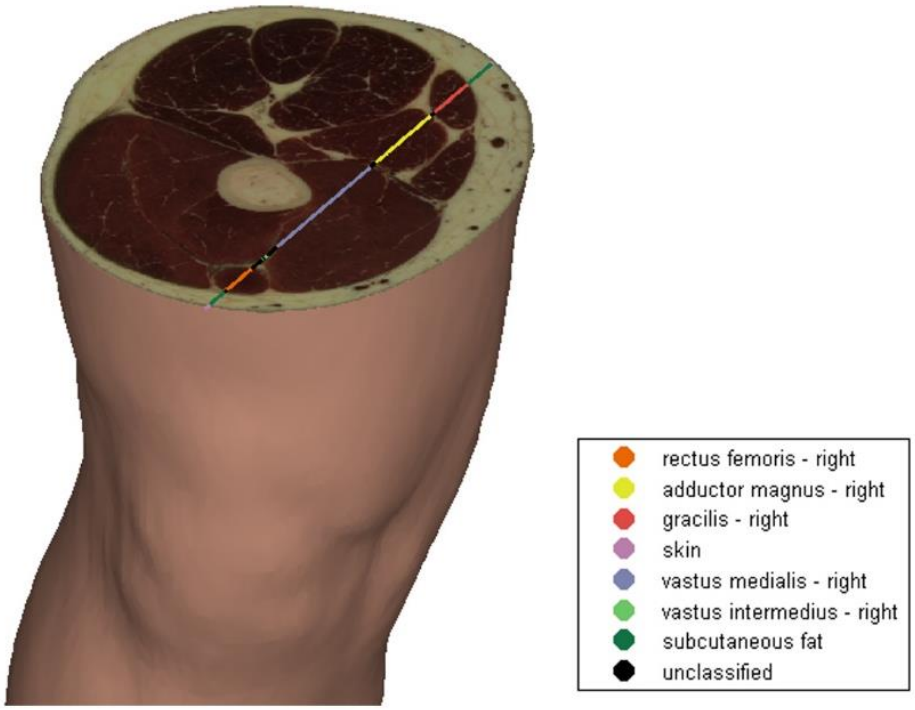

Figure 3.29 – Spatial inclusion analysis.

Performing a spatial inclusion analysis by identifying the anatomical structures crossed by a needle.

The inclusion analysis function has the ability to identify all the structures classified after segmentation and, additionally, creates the unclassified item in the legend to represent non-classified areas.

In the prototype, the neighborhood analysis is based on the same type of topology explicitly described in the model. One of the advantages of using explicit topology is the time gain in spatial analysis operations. To check this time gain, analyzes with and without topology were carried out. Three structures were selected: the femur, the *rectus femoris* and the *vastus lateralis* the left leg. For these structures, their neighbor muscles were determined (Figure 3.30). The first group of analyzes reads the topological neighborhood tables. In the second experience, a non-topological system was simulated, requiring on-the-fly determination of the requested topology.

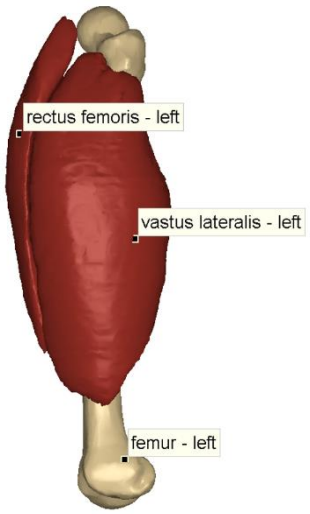

Figure 3.30 – Global spatial neighborhood analysis.

Structures for which was made a neighborhood analysis having as target the whole left leg muscles.

The results and the run times of analyzes are shown in Table 3.4. The analysis of this table shows that the non-inclusion of topology in the model leads to a runtime, which is, in average, 254.5 times higher. The magnitude of this value shows the importance of having a topological model to perform neighborhood spatial analysis.

Structure	**Analysis result**	**Running time (in seconds) with / without topology**
Femur	*adductor brevis, adductor magnus, gluteus medius, obturator externus, quadratus femoris, biceps femoris, vastus intermedius, vastus lateralis, vastus medialis*	0.04 / 8.05
Rectus femoris	*sartorius, tensor fasciae latae, vastus intermedius, vastus lateralis, vastus medialis*	0.04 / 8.38
Vastus lateralis	*rectus femoris, tensor fasciae latae, vastus intermedius*	0.04 / 14.11

Table 3.4 - Determination of the left leg muscles that are neighbors of a predetermined structure.

The expansion of the neighborhood topological component takes place with the implementation of tables that describe the neighboring structures at the vertex level. With this information available, it becomes possible to determine the structures in the neighborhood of a sub-region of a predefined structure. Table 3.5 shows the neighboring muscles of the femur: in the first column, the analysis is

made to the whole structure and, in the second, to the upper half of the bone. By analyzing this table it can be seen that the short head of *biceps femoris* is taken from the result of the second analysis. The position of this structure relative to the femur is shown in Figure 3.31, where it can be seen that it is not neighbor of the upper half of the femur.

Adjacent muscles of the femur	**Adjacent muscles of the upper half of the femur**
adductor brevis, adductor magnus, gluteus medius, obturator externus, quadratus femoris, short head of the biceps femoris, vastus intermedius, vastus lateralis, vastus medialis	*adductor brevis, adductor magnus, gluteus medius, obturator externus, quadratus femoris, vastus intermedius, vastus lateralis, vastus medialis*

Table 3.5 - Spatial neighborhood analysis. Determination of the left leg muscles that are neighbors of the total and the top half of the femur.

Figure 3.31 – Restricted spatial neighborhood analysis.

Verifying that the short head of *biceps femoris* is not neighbor of the upper half of the femur.

4. DISCUSSION

Considering the objectives of this study, the following items emerge as fundamental to validate the model:

- Construction of the volume model: the integration of surface and internal components was implemented in the model structure. The tools for simultaneous display of the two components, based on cutting planes defined by the user, were also developed;
- Realistic vector model: after reducing the density of the triangles and smoothing the vector component, it is possible to eliminate the pixelization effect;
- RMSE: the obtained value of 0.18 mm means that the vector model, although manipulated in order to optimize the visual appearance, adheres significantly to the raster data set;
- Representation in GUI: the algorithm that converts the structural model in a visual temporary model allows a realistic viewing and an effective interaction;
- Inclusion analysis: the raster-vector integration transforms an inclusion analysis into a simple data reading operation.

This model fulfils the purpose of representing the surface of the body integrated with its interior, i.e., it constitutes a volume model for the human body. The vector component of the model accomplishes the goal of reproducing the properties of the vector model mentioned in Section 3.5. The raster component comprises 3D matrices, obtained from a sequence of axial images of the body. The integration of the vector component with the raster matrices occurs not only in terms of visualization but also in terms of the model structure. For this purpose, the voxels of the LM are connected to the layer of the surface to which they belong. This connection allows the integrated representation of the surface and the interior of the human body, and provides, e.g., point-in-polyhedron analysis capability in a simple way.

The visualization method of the internal component constitutes a relevant characteristic of the model: the use of cutting planes, the model structure and its previous manipulation, were conceived to minimize the data used in the graphic environment. This characteristic optimizes the visualization and interaction with the model.

The design, development and implementation of the final prototype, the 3DBodyGIS, involved several processes that lead to intermediate and final results, which are discussed in this chapter. The topics relevant to draw conclusions are ordered in a way to make understandable the procedure from the input data until the implementation of 3DBodyGIS. In practice, the relationship of interdependence between the various processes that contributed to the construction of the model, the results obtained

at intermediate stages and at different times, led to iterations, corrections and optimizations that change, to some extent, the actual procedure from the sequence used in the presentation.

The implementation of much of the prototype functionality was carried out using methods and algorithms widely known in the field of GIS. The methods, specifically developed in this work, are related to tasks linked to the development of the software and of some components of the model, as well as model-specific features for problem solving. An example of the latter situation is the sub-set of tasks involved in defining cutting planes in a model with the features of the one that is presented in this dissertation: this procedure required the implementation of solutions specifically designed to operate on the integrated model.

In the sections that follow, the main steps that have guided this work are analyzed and discussed.

4.1. Segmentation Environment: Integration of RGB and CT Images

The developed segmentation tools are presented in two modules that were integrated through functions for converting the segmentations of a coordinate system into the other. In the initial phase of the work, a module that operated on RGB images was developed. This is a usual way to operate with the type of data used in this work as was referenced in previous chapters. Another option was to create a semi-automatic environment that attempts to approximate as much as possible the manual intervention with the automatic procedures.

The choice of a semi-automatic method, on the one hand, proved to be mandatory in this type of work because, considering 3D reconstruction of anatomical structures based on the results of 2D segmentation, the acceptance of a certain margin of error in the segmentation procedures would, in certain cases, result in deformed 3D models. On the other hand, the deepening of the manual-automatic integration, allows to maximize the efficiency of manual interventions whenever they are required.

The use of RGB images on segmentation procedures presents difficulties, particularly in two situations, by the number of times they occur and by the time spent in its resolution. The first relates, for example, to the existence of the same tissue, which has distinct classifications in neighboring regions (the muscle tissue is a recurring situation of this kind of difficulty). The second situation has to do with the existence of joints and tendons in the neighborhood of bones. In the segmentation module two procedures were developed that mitigated this kind of difficulties. In addition to the automatic application of an RGB ellipsoid, after the manual definition of a study area to propose an initial segmentation region, a

manual construction of polygons that frames the segmentation zone allows to restrict the segmented area in the regions where it exceeds the area to classify. The incorporation of an image-matching technique allows, once a segmentation polygon is properly set, its transfer to the next image. This polygon can be adjusted by manual intervention.

In a second iteration of the work, another module was developed aimed at solving the problem involving the segmentation of bones. In fact, although this segmentation has been performed specifically with the tools developed in the first module, it was necessary to use some images previously segmented by professionals on this type of data. Still, the adjustment of the area to segment involves always some degree of ambiguity given the similarity with some of its neighboring structures. The second segmentation module uses the CT images also made available by the VHP. The segmentation principle of this module comprises applying a threshold value such that only hard tissues are highlighted. This type of segmentation solves the problem encountered in bones but requires an additional procedure given the fact that RGB and CT images have different dimensions and spatial resolutions, which results in different coordinate systems. This means that the segmentation results of the two modules cannot be directly overlaid. The integration of the two modules was made through a system that allows operating interactively on the CT segmented images and through the application of translations and scaling factors, making it possible to convert the CT image coordinate system to the one of the RGB image.

The semi-automatic method has been employed to obtain 43278 segmentations. We note that the knowledge of human anatomy is essential in this type of operation and, in the particular case of this work, the morphology of anatomical structures arranged in sectional images. In this study, this requirement has been met by consulting images that reproduce segmentations of anatomical structures on axial images.

4.2. Point Clouds and Reconstruction of Vector Components

From the point of view of 3D reconstruction of anatomical structures, the segmentations provide points in horizontal planes, separated by 1-mm distance, corresponding to the periphery of the anatomical structure.

To reach the final 3D reconstruction procedure, algorithms and additional filtering were tested in order to obtain visually acceptable results.

Tests conducted with alpha-shape algorithms failed to produce the desired closed boundary surfaces of anatomical structures. These tests highlighted the specific characteristics of the data used in the 3D reconstruction. The works involving reconstruction of 3D objects usually use thick clouds of points obtained by 3D scanners. In this study, the cloud of points materializes, in each horizontal plane, the equivalent to contour lines similar to the ones used in cartographic representations. A consequence of providing the data in this way is that in areas of low slope the spacing between lines increases.

This means that in the point cloud produced, whenever there are areas with lower slope, the spacing between border points increases. This can be seen, for example, in the upper shoulder region. In these regions, the alpha-shape method was not able to connect the dots, thereby producing open areas. The tuning of alpha-shapes for these areas leads, on one hand, to a loss of sensitivity in more pronounced curvature areas, leading to degradation of the final result. The screened Poisson method led to satisfactory results, and has been complemented by filtering in order to smooth the final surface. To some extent it was also possible to reduce the final number of triangles of each surface with the goal of reducing the amount of data present in the GUI. For that, the observable morphology of the anatomical structure should be preserved. The reduction percentage differs, therefore, from structure to structure.

The 3D model reconstruction showed that the methods employed in this procedure can be somewhat difficult to operate with the kind of data used in this work. An illustrative example of this situation are the intestines. Due to the way they are accommodated inside the body, the small intestine, for example, is very compacted in multiple regions and folded upon itself. The use of 3D reconstruction procedures on this structure only models the border regions corresponding to the segmentations, which means that many of the actual peripheral areas of the intestine are lost. This feature prevents, for example, a correct definition of the central axes of the intestines.

4.3. Integration of Raster and Vector Components

This phase corresponds to the implementation of the geometric component of the integrated model. The raster model components are composed by the voxel matrix, which comes from the RGB input images and contains true color information from within the anatomical structures, and by the LM matrix, which contains the segmentation information carried out in the first phase of work.

The second matrix contains the ID number of the several segmented structures, information which is used to integrate the surface vector components of the anatomical structures. The integration of the two components allows the GUI to reproduce the 3D shape of each structure across the surface, being

the raster component used visually only when called to render cutting planes when these are defined. This way of operating allows to reduce the volume of this data in the GUI, which is vital to improve the experience of handling the 3D model. Another aspect of the geometric construction of the model consists in defining central axes of anatomical structures which may be regarded as progressing linearly in space. This model component, although having no actual anatomical existence, allows the development of one of the topological components of the model.

4.4. DIRECT USE OF VHP DATA AND VISUALIZATION OF THE MODEL INTERIOR

The input data obtained from a 3D body are, per se, 2D. Before reproducing the model in 3D, a module that allows to explore the data directly was developed, i.e., the axial images of the human body. Although this kind of functionality does not allow to go far beyond the data, it is a direct way to perceive them, since the various images can be successively made available and, ultimately, be displayed successively simulating a video sequence. The application of an identification function in this module and the inclusion of the coronal and sagittal planes adds information regarding the simple observation of images.

One of the fundamental features of the prototype is the possibility of observing the morphology of the anatomical structures in a 3D space and, simultaneously, to show the interior interactively with user defined areas (and not just in horizontal planes corresponding to the input data).

The definition of cutting plans can be made with two different tools. The interactive enforcement of three points on the surface of a structure and the simulation of the insertion of a needle, which in turn defines a cutting plane.

In the first case, a plane is set passing by three points and, in the second case, the plane, whose line of maximum gradient contains the needle inserted interactively, is built. This way of accessing the model's interior surpasses the traditional approaches, in which the anatomical structures are classified in a finite set of images / maps, that is, the user cannot observe the whole structure or any desired plane and, much less, a plane set interactively in a region with a user defined orientation.

4.5. TOPOLOGY CONSTRUCTION

One of the typical characteristics of GIS is the existence of topological relationships explicitly defined in their data models, including neighborhood, inclusion and connectivity.

The explanation of the segmented structures via the LM sets, for itself, a form of inclusion topology. In GIS, the inclusion of topology consists in defining this kind of relationships that exist between objects of the model, which is not defined in the current model. However, the information in the LM may be used to support point-in-polyhedron inclusion analysis by reading directly the contents of this matrix. This model feature supported the function of simulating the insertion of a needle into the human body returning the crossed structures in the process.

The neighborhood topology has been implemented in the model on two levels: the first is accomplished by defining comprehensive listings of nearby structures (within the segmented structures) of each of the anatomical structures. This type of information allows us to respond efficiently to the question of which are the neighboring structures of a predetermined structure. The other type of topological neighborhood information is similar to the above but occurs at each vertex structure, i.e., for each vertex of surface components of each anatomical structure, the model contains the information of the neighboring structures. This second level of information allows also to perform neighborhood analysis but, in this case, with the possibility to determine on the neighboring structures of a predetermined structure sub-region.

Although this information allows to replicate the analysis made in the first case, this first information remains in the model structure because, in that particular context, it allows to obtain results more quickly.

As verified in this work, the execution of this kind of analysis with the support of neighborhood topology contributed to a very substantial reduction in involved operating times.

4.6. Integrating the Model in a GIS Prototype

The emulation of a GIS platform comprises the topological data model, a GUI and a set of functions that give the system an analogous functionality to the GIS when implemented using SI.

In the current system these three components were developed and integrated following closely the implementation of GIS software: the model contains topological properties and their geometric component can be accessed through the GUI. The interaction with the model allows the access to alphanumeric information and to perform a series of operations to explore the data and produce new information from spatial analysis operations.

The greatest difficulty in the approach of the current system to traditional GIS has to do with the fact that it is a 3D system that offers tools to interact and analyze a 3D model. This situation is not also the most common in modern GIS.

4.7. PROTOTYPE FUNCTIONS

With the development of the model and its integration in a GUI, it is imperative to enable the exploitation of the information contained therein.

Navigation Tools

A first set of functions are the tools that allow to visually explore the model, i.e., the navigation tools. Through these, it is possible to rotate, move and scale the model. When the volume of information in the GUI is high, these operations become more time-consuming. Thus, some typical anatomy predefined views were included to position the model more quickly.

Multilayer Management

The layer concept is inseparable from the GIS software implementation. This concept allows not only to structure the information contained in the system but also to perform operations on specific pre-selected layers. The developed interface includes this type of information management. Being the anatomical atlas, a very specific case of type and organization of information, the system interface was provided with a TOC that hosts three classification systems. These systems reproduce the hierarchical classification of anatomical structures found in the platforms that operate with anatomical information. This approach has three main advantages: the first comes from having a multilayer system, as usually happens in GIS, allowing to handle the visualization of structures as overlaid transparencies, each one with its structure; the second advantage concerns the option of implementing in the TOC an hierarchical tree which enables the access to the desired information more efficiently in comparison with a system that would only list the anatomical structures in alphabetical order. Finally, the third advantage relates to the possibility of opting for alternative classifications as some selections may work better with a certain type of classification: to choose all the leg muscles, it will be more efficient to use a classification system for regions than for tissues, noting that within each region, the muscles subgroup arise.

Identification and editing Functions

The identification function included in the prototype has various functionalities with different features.

The identification of the raster component can occur in two ways: the first is to produce a label showing the name of the region indicated interactively; the second mode joins a segmented image to an RGB image that is being displayed and creates a legend where its structures are described (as long as segmented) in that RGB image.

The identification function on the vector component presents four distinct modes: the first, similar to what happens with the raster component, generates a label with the name of the structure selected interactively; the second corresponds to the detail information and displays the name of an anatomic region in a given structure; the third allows to connect the selected structure to a specific page of a document in the computer while the fourth connects via URL to a page or document on the Internet.

The editing function allows to draw over the 3D component a given sub-region of an anatomical structure that, after validation, could be used by the detailed identification function.

Measurement Tools: Volume, Area, Distance and Length of Anatomical Structures

The anthropometry issue is very relevant in the health area being the subject of many works as verified in the course of this study. In GIS, the existence of measurement tools is common as these systems aim to provide accurate SI. The present system takes advantage of model features to implement several measurement tools, except for the distance between two measuring points which depends only on these points. The volume measurement of an anatomical structure is carried out counting the voxels of the structure which are described in the LM; the measurement of the surface area of the structures consists in determining the areas of the triangles that constitute them; and finally, the measurement along the structures with possible branches, makes use of the central axes of these structures and connectivity topology implemented through the arc-node tables.

The measurements obtained with these tools were compared with reference values / ratios. Assuming that the model may have values outside the benchmarks, several measurements fall within these ranges.

Visualization Functions: False Color, Segmentation Color and Real Color

A good implementation of GIS should take into account the problem of cartographic communication. GIS, as a tool that allows to map a given space, must have the ability to communicate in an accessible and direct way the information represented. The ability to communicate directly and unambiguously the available maps is related with the adequate choice of symbols used, which implies a good selection of various visual variables (e.g., color, brightness, saturation, patterns, texture, etc.) and non-unnecessarily burdening the representation. The ability to choose different types of color components on the raster and vector model allows a better reading of the structures: (i) the texturing of 3D structures with true color allows a more realistic reading. However, the use of false color overloads less the GUI allowing to operate more quickly; (ii) the identification of a structure on a sectional image may not be fully informative about which is the boundary line on that structure. The combined use of segmentation color enables not only to display the structure but also to know the region occupied by it.

Spatial Analysis

The spatial analysis functions take advantage of topological components of the model. The development of a function that simulates the insertion of a needle into the human body activates the cut of the structure according to the interactively defined insertion parameters and analyzes which anatomical structures were crossed in these conditions. The results are shown through a label that identifies the colors created along the needle, which correspond to the different crossed anatomical structures.

Given the type of neighborhood topology tables included in the system, the neighborhood analysis functions have the ability to determine the neighboring structures of a preselected structure, or just a part of it.

These functions materialize one of the typical characteristics of GIS: the ability to produce new information from the data available, in contrast to systems that only allow the displaying of the available information.

5. CONCLUSIONS

The final result of this work is the 3DBodyGIS prototype which operates with SI of the human body. This prototype was developed to meet the main objective of this work, i.e. to develop an anatomical atlas of the human body through a GIS approach. This objective and the working assumptions, the feasibility and the opportunity of such system, were established in section 1.2. Thus, to validate the final result of the thesis, the 3DBodyGIS prototype, it is necessary to verify whether the objectives have been achieved and the assumptions were validated.

The objective and the first assumption underlying the present work are demonstrated by the implementation of the 3DBodyGIS prototype. As stated in section 1.2, the second assumption, the opportunity of the developed system, could be evaluated regarding (i) its capacity in delivering the information typically available in anatomical atlases and (ii) the added value brought to these documents / systems through the GIS approach.

The first question is, therefore, whether the system can replicate the information provided by anatomical atlases? To answer this question two types of anatomical atlases, related with the developed system, are observed. The first type comprises the sectional anatomy atlases and the second type, the anatomical 3D atlases.

The sectional anatomy atlases are closely linked to the type of input data in this study. In this type of systems it is usual to present a finite number of cross-sectional images of the human body. These images can be RGB, CT, designed manually or other. Alongside each of these images, a representation is done, for example, using a drawing that shows the definition of the anatomical structures depicted in the first image, which are associated, for example, to the numbering which originates a legend with the respective identification. The set of input images of this work allows to show more than 1,800 of these images (a number higher than normally found in sectional anatomy atlases) but does not generate more information than that. With the production of segmentations it is possible to add a segmented image of any of the original RGB images and, through the developed identification functions, to create labels of any structure or generating legends discriminating all structures present in the image. Thus, the replication of the information provided by sectional anatomy atlases is achieved.

The 3D anatomy atlases present models of the human body in a 3D space. These atlases usually have a layer system to manage information (show / hide anatomical structures) and have identification functions that allow returning the names of the requested structures. Many of these systems are purely surface vector being the inner component hollow. So, they allow only to observe the

morphological and color on the surface of the structures which, although well designed, do not really correspond to the real color. Some systems, for example, the ones developed from the VHP data, allow to observe the interior of the anatomical structures. The metric capabilities are quite unusual in these systems and, although present, all the description given so far about the 3D anatomical atlases is only a small part of the 3DBodyGIS. All other features, including interactive cutting planes setting, spatial analysis functions, length measurements along the structures, connection to external documentation, eventually created by the user, are presented as added-value provided by the GIS approach in mapping the human body.

5.1. MODEL LIMITATIONS

As in any model that seeks to represent a certain reality, this one has its own limitations. Some of these limitations are related to the nature of the input data, other with the processes used in its construction.

Regarding the 3D reconstruction process, the vector surface components lose texture, present in the real structures, after the filtering procedures. However, the absence of these filtering procedures, would lead to surfaces with pixelated aspect given the nature of the data. Another problem in the 3D reconstruction is the one that was described in the case of compact structures and are folded upon themselves. In this case, the 3D reconstruction routines cannot detect the entire outer surface of the anatomical structures, joining areas that are actually just nearby. This phenomenon results in an incorrect representation of the anatomical structure itself and leads, therefore, to an inadequate definition of the central axis of the structure.

Another limitation of the prototype is related to the performance on the 3D interface. Indeed, the environment in which the prototype was developed has very favorable characteristics to the implementation of this research work. However, its performance in terms of graphics capability is below that of other environments that use lower-level programming languages.

The initial model itself constitutes a clear limitation regarding the representation of an anatomical model: in the study of anatomical models it is usual to dispose them in an anatomical position. In this model, we can observe the hands on the abdomen and the foot soles are somewhat facing each other.

Finally, although the GIS tool set has been tested, further testing will be required in the most appropriate medical context. In fact, it is not enough that the tools execute several tasks, being also necessary to check its suitability to the medical area requirements. The development of various measuring tools illustrates this situation. Several tests were performed and compared with reference

values obtained in scientific papers. It would however be necessary to test these tools in specific medical conditions to verify their actual accuracy and, moreover, notice how it would be interesting to expand its functionality to answer relevant questions: beyond measuring total volumes of anatomical structures is it relevant to measure parts thereof? How to define these regions? The same questions could be placed for the area measurements.

5.2. FUTURE RESEARCH

Some of the future research possibilities opened up by this work are related to the limitations described. The current model only uses VHP data. However, its structure may contain higher resolution images representing specific areas of the human body. In this case, after their geo-referencing, according to the coordinates of the 3D model, they can be associated with intervals of predefined scales. This GIS typical feature allows to manage the images visualization by selecting those with the most suitable detail according to the actual scale.

A possibly more complex problem relates to the use / design of 3D reconstruction methods which present better results with the specific data of this work, especially in the situations in which they present more difficulties, namely, the application of filters to remove the pixelation effect with loss of the original texture, and poor reproduction of structures that fold upon themselves.

The exploration of dynamic handling of the model is another aspect to consider. This issue could be addressed as follows: (i) consider the segmented bone structure, laid out in as many layers as the individual bones present; (ii) reproduce a skeleton to define the joint areas and to create a file to provide motion parameters as, for example, a Biovision hierarchical data file (BVH); (iii) with this file, define a set of routines that lead this dynamic skeleton to take an anatomical position; (iv) finally, by combining the real skeleton with the dynamic skeleton, we will put the skeleton of the VHP in an anatomical position.

The incorporation of information in semi real-time by the system is another possibility for future research. In this case, the system would be supplied with one set of images obtained on patient, reproducing a model with the approximate characteristics of the developed model. Then, it would be possible to apply the functions developed for this platform.

Spatio-temporal models are present in many GIS applications. (Caluwe et al. 2013). With regard to the representation of the human body, this issue can be reflected in the creation of two or more models that may then be compared with the proper tools. For instance, a first standard model can be built to

simulate a clinically healthy body. The system can then be loaded with models derived from real bodies, which can be compared to the standard model in order to study and evaluate eventual differences.

Finally, it would be relevant to validate the prototype on a global basis in conditions closer to the medical requirements with the participation of experts in order to contribute with their vision and with an informed opinion on limitations and model development possibilities in terms of making adjustments or increase functionality.

6. REFERENCES

Abdul-Rahman, A. & Pilouk, M., 2008. *Spatial data modelling for 3D GIS*, Berlin ; New York: Springer. Available at: http://www.loc.gov/catdir/enhancements/fy0904/2007932286-d.html.

Abrahams, P.H. et al., 1998. *McMinn's Color Atlas of Human Anatomy*, Mosby. Available at: https://books.google.pt/books?id=i6tqAAAAMAAJ.

Aggarwal, J.K. & Xia, L., 2014. Human activity recognition from 3D data: A review. *Pattern Recognition Letters*, 48(0), pp.70–80. Available at: http://www.sciencedirect.com/science/article/pii/S0167865514001299.

Agur, A.M.R., Dalley, A.F. & Grant, J.C.B., 2013. *Grant's Atlas of Anatomy*, Wolters Kluwer Health/Lippincott Williams & Wilkins. Available at: https://books.google.pt/books?id=SmflHHbed4EC.

Akkiraju, N. et al., 1995. Alpha shapes: definition and software. In *Proceedings of the 1st International Computational Geometry Software Workshop*. pp. 63–66.

Alliez, P. et al., 2007. Voronoi-based variational reconstruction of unoriented point sets. In *Symposium on Geometry processing*. pp. 39–48.

Anatronica, 2010. Interactive Anatomy 3D. Available at: http://www.anatronica.com/systems.html [Accessed May 20, 2015].

Argosy Publications, 2008. Visible Body. Available at: http://www.visiblebody.com/index.html [Accessed June 20, 2014].

Auchincloss, A.H. et al., 2012. A review of spatial methods in epidemiology, 2000--2010. *Annual review of public health*, 33, p.107.

Barbeito, A. et al., 2014. An Integrated Model of the Human Body. In *Portuguese Association for Information Systems (CAPSI), 2014 14th Conference on Health Information Systems*.

Barbeito, A., Cabral, P. & Painho, M., 2011. Human body modeling in geographic information systems. In *Information Systems and Technologies (CISTI), 2011 6th Iberian Conference on*. pp. 1–6.

Berger, M. et al., 2014. State of the Art in Surface Reconstruction from Point Clouds. In *Eurographics 2014 - State of the Art Reports*. EUROGRAPHICS star report. Strasbourg, France, pp. 161–185. Available at: https://hal.inria.fr/hal-01017700.

Beveridge, E. et al., 2013. 3D visualisation for education, diagnosis and treatment of lliotibial band syndrome. In *Computer Medical Applications (ICCMA), 2013 International Conference on*. pp. 1–6.

Beylot, P. et al., 1996. 3D interactive topological modeling using visible human dataset. In *Computer Graphics Forum*. Wiley Online Library, pp. 33–44.

Biodigital Human, 2013. Biodigital Human. , (25/4/2015). Available at: https://human.biodigital.com/index.html.

Bonham-Carter, G.F., 2014. *Geographic information systems for geoscientists: modelling with GIS*, Elsevier.

Bracewell, R.N., 2000. *The Fourier Transform and Its Applications*, McGraw Hill. Available at: https://books.google.pt/books?id=ecH2KgAACAAJ.

Burrough, P.A., 1986. *Principles of geographical information systems for land resources assessment*, Clarendon Press. Available at: https://books.google.pt/books?id=KsMsAQAAMAAJ.

Burrough, P.A., McDonnell, R.A. & Lloyd, C.D., 2015. *Principles of Geographical Information Systems*, OUP Oxford. Available at: https://books.google.pt/books?id=kvoJCAAAQBAJ.

Butwilowski, E. & Breunig, M., 2010. Requirements and implementation issues for a topology component in 3D geo-databases. In *13th AGILE International Conference on Geographic Information Science, Portugal*.

de By, R.A., 2004. *Principles of Geographic Information Systems: An Introductory Textbook*, International Institute for Geo-Information Science and Earth Observation. Available at: https://books.google.pt/books?id=a9AsAQAAMAAJ.

Caluwe, R. de, Tre, G. de & Bordogna, G., 2013. *Spatio-Temporal Databases: Flexible Querying and Reasoning*, Springer Berlin Heidelberg. Available at: https://books.google.pt/books?id=7xzpCAAAQBAJ.

Canty, M.J., 2014. *Image Analysis, Classification and Change Detection in Remote Sensing: With Algorithms for ENVI/IDL and Python*, Crc Press.

Caon, M., 2004. Voxel-based computational models of real human anatomy: a review. *Radiation and environmental biophysics*, 42(4), pp.229–235.

Casaca, J.M., Matos, J. & Baio, M., 2005. *TOPOGRAFIA GERAL* 4th ed. Lidel, ed., LTC. Available at: https://books.google.pt/books?id=VswhPwAACAAJ.

CG Studio, 2014. Human Body. Available at: https://www.cgstud.io/3d-models/human_body [Accessed May 20, 2015].

Chang, Y.-J., 1996. The NPAC Visible Human Viewer. , (2015/4/8). Available at: http://zatoka.icm.edu.pl/vh/paper/index.htm [Accessed April 14, 2015].

Conti, J., 2004. File Exchange - MATLAB Central. , 1/5/2015. Available at: http://www.mathworks.com/matlabcentral/fileexchange/.

Coppock, J.T. & Rhind, D.W., 1991. The History of GIS. In D. J. Maguire, M. F. Goodchild, & D. W. Rhind, eds. *Geographical Information Systems : Principles and Applications, Volume 1*. pp. 21–43.

Cornea, N.D., Silver, D. & Min, P., 2007. Curve-skeleton properties, applications, and algorithms. *Visualization and Computer Graphics, IEEE Transactions on*, 13(3), pp.530–548.

Curtis, H. & Barnes, N.S., 1994. *Invitation to Biology*, W. H. Freeman. Available at: https://books.google.pt/books?id=Et0MnwEACAAJ.

Daintith, J., 2008. *Biographical Encyclopedia of Scientists, Third Edition*, CRC Press. Available at: https://books.google.pt/books?id=vqTNfnKJVPAC.

Database Center for Life Science, 2009. BodyParts3D. , (25/4/2015). Available at: http://lifesciencedb.jp/bp3d/.

Davis, B.E., 2001. *GIS: A Visual Approach*, Delmar Thomson Learning. Available at: https://books.google.pt/books?id=sRNcW3jFYLYC.

Dijkstra, E.W., 1959. A note on two problems in connexion with graphs. *Numerische mathematik*, 1(1), pp.269–271.

Dixon, A.K. et al., 2015. *Human Sectional Anatomy: Atlas of Body Sections, CT and MRI Images, Fourth Edition*, CRC Press. Available at: https://books.google.pt/books?id=Mt8_CQAAQBAJ.

Dogdas, B., Shattuck, D.W. & Leahy, R.M., 2005. Segmentation of skull and scalp in 3-D human MRI using mathematical morphology. *Human Brain Mapping*, 26(4), pp.273–285.

Drake, R., Vogl, A.W. & Mitchell, A.W.M., 2014. *Gray's Anatomy for Students*, Elsevier Health Sciences. Available at: https://books.google.pt/books?id=Lh20BQAAQBAJ.

Egenhofer, M.J. & Franzosa, R.D., 1991. Point-set topological spatial relations. *International Journal of Geographical Information System*, 5(2), pp.161–174.

Egenhofer, M.J. & Herring, J., 1990. A mathematical framework for the definition of topological relationships. In *Fourth International Symposium on Spatial Data Handling*. Zurich, Switzerland, pp. 803–813.

Egenhofer, M.J., Sharma, J. & Mark, D.M., 1993. A critical comparison of the 4-intersection and 9-intersection models for spatial relations: formal analysis. In *AUTOCARTO-CONFERENCE-*. p. 1.

ESRI, 2012. Reveal More Value in Your Data with Location Analytics. Available at: http://www.esri.com/library/whitepapers/pdfs/reveal-more-value.pdf [Accessed May 19, 2015].

Feldesman, M.R., Kleckner, J.G. & Lundy, J.K., 1990. Femur/stature ratio and estimates of stature in mid- and late-pleistocene fossil hominids. *American Journal of Physical Anthropology*, 83(3), pp.359–372. Available at: http://dx.doi.org/10.1002/ajpa.1330830309.

Flores, J.M. & Schmitt, F., 2005. Segmentation, reconstruction and visualization of the pulmonary artery and the pulmonary vein from anatomical images of the visible human project. In *Computer Science, 2005. ENC 2005. Sixth Mexican International Conference on*. pp. 136–144.

Frank, A.U., Kuhn, W. & others, 1986. *Cell graphs: A provable correct method for the storage of geometry*, Eidgen{ö}ssische Technische Hochschule, Institut f{ü}r Geod{ä}sie und Photogrammetrie.

Frigo, M. & Johnson, S., 2014. FFTW. Available at: http://www.fftw.org/ [Accessed July 27, 2014].

Garb, J.L. et al., 2007. Using GIS for spatial analysis of rectal lesions in the human body. *Int J Health Geogr*, 6, p.11. Available at: http://www.ncbi.nlm.nih.gov/entrez/query.fcgi?cmd=Retrieve&db=PubMed&dopt=Citation&lis

t_uids=17362510.

Goodchild, M.F., 1992. Geographical information science. *International Journal of Geographical Information Systems*, 6(1), pp.31–45.

Goodchild, M.F., 2005. Geographical information science fifteen years later. Available at: http://www.geog.ucsb.edu/~good/papers/424.pdf [Accessed May 21, 2015].

Gröger, G. & Plümer, L., 2012. Transaction rules for updating surfaces in 3D GIS. *ISPRS Journal of Photogrammetry and Remote Sensing*, 69(0), pp.134–145. Available at: http://www.sciencedirect.com/science/article/pii/S0924271612000573.

Hahmann, S. & Burghardt, D., 2013. How much information is geospatially referenced? Networks and cognition. *International Journal of Geographical Information Science*, 27(6), pp.1171–1189.

Harley, J.B. & Woodward, D., 2001. " The History of Cartography. *Newsletter*.

Heywood, D.I. et al., 2011. *An Introduction to Geographical Information Systems*, Prentice Hall. Available at: https://books.google.pt/books?id=m8pYewAACAAJ.

Höhne, K.H. et al., 2000. *VOXEL-MAN 3D-Navigator: inner organs: regional, systemic and radiological anatomy*, Springer.

Höhne, K.H. & MAN, U., 2009. *Voxel-Man 3D-navigator: brain and skull; regional, functional, and radiological anatomy; English, German, French, Latin, Japanese*, Springer.

Hoppe, H. et al., 1992. Surface reconstruction from unorganized points. *SIGGRAPH Comput. Graph.*, 26. Available at: http://dx.doi.org/10.1145/142920.134011.

Imelińska, C., Downes, M.S. & Yuan, W., 2000. Semi-automated color segmentation of anatomical tissue. *Computerized Medical Imaging and Graphics*, 24(3), pp.173–180. Available at: http://www.sciencedirect.com/science/article/pii/S0895611100000173.

Imielinska, C. et al., 2000. Hybrid segmentation of the visible human data. In Citeseer.

Jamshidi, D.N., Esfahani, M.A. & Sharifi, M., 2014. *Biomechanic of Heart: 3D Heart Modeling Using CT or MRI Images*, USA: CreateSpace Independent Publishing Platform.

Jasika, N. et al., 2012. Dijkstra's shortest path algorithm serial and parallel execution performance analysis. In *MIPRO, 2012 Proceedings of the 35th International Convention*. IEEE, pp. 1811–1815.

Jones, C.B., 2014. *Geographical Information Systems and Computer Cartography*, Taylor & Francis. Available at: https://books.google.pt/books?id=5Ix9AwAAQBAJ.

Juanes, J.A. et al., 2012. Development of anatomical and radiological digital brain maps. *European Journal of Anatomy, European Journal of Anatomy*, 16, pp.91–97.

Kan, M.K. & Hopkins, G.B., 1979. Measurement of liver volume by emission computed tomography. *Journal of nuclear medicine: official publication, Society of Nuclear Medicine*, 20(6), pp.514–520.

Kang, H.S. et al., 2000. The Visible Man: Three-dimensional Interactive Musculoskeletal Anatomic Atlas of the Lower Extremity1. *Radiographics*, 20(1), pp.279–286. Available at:

http://radiographics.rsna.org/content/20/1/279.abstract.

Kazhdan, M. & Hoppe, H., 2013. Screened poisson surface reconstruction. *ACM Trans. Graph.*, 32(3), pp.1–13.

Kennedy, M.D., Dangermond, J. & Goodchild, M.F., 2013. *Introducing Geographic Information Systems with ArcGIS: A Workbook Approach to Learning GIS*, Wiley. Available at: https://books.google.pt/books?id=v6WcvrT8jRsC.

Kim, S.-H. & Chung, K.-Y., 2013. Medical information service system based on human 3D anatomical model. *Multimedia Tools and Applications*, pp.1–12. Available at: http://dx.doi.org/10.1007/s11042-013-1584-8.

Koussa, C. & Koehl, M., 2009. A simplified geometric and topological modeling of 3D buildings: combination of surface-based and solid-based representations. In *ASPRS 2009 annual Conference: Reflection of the past, vision of the future*.

Lee, J. & Zlatanova, S., 2008. A 3D data model and topological analyses for emergency response in urban areas. *Geospatial information technology for emergency response*, 143, p.C168.

LI, R., 1994. *Data structures and application issues in 3-D geographic information systems*, Nepean, ON, CANADA: Canadian Institute of Geomatics.

Lingle, V.A., 1999. Atlas of Human Anatomy. *Bulletin of the Medical Library Association*, 87(2), pp.227–228. Available at: http://www.ncbi.nlm.nih.gov/pmc/articles/PMC226566/.

Liu, B. et al., 2014. A simple method of rapid and automatic color image segmentation for serialized Visible Human slices. *Computers & Electrical Engineering*, 40(3), pp.870–883. Available at: http://www.sciencedirect.com/science/article/pii/S0045790613001389.

Liu, G. et al., 2009. *3D GIS Database Model for Efficient Management of Large Scale Underground Spatial Data* L. Di & A. Chen, eds., New York: Ieee. Available at: <Go to ISI>://WOS:000277622400145.

Longley, P. a. et al., 2005. *Geographic Information Systems and Science*, Wiley. Available at: http://www.amazon.com/Geographic-Information-Systems-Science-Longley/dp/047087001X/ref=sr_1_1?ie=UTF8&s=books&qid=1255777587&sr=1-1.

Mackenzie, J., 2013. GIS Analyses of Snow's Map. Available at: https://www.udel.edu/johnmack/frec682/cholera/cholera2.html [Accessed January 1, 2013].

Maguire, D.J., Goodchild, M.F. & David W, R., 1991. *Geographical Information Systems: Principles and Applications*, Longman.

Meade, M.S. & Emch, M., 2010. *Medical Geography*, Guilford Press. Available at: https://books.google.pt/books?id=LhnmiNYRj7kC.

Milner, J., Wong, K. & Ellul, C., 2014. Beyond Visualisation in 3D GIS.

Molenaar, M., 1990. A Formal Data Structure for Three-Dimensional Vector Maps D. A. Ondaatje, ed. *EGIS'90, First European Conference on Geographical Information Systems*, 2, pp.770–781.

Mosteller, R.D., 1987. Simplified calculation of body-surface area. *The New England journal of medicine*, 317(17), p.1098.

Netter, F.H., 2014. *Atlas of Human Anatomy*, Elsevier Health Sciences. Available at: https://books.google.pt/books?id=P73zAgAAQBAJ.

Painho, M. & Curvelo, P., 2012. Building dynamic, ontology-based alternative paths for GIS&T curricula. *Teaching Geographic Information Science and Technology in Higher Education*, pp.97–115.

Park, J.S. et al., 2006. Visible Korean human: its techniques and applications. *Clinical Anatomy*, 19(3), pp.216–224.

Peuquet, D.J., 1984. Data structures for a knowledge-based geographic information system. In *Proc. Spatial Data Handling*.

Pommert, A. et al., 2001. Creating a high-resolution spatial/symbolic model of the inner organs based on the Visible Human. *Medical Image Analysis*, 5(3), pp.221–228.

Pouncey, R., Swanson, K. & Hart, K., 1999. ERDAS Field Guide™ R. Pouncey, K. Swanson, & K. Hart, eds.

Primal Pictures, 2014. 3D Anatomy & Physiology. Available at: https://www.primalpictures.com/Home.aspx [Accessed May 20, 2015].

Ramsay, M.A.E., 2006. John Snow, MD: anaesthetist to the Queen of England and pioneer epidemiologist. *Proceedings (Baylor University. Medical Center)*, 19(1), pp.24–28. Available at: http://www.ncbi.nlm.nih.gov/pmc/articles/PMC1325279/.

Rana, M.A., Setan, H. & Chong, A.K., 2005. Computer-based modeling of soft tissues for medical and GIS applications. *International Symposium & Exhibition on Geoinformation*.

Richardson, D.B. et al., 2013. Spatial Turn in Health Research. *Science (New York, N.Y.)*, 339(6126), pp.1390–1392. Available at: http://www.ncbi.nlm.nih.gov/pmc/articles/PMC3757548/.

Riemer, M. et al., 2007. Improving the 3D Visualization of the Visible Korean Human via Data Driven 3D Segmentation in RGB Color Space. In R. Magjarevic & J. H. Nagel, eds. *World Congress on Medical Physics and Biomedical Engineering 2006*. Springer Berlin Heidelberg, pp. 4200–4203. Available at: http://dx.doi.org/10.1007/978-3-540-36841-0_1065.

Rinehart, H. et al., 1998. *Holt Biology: Visualizing Life: Teaching Resources*, Holt McDougal. Available at: https://books.google.pt/books?id=TbvzAQAACAAJ.

Schiemann, T., Tiede, U. & Höhne, K.H., 1997. Segmentation of the Visible Human for high-quality volume-based visualization. *Medical Image Analysis*, 1(4), pp.263–270. Available at: http://www.sciencedirect.com/science/article/pii/S1361841597850013.

Schlich, E., Schumm, M. & Schlich, M., 2010. 3-D-Body-Scan als anthropometrisches Verfahren zur Bestimmung der spezifischen Körperoberfläche. *Ernährungs Umschau*, 57, pp.178–183.

Schön, B., Laefer Debra, M.S. & Bertolotto, M., 2009. Three-Dimensional Spatial Information Systems -- State of the Art Review. *Recent Patents on Computer Science*, 2, pp.21–31.

Smith, B. et al., 2005. Anatomical information science. *Spatial Information Theory, Proceedings*, 3693, pp.149–164.

Smith, S.W., 1997. *The Scientist and Engineer's Guide to Digital Signal Processing*, California Technical Pub. Available at: https://books.google.pt/books?id=rp2VQgAACAAJ.

Sobotta, J. et al., 1997. *Sobotta Atlas of Human Anatomy*, Williams & Wilkins. Available at: https://books.google.pt/books?id=08tpAAAAMAAJ.

Španěl, M. et al., 2007. Delaunay-Based Vector Segmentation of Volumetric Medical Images. In W. Kropatsch, M. Kampel, & A. Hanbury, eds. *Computer Analysis of Images and Patterns SE - 33*. Lecture Notes in Computer Science. Springer Berlin Heidelberg, pp. 261–269. Available at: http://dx.doi.org/10.1007/978-3-540-74272-2_33.

Spitzer, V. et al., 1996. The visible human male: a technical report. *Journal of the American Medical Informatics Association*, 3(2), pp.118–130.

Spitzer, V. et al., 2004. VH Dissector: a platform for curriculum development and presentation for the anatomical arts and sciences. *Medicine Meets Vitual Reality*, 12, pp.127–129.

Starbuck, R. et al., 2014. A stereo vision-based approach to marker-less motion capture for on-site kinematic modeling of construction worker tasks. In *Proceedings of the 15th International Conference on Computing in Civil and Building Engineering (ICCCBE), Orlando, FL*.

Strecker, W. et al., 1997. Length and torsion of the lower limb. *Journal of Bone & Joint Surgery, British Volume*, 79(6), pp.1019–1023.

Suri, J.S., Singh, S. & Reden, L., 2002. Computer vision and pattern recognition techniques for 2-D and 3-D MR cerebral cortical segmentation (part I): A state-of-the-art review. *Pattern Analysis & Applications*, 5(1), pp.46–76.

Suveg, I. & Vosselman, G., 2000. 3D reconstruction of building models. *International archives of photogrammetry and remote sensing*, 33(B2; PART 2), pp.538–545.

Suwardhi, D. & Setan, H., 2006. 3D Geo-database Implementation using Craniofacial Geometric Morphometrics Database System Innovations in 3D Geo Information Systems. In A. Abdul-Rahman, S. Zlatanova, & V. Coors, eds. Springer Berlin Heidelberg, pp. 279–294. Available at: http://dx.doi.org/10.1007/978-3-540-36998-1_22.

Swartz, A., 2006. Open Library. Available at: https://openlibrary.org [Accessed June 2, 2014].

Takanashi, I. et al., 2002. Segmentation and 3D visualization of high-resolution human brain cryosections. In pp. 55–61. Available at: http://dx.doi.org/10.1117/12.458810.

Tanton, J.S., 2009. *Encyclopedia of Mathematics*, Facts On File, Incorporated. Available at: https://books.google.pt/books?id=MfKKMSuthacC.

Tao, V., 2004. 3D Data Acquisition and Object Reconstruction for AEC/CAD. *Directions Magazine*. Available at: http://www.directionsmag.com/entry/3d-data-acquisition-and-object-reconstruction-for-aeccad/123668 [Accessed June 9, 2015].

Tegtmeier, W. et al., 2014. 3D-GEM: Geo-technical extension towards an integrated 3D information

model for infrastructural development. *Computers & Geosciences*, 64(0), pp.126–135. Available at: http://www.sciencedirect.com/science/article/pii/S0098300413002902.

Thurston, J., Moore, J.P. & Poiker, T.K., 2003. *Integrated Geospatial Technologies: A Guide to GPS, GIS, and Data Logging*, Wiley. Available at: https://books.google.pt/books?id=WYyP4cr3VqgC.

TolTech, 2014. VH Dissector for Medical Education. , (1/5/2015). Available at: http://www.toltech.net/anatomy-software/solutions/vh-dissector-for-medical-education.

Tomlinson, R.F., Calkins, H.W. & Marble, D.F., 1976. *Computer handling of geographical data*, UNESCO press.

U.S. National Library of Medicine, 2001. The Visible Human Poject Projects Based on the Visible Human Data Set Applications for viewing images. Available at: http://www.nlm.nih.gov/research/visible/applications.html [Accessed May 20, 2014].

Ungar, P.S. & M'Kirera, F., 2003. A solution to the worn tooth conundrum in primate functional anatomy. *Proc Natl Acad Sci U S A*, 100(7), pp.3874–3877. Available at: http://www.ncbi.nlm.nih.gov/entrez/query.fcgi?cmd=Retrieve&db=PubMed&dopt=Citation&list_uids=12634426.

Verbraecken, J. et al., 2006. Body surface area in normal-weight, overweight, and obese adults. A comparison study. *Metabolism*, 55(4), pp.515–524.

Vongkornvoravej, P., Roongmangsorakarn, S. & Chaisaowong, K., 2006. Segmentation of Medical Images from Computerized Tomography to Create a 3-Dimensional Model of Human Skull. *King Mongkut's Institute of Technology North Bangkok*.

Wang, G. et al., 2015. 3D geological modeling for prediction of subsurface Mo targets in the Luanchuan district, China. *Ore Geology Reviews*. Available at: http://www.sciencedirect.com/science/article/pii/S0169136815000682 [Accessed May 3, 2015].

Wang, G. et al., 2014. 3D-GIS Analysis for Mineral Resources Exploration in Luanchuan, China. In *Mathematics of Planet Earth*. Springer, pp. 295–298.

Wang, G. & Huang, L., 2012. 3D geological modeling for mineral resource assessment of the Tongshan Cu deposit, Heilongjiang Province, China. *Geoscience Frontiers*, 3(4), pp.483–491.

Wang, Y., 2006. *3D GIS Spatial Modeling for City Surface and Subsurface Integration*, New York: Ieee. Available at: <Go to ISI>://WOS:000260989400386.

Wang, Y. et al., 2006. 3D Integral Modeling for City Surface & Subsurface. In A. Abdul-Rahman, S. Zlatanova, & V. Coors, eds. *Innovations in 3D Geo Information Systems*. Springer Berlin Heidelberg, pp. 95–105. Available at: http://dx.doi.org/10.1007/978-3-540-36998-1_7.

Wang, Y. et al., 2007. On 3D GIS Spatial Modeling. In *ISPRS Workshop on Updating Geo-spatial Databases with Imagery & The 5th ISPRS Workshop on DMGISs*. pp. 237–240.

Wenzel, V. et al., 1998. Respiratory system compliance decreases after cardiopulmonary resuscitation and stomach inflation: impact of large and small tidal volumes on calculated peak

airway pressure. *Resuscitation*, 38(2), pp.113–118.

van Wilgenburg, R. & SPINlab, V.U., 2013. GIS and epidemiology, a SWOT analysis.

Woodford, O., 2011. File Exchange - MATLAB Central. , (1/5/2015). Available at: http://www.mathworks.com/matlabcentral/fileexchange/.

World Health Organization, 2013. BMI classification 2013. *World Health Organization. URL: http://apps. who. int/bmi/index. jsp*.

World Health Organization, 2015. Geographic Information Systems. Available at: http://www.who.int/topics/geographic_information_systems/en/ [Accessed May 24, 2015].

Wu, L., 2004. Topological relations embodied in a generalized tri-prism (GTP) model for a 3D geoscience modeling system. *Computers & Geosciences*, 30(4), pp.405–418. Available at: http://www.sciencedirect.com/science/article/pii/S0098300404000196 [Accessed May 3, 2015].

Wu, Y. et al., 2012. Creation of a female and male segmentation dataset based on Chinese Visible Human (CVH). *Computerized Medical Imaging and Graphics*, 36(4), pp.336–342.

Xu, D. & Zlatanova, S., 2013. An approach to develop 3d Geo-DBMS topological operators by re-using existing 2d operators. In *8th 3DGeoInfo Conference & WG II/2 Workshop, Istanbul, Turkey, 27–29 November 2013, ISPRS Archives Volume II-2/W1*. ISPRS.

Xue, Z. et al., 2014. Body Segment Classification for Visible Human Cross Section Slices. In *Computer-Based Medical Systems (CBMS), 2014 IEEE 27th International Symposium on*. IEEE, pp. 199–204.

Yin, L. & Shiode, N., 2014. 3D spatial-temporal GIS modeling of urban environments to support design and planning processes. *Journal of Urbanism: International Research on Placemaking and Urban Sustainability*, 7(2), pp.152–169.

Yuan, Y., Qi, L.N. & Luo, S.Q., 2008. The reconstruction and application of virtual Chinese human female. *Computer Methods and Programs in Biomedicine*, 92(3), pp.249–256. Available at: <Go to ISI>://000261246500004.

Zhang, S.-X., Heng, P.-A. & Liu, Z.-J., 2006. Chinese visible human project. *Clinical Anatomy*, 19(3), pp.204–215. Available at: http://dx.doi.org/10.1002/ca.20273.

Zlatanova, S., 2006. 3D Geometries in Spatial DBMS. In A. Abdul-Rahman, S. Zlatanova, & V. Coors, eds. *Innovations in 3D Geo Information Systems SE - 1*. Lecture Notes in Geoinformation and Cartography. Springer Berlin Heidelberg, pp. 1–14. Available at: http://dx.doi.org/10.1007/978-3-540-36998-1_1.

Zlatanova, S., Rahman, A.A. & Pilouk, M., 2002. *Trends in 3D GIS Development*,

Zygote Body Media, 2011. Zygote Body. , (25/4/2015). Available at: https://zygotebody.com/.